UNIVERSITAT POLITÈCNICA DE VALÈNCIA
Escuela Técnica Superior de Ingeniería del Diseño

DESIGN, IMPLEMENTATION AND CONTROL OF A REACTION WHEEL BASED POSITIONING MECHANISM

DISEÑO, IMPLEMENTACIÓN Y CONTROL DE UN MECANISMO DE POSICIONAMIENTO BASADO EN RUEDA DE REACCIÓN

TRABAJO FINAL DEL

Máster Universitario en Ingeniería Mecatrónica

REALIZADO POR

Onur Cimen

TUTORIZADO POR

Vicente Fermín Casanova Calvo

CURSO ACADÉMICO: 2020/2021

Valencia 15.07.2021

Abstract

Autor   **Tutor**

Onur Cimen   Dr. Vicente Fermín Casanova Calvo

Design, Implementation and Control of a Reaction Wheel Based Positioning Mechanism

Diseño, Implementación y Control De Un Mecanismo de Posicionamiento Basado en Rueda De Reacción

Reaction Wheels, Controlling Position, Simscape, Hardware-in-the-Loop

This master thesis presents the mechatronics design, modelling simulation, implementation, and development of a control algorithm for position by using reaction wheels. This thesis focuses on a method for simulating a three-dimensional multibody system with MATLAB Simulink/Simscape.

A strategy for the control of the system is to control the angles of three axes, compared the results of the simulation, verifying the system is controllable with the desired angle parameters. The mechanical design of this master thesis is a satellite for developing the control algorithm of pointing and balance control.

Further this master thesis implements an experimental design of the system for a single axis for measurements and position control with MATLAB/Simulink (Hardware-in-the-Loop).

En esta tesis de máster se presenta el diseño mecatrónico, la simulación de modelos, la implementación y el desarrollo de un algoritmo de control mediante el uso de ruedas de reacción. Esta tesis demuestra un método de simulación con el sistema multicuerpo tridimensional con MATLAB Simulink/Simscape.

Una estrategia para el control del sistema consiste en controlar los ángulos de tres ejes, comparando los resultados de la simulación, verificando que el sistema es controlable con los parámetros de ángulo deseados. El diseño mecánico de esta tesis de máster es satélite para desarrollar el algoritmo de control de apuntamiento y equilibrio.

Además, esta tesis de máster implementa un diseño experimental del sistema para un solo eje para mediciones y control de posición con MATLAB/Simulink (Hardware-in-the-Loop).

Acknowledgements

First and foremost, I greatly appreciate the support and guidance provided by Dr. Vicente Fermín Casanova Calvo. I am very thankful for teaching me how to think simple during the master thesis. This master thesis would have not been completed without his helping, valuable ideas, and unending patience.

I am especially thankful to my parents, my father, my mother and my brother for their support, and positive attitude toward my master's degree.

Finally, I would like to thank all the individuals who directly or indirectly contributed towards the completion of this master thesis and my master's degree.

Contents

1. Introduction

1.1. Background and Motivation

This master thesis has different motivations. The initial idea of the topic of the master thesis is born from the control of the position with reaction wheel for multibody system (MBD), including all the development phases. The development phases are covered to mechatronic system (actuators, sensors, mechanical parts, control theory) and designing all mechanical part for simulation, developing a control algorithm for multibody dynamic system (MBD) in three-dimension world and real implementation to see the behavior of multibody system.

Furthermore, some new ideas and questions have risen on the duration of working project. One of them is to decide which real systems would be suitable to implement this project. And these last a few years a new spacecraft technology has been developed which is called CubeSats. This satellite technology is small and economic when it is compared to other satellites. CubeSats are considered as a spacecraft and affordable price to explore outer space and Earth observation.

CubeSats need some subsystems for controlling on the orbit. An Attitude Determination and Control Subsystem (ADCS) in a CubeSats is important to control the orientation towards a desired point in space. Especially, when CubeSat is in outer space, it would be the better solution of orientation CubeSat is reaction wheels.

In deep space, position determination and orbit changing have a different approach which using spacecraft propulsion for accelerating spacecraft from one point to another point. The direction of the satellite has to be stable during the changing trajectory to charging battery, communication etc. Controlling the direction is vital system for satellites.

In the past many projects have already been done on these subsystems of satellites. Many of them were simulated in MATLAB/Simulink with all equations. Recently, MATLAB had a new library which is Simscape inside Simulink. This library enables to design control systems for multibody systems in a three-dimension environment. Simscape provides to see behavior of systems in every change in the three-dimension environment. In this thesis all simulation and control algorithms are designed in Simulink/Simscape.

1.2. Objectives

All work is focused to improve efficiency and performance through the process of developing. MATLAB-Simulink/Simscape provides to simulate multibody dynamic model in a three-dimensions world. In addition to this, the other goal is the implementation of position control with hardware. The objectives of this work for this thesis are explained in the below.

- Objective 1; Designing all mechanical parts in SolidWorks to simulate in MATLAB/Simulink Simscape.
- Objective 2; The objective is to control the position of the angle in the three-axis with reaction wheels. The development of a control algorithm for three-axis in MATLAB/Simulink Simscape.
- Objective 3; The final objective of the thesis work is that implementation hardware-in-the-loop test (HIL) for a single axis with Arduino Due in MATLAB/Simulink.
- Objective 4; Design the prototype of the control position using reaction wheels for the master's course.

1.3. CubeSats

CubeSats are a class of nanosatellite which were developed by California Polytechnic State University (Cal Poly) and Stanford University's Space Systems Development Laboratory (SSDL). The main mission objective of CubeSats is to provide affordable access to space and doing scientific study in outer space.

After the development of CubeSat technology, it attracted the attention of universities and small companies because of the low cost to reach space and opening new business areas. The purpose of universities is to develop CubeSats for scientific research and take a part of the

space field. Many companies are building CubeSat for Earth observation, exploring space, and testing new technologies.

Figure 1.1 CubeSats fly free after deploying from International Space Station[1]

CubeSats have a size and form standard. The standard dimension is called "One Unit" or "1U" which is 10X10X10 cm. Typically 1U CubeSats' weight is between around 1 kg and 2 kg. In addition to this, the standard specification has changed in time and nowadays CubeSats are extendable, and there are various sizes 1U,1.5U, 2U, 3U, 6U and 12U with the following main feature (Figure 1.2).

- 1U CubeSat's dimension is 10X10X10 cm with a maximum weight of 2 kg.

- 1.5U CubeSat's dimension is 10X10X17.2 cm with a maximum weight of 3 kg.

- 2U CubeSat's dimension is 10X10X27.7 cm with a maximum weight of 4 kg.

- 3U CubeSat's dimension is 10X10X34.5 cm with a maximum weight of 6 kg.

- 6U CubeSat's dimension is 10X26.63X36.6 cm with a maximum weight of 12 kg.

- 12U CubeSat's dimension is 26.63X26.63X36.6 cm with a maximum weight of 24 kg. [1][2]

---

[1] Website of Nasa, Crew Researching How Life Adapts to Spaceflight

[2] Alicia Johnstone, CubeSat Design Specification (1U-12U) REV14 CP-CDS-R14, California Polytechnic State University (Cal Poly), July 2020, page 12.
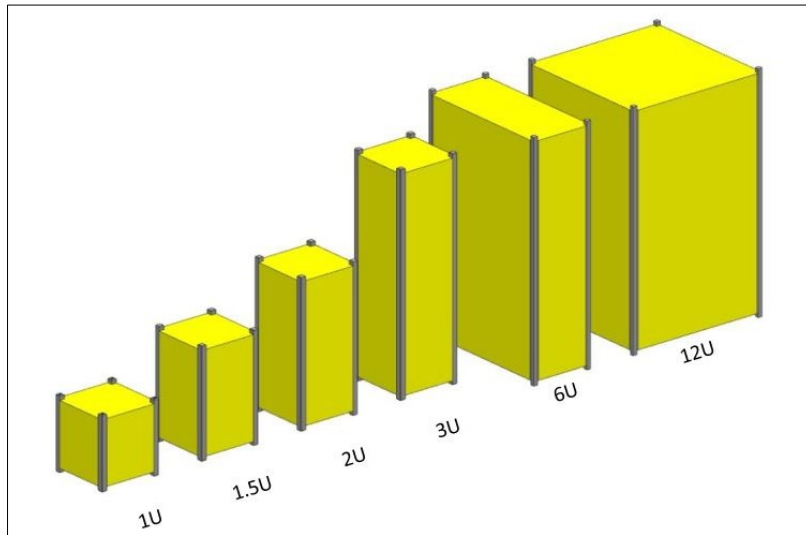
Figure 1.2 CubeSats Family[3]

The design of CubeSats depends on a mission goal. Every mission goal needs some essential subsystems. For example, the following subsystems

- Payload
- Structures Subsystem
- Electric Subsystem
- Thermal Subsystem
- Propulsion Subsystem
- Attitude Determination and Control Systems (ADCS) and Guidance Navigation and Control (GNC)
- Communications
- Data Handling
- Ground Segment
- Ground Networks

The platform of CubeSats has a special deployment mechanism which is called "the dispenser". The dispenser is assembled on the launch vehicle (rocket) to protect the CubeSats against any damage during the launch. The dispenser releases the CubeSats into space when the launch vehicle is in the desired orbit.

After launch into space, CubeSats should be controlled for desired orbit, point and a given task. Some subsystems are necessary to control CubeSats during trajectory correction and maneuvers such as Attitude determination and control systems (ADCS) and Guidance Navigation and Control (GNC). These subsystems have some actuators which use for satellite attitude control and guidance navigation include reaction wheel, magnetorquers, thrusters.

---

[3] Alicia Johnstone, CubeSat Design Specification (1U-12U) REV14 CP-CDS-R14, California Polytechnic State University (Cal Poly), July 2020, page 8.
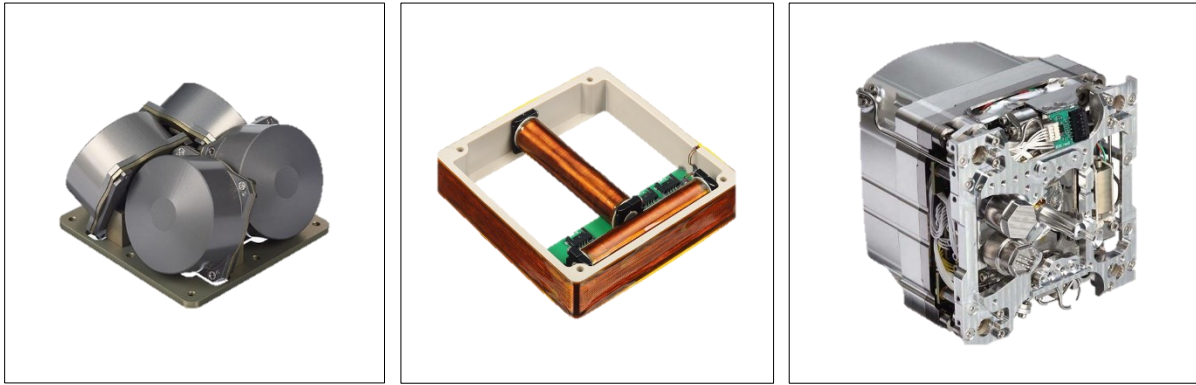
Figure 1.3 Reaction Wheel, Magnetorquers and Thrusters[4]

These actuators (Figure 1.3) are helping to arrange in any change of the trajectory and attitude during correction maneuvers. Reaction wheels provide CubeSats with three axis (yaw, roll and pitch) controlling capability. Magnetorquers are often used in low-Earth orbit because they take advantage of Earth's magnetic field. Lastly, thrusters help to CubeSats acceleration and pointing accuracy in space.

2. Theoretical Model

This chapter provides a mathematical equation of the systems with reaction wheel assembly configurations dynamics equations.

2.1. Design of Reaction Wheels

There are some specifications for designing reaction wheels. As it is known, CubeSat structural has a volume limitation. The volume limitation of CubeSat is considered for the designing reaction wheels. The other specifications of the reaction wheel are mass and dimensions [2].

The calculation of the mass for the reaction wheel is shown below equation (2.1).

$$m_{total} = m_{disc} + m_{ring} \tag{2.1}$$

The expression for the equation is shown that the radius of ring can be calculated for specific inner radius by using the equation (2.2) Some terms of equation are needed for the calculation which are the density of material, design requirement of radius and the height of reaction wheel. As it knows, it is necessary to know density and volume for the mass calculation.

$$m_{total} = \rho \pi r_{disc}^2 h_{disc} + \rho \pi (r_{disc}^2 - r_{ring}^2) h_{ring} \tag{2.2}$$

Having a high level of momentum, the reaction wheels are designed with ring. Inner and outer radius provides more inertia while the mass is the same (2.3).

$$I_{disc} = \frac{1}{2} m_{disc} r_{disc}^2 \tag{2.3}$$

Having a high level of momentum, the reaction wheels are designed with ring. Inner and outer radius provides more inertia while the mass is the same (2.4).

$$I_{ring} = \frac{1}{2} m_{ring} (r_{in}^2 + r_{out}^2) \tag{2.4}$$

The calculation of total inertia for reaction wheel can be calculated with below equation.

$$I_{total} = I_{disc} + I_{ring} \tag{2.5}$$

---

[4] CubeSat components - Flight Proven subsystems https://nanoavionics.com/cubesat-components/

The electric motor is the other important component. After selection of the motor, maximum angular momentum is calculated with maximum motor speed.

$$h_{max} = I_{total} \, \omega_{max} \qquad (2.6)$$
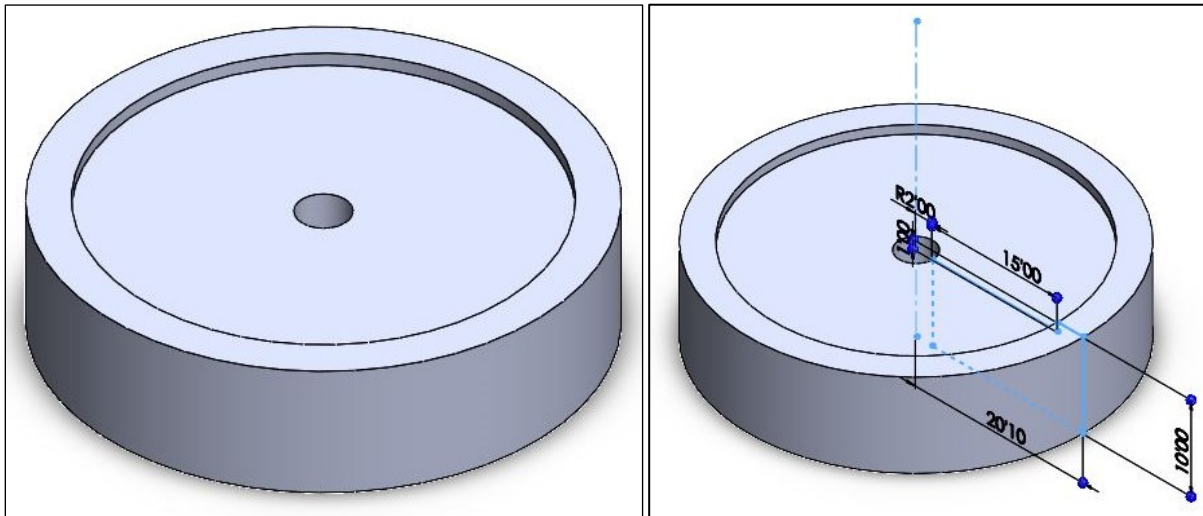
Figure 2.1 Reaction Wheel and Dimensions

Design Parameters of Reaction Wheel

Parameters	Values	Unit
Radius of disc	15	mm
Height of disc	10	mm
Radius of ring	20.1	mm
Height of ring	1	mm
Total Mass of Reaction Wheel	0.0351	kg
Density	2700	kg/m^3

Table 1 Design Parameters of Reaction Wheel

For control of the CubeSat attitude, it needs to be assembled with Simscape. The below figure (Figure 2.2) shows that inertia of reaction wheel and derived values. This information provides to solve mathematical model for development control systems.
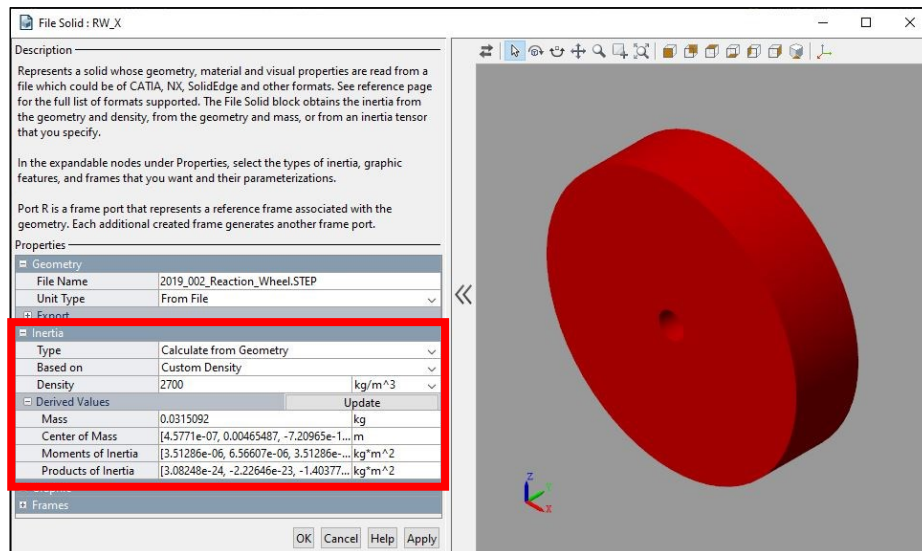
Figure 2.2 Reaction Wheel Simscape Configuration

When reaction wheel rotates in one direction around the axis, meanwhile providing the force the multibody systems (satellite) to rotate in the other direction. Therefore, the positions of the satellite are controlled.

2.2. Mathematical Model of the System

Mathematical equations of 3-axis control system are defined with especial angles. These angles are named as Euler angel. The angle of rotation about the X body axis is (∅), the angle of rotation about the Y body axis is (θ) and lastly the angle of rotation about the Z body axis is (Ψ). All Euler angle matrices about each axis are explained in the below.

$$R_x(\emptyset) = \begin{bmatrix} 1 & 0 & 0 \\ 0 & \cos\emptyset & \sin\emptyset \\ 0 & -\sin\emptyset & \cos\emptyset \end{bmatrix} \tag{2.7}$$

$$R_x(\theta) = \begin{bmatrix} 1 & 0 & 0 \\ 0 & \cos\theta & \sin\theta \\ 0 & -\sin\theta & \cos\theta \end{bmatrix} \tag{2.8}$$

$$R_z(\Psi) = \begin{bmatrix} \cos\Psi & -\sin\Psi & 0 \\ \sin\Psi & \cos\Psi & 0 \\ 0 & 0 & 1 \end{bmatrix} \tag{2.9}$$

The inertia of the body frame 'I' can be explained following equation. Assuming the body frame homogenous displacement of mass through the principal axes, the inertia matrix can be reduced to a diagonal matrix:

$$I = \begin{bmatrix} I_x & -I_{xy} & -I_{xz} \\ -I_{yx} & I_y & -I_{yz} \\ -I_{zx} & -I_{zy} & I_z \end{bmatrix} = \begin{bmatrix} I_x & 0 & 0 \\ 0 & I_y & 0 \\ 0 & 0 & I_z \end{bmatrix} \tag{2.10}$$
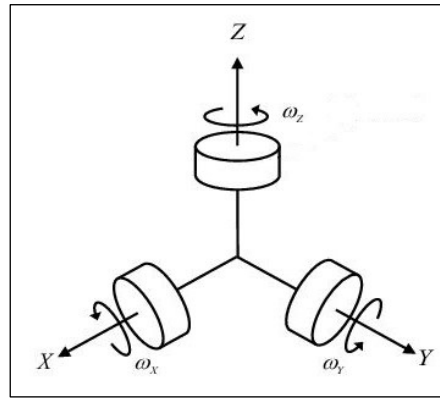
Figure 2.3 Configuration of Three Reaction Wheels

L_{3x3} The distribution matrix of standard orthogonal 3-wheel configuration can be defined as:

$$L = \begin{bmatrix} 1 & 0 & 0 \\ 0 & 1 & 0 \\ 0 & 0 & 1 \end{bmatrix} \tag{2.11}$$

The angular velocity of the dynamic system is defined as follows.

$$\omega_{IE/B} = \begin{bmatrix} \omega_x \\ \omega_y \\ \omega_z \end{bmatrix} \tag{2.12}$$

T_w is the applied reaction wheel torques and T_d is the external disturbance torques vector. Sum all, the total torques matrix is defined as follows.

$$T_w = \begin{bmatrix} T_1 \\ T_2 \\ T_3 \end{bmatrix} \tag{2.13}$$

As it is mentioned (2.13) the torque of reaction wheel matrix and the moment acted on the body frame with reaction wheel

$$\begin{bmatrix} T_x \\ T_y \\ T_z \end{bmatrix} = L_{3x3} \begin{bmatrix} T_1 \\ T_2 \\ T_3 \end{bmatrix} \tag{2.14}$$

h_w is the reaction wheel angular momentum vector. Finally, the dynamics equation of the system with reaction wheels is represented in the below equation (2.15). [3]

$$I\,\dot{\omega}_{IE/B} = T_d - \omega_{IE/B} \times \left(I\,\omega_{IE/B} + h_w\right) - T_w \tag{2.15}$$

Applied all equations in the above it can be obtained all angles as follows.

$$\emptyset = \dot{\omega}_x = \frac{T_x - (I_y - I_z)\omega_z\,\omega_y + h_{wz}\,\omega_y - h_{wy}\,\omega_z}{I_x} \tag{2.16}$$

$$\theta = \dot{\omega}_y = \frac{T_y - (I_z - I_x)\omega_x\,\omega_z + h_{wx}\,\omega_z - h_{wz}\,\omega_x}{I_y} \tag{2.17}$$

$$\Psi = \dot\omega_z = \frac{T_z - (I_x - I_y)\omega_y\,\omega_x + h_{wy}\,\omega_x - h_{wx}\,\omega_y}{I_x} \qquad (2.18)$$

In order to design control algorithm for 3-axis, it can be considered more expressions, but in this work, some of expression do not include such as earth gravity, friction etc. All mathematical model is calculated by Simscape blocks in three dimensional environments.

3.   Control Model Design with Simspace
3.1. Mechanical Part Model Design
3.1.1. CubeSat Design Specification

Design of CubeSat is a long process from the ground to space. According to NASA this process will take 1-6 months[5]. During the development process there are different kinds of test procedures which CubeSat should pass for the launch. To know all the procedures Cal Poly SLO have published the last version of CubeSat design specification which is named CubeSat Design Specification (1U-12U) REV14 CP-CDS-R1.

Finally, the aim of the design of CubeSat for this work is to design control algorithms within Simulink/Simscape and analyze the response of CubeSat in a three-dimensions environment.

3.1.2. Design Specification

For simulation of multibody dynamic models, it is necessary to design mechanical parts of CubeSat. CubeSat was chosen for this project. When the model is chosen, the structure of CubeSat must be designed according to requirements. In this work a few main requirements were considered for the design. These requirements are mentioned in the below.

2.2.7   The edges of the rails should be rounded to a radius of at least 1 mm.

2.2.8   The ends of the rails on the +/- Z face shall have a minimum surface area of 6.5 mm x 6.5 mm contact area with neighboring CubeSat rails (as per drawing in Appendix B).

2.2.10 Note: Table 1 shows the typical maximum mass for each U configuration.

1U CubeSat's maximum weight is 2 kg.

2.2.12.1 Note: Typically, Aluminum 7075, 6061, 6082, 5005, and/or 5052 are used for both the main CubeSat structure and the rails. If materials other than aluminum are used, the CubeSat developer should contact the Launch Provider or dispenser manufacturer.[6]

---

[5] CubeSat101 Basic Concepts and Processes for First-Time CubeSat Developers NASA CubeSat Launch Initiative for Public Release – Revision Dated October 2017 page 9.

[6] Alicia Johnstone, CubeSat Design Specification (1U-12U) REV14 CP-CDS-R14, California Polytechnic State University (Cal Poly), July 2020, page 11-12
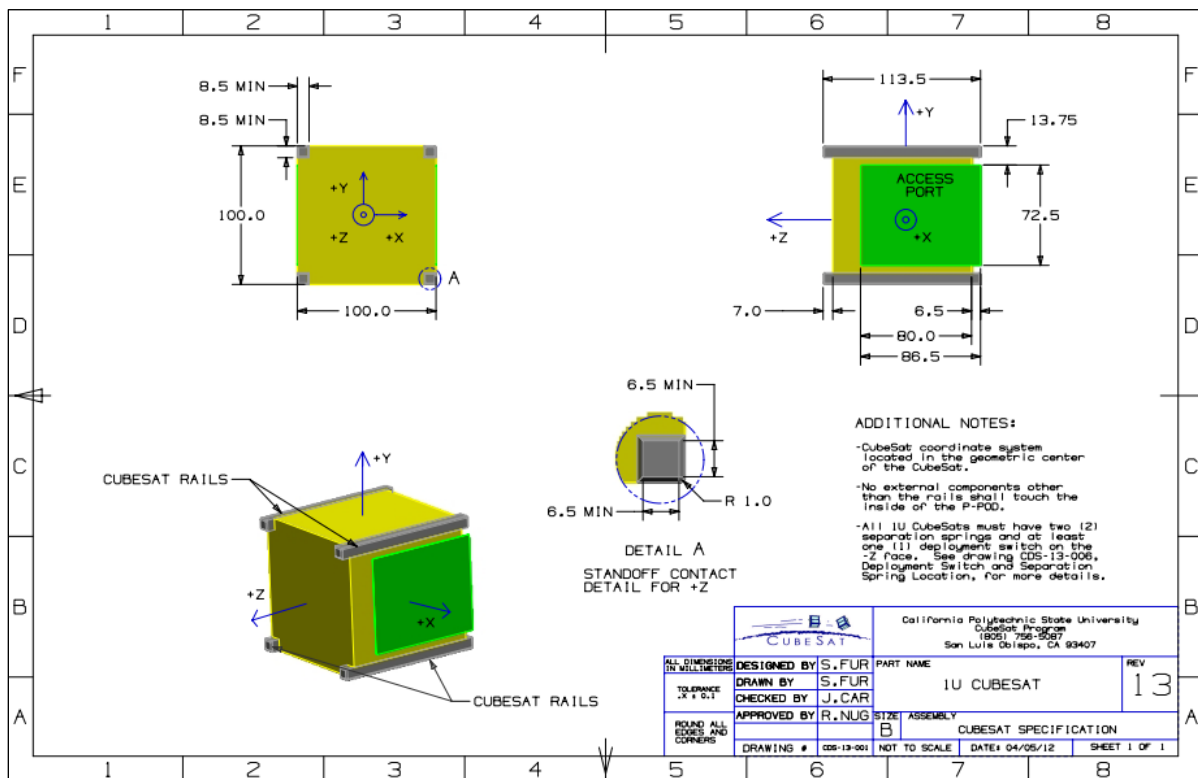
Figure 3.1 1U CubeSat[7]

For the design of structural using Student Edition of SolidWorks all parts and the assembly were created.

3.1.3. Design of CubeSat

The structural design has four main parts, carrying all payload. These parts are named rails. CubeSat rails are connected to other small rails which are assembled side +X, -X and side +Y, -Y. CubeSat rails (Figure 3.2Figure 3.2) provide slip from dispensers during the launch process. The other rails (Figure 3.3) are connected CubeSat rails to create a cube shape.
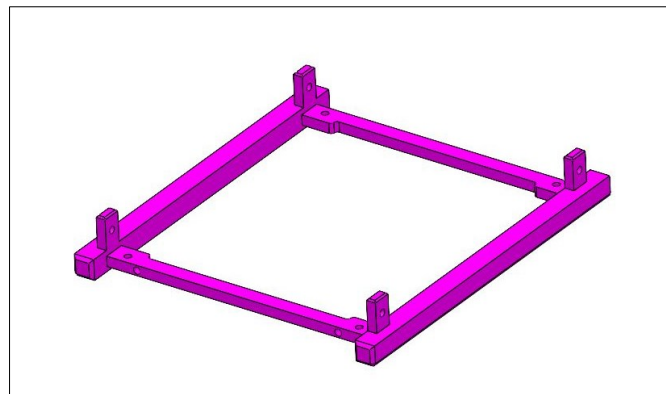
Figure 3.2 CubeSat Rail 1

---

[7] Alicia Johnstone, CubeSat Design Specification (1U-12U) REV14 CP-CDS-R14, California Polytechnic State University (Cal Poly), July 2020, page 31
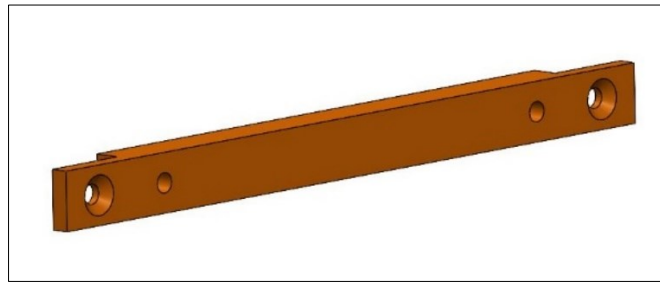
Figure 3.3 CubeSat Rail 2
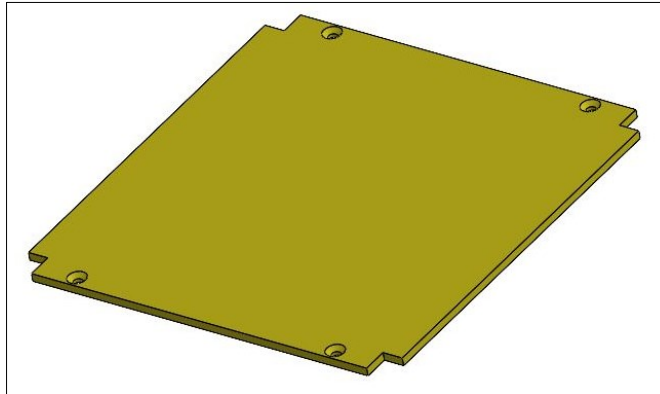
Figure 3.4 CubeSat Top and Bottom Plate
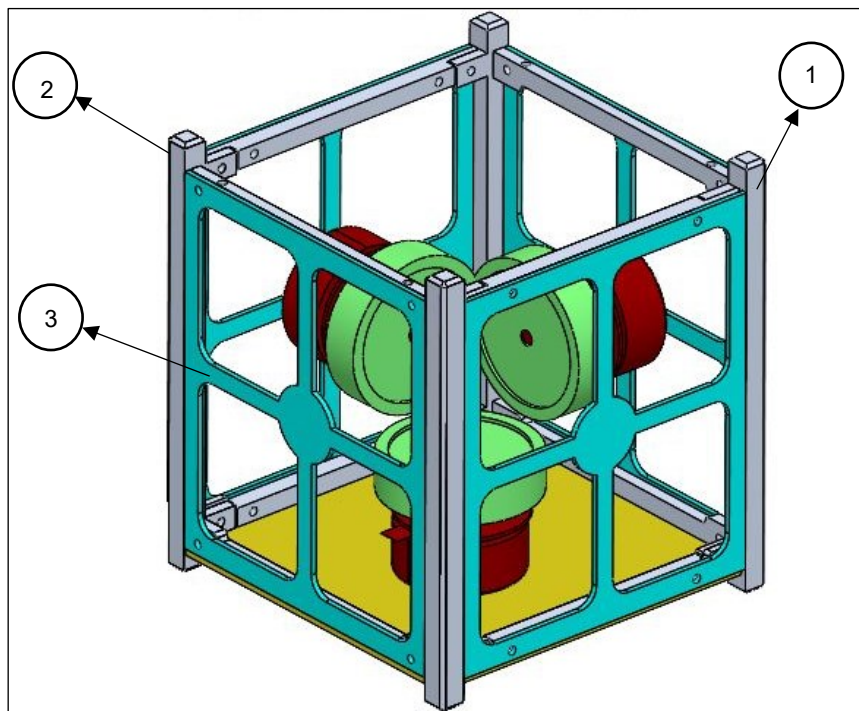
Figure 3.5 Structure of CubeSat

CubeSat (Figure 3.5) shows structure alone on an isometric view. It is formed by three main parts. These three main parts are used to all assembly of the structure.

- Label 1 is CubeSat Rail 1 (Figure 3.2) and there are two of them which are connected perpendicular to Y direction.
- Label 2 is CubeSat Rail 2 (Figure 3.3) and there are twelve. And these parts are connected lateral panels perpendicular to X direction.
- Label 3 is a plate for Solar Panel and access to inside of CubeSat. There are four and they are connected X direction and Y direction.

- Figure 3.4 shows top and bottom plate. Top and bottom plates are assembled to lateral to Z direction. This perpendicular to Z direction
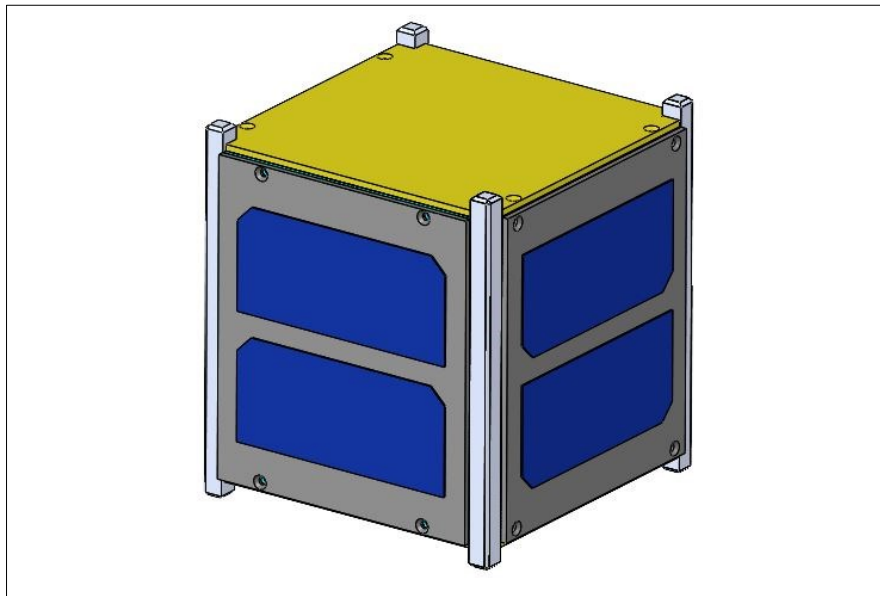
Figure 3.6 Assembly of CubeSat with Solar Panels

All satellites have different missions and goals. Power subsystems are necessary with rechargeable batteries and solar panels for a longer operating time. Figure 3.6 shows the views with solar panels.

The CubeSat structure is made of Aluminium 6061-T6. Material properties are explained in the below table (Table 2).

Property	Value	Units
Elastic Modulus	69000.00067	N/mm^2
Poisson's Ratio	0.33	N/A
Tensile Strength	310.0000021	N/mm^2
Yield Strength	275.0000009	N/mm^2
Tangent Modulus	N/A	N/mm^2
Thermal Expansion Coefficient	$2.4\,e^{-5}$	/K
Mass Density	2700	kg/m^3
Hardening Factor	0.85	N/A

Table 2 Material Properties for Aluminium 6061-T6

Material properties are important for Simscape simulation. For development of control algorithms, it is necessary to use some properties to calculate equations with Simscape. Therefore, density of Al 6061 T6 (Aluminium 6061) is 2700 kg/m^3. The below figure (Figure 3.7) shows how to configure the Simscape simulation. The density of all parts of the structural should be entered in configurations of Simscape.
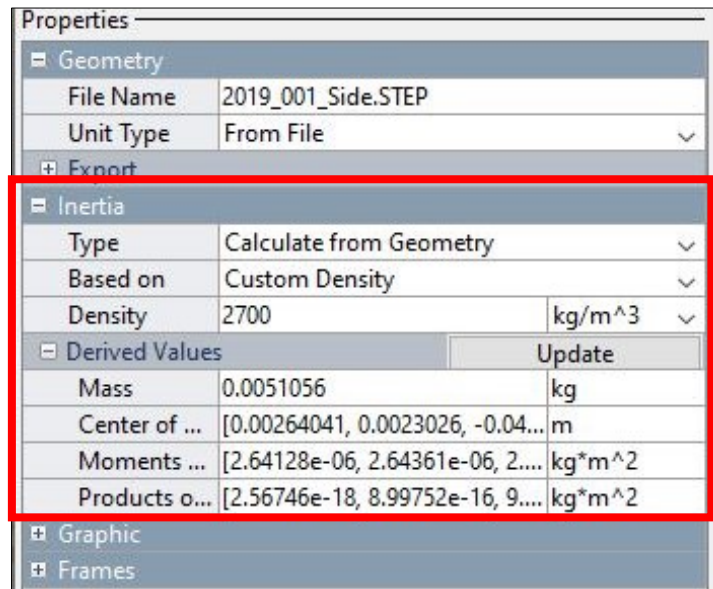
Figure 3.7 Simscape Configuration

After the material properties the other critical properties are mechanical properties such as center of mass, moments of inertia. The below table (Table 3) was taken from Student Edition of SolidWorks

Mass properties of CubeSat
Mass = 382.06 grams
Volume = 765690.95 cubic millimeters
Volume = 270806.88 cubic millimeters
Center of mass: (millimeters)
X =40.57
Y = 94.92
Z = 95.66

Principal axes of inertia and principal moments of inertia: (grams * square millimeters)	
Taken at the center of mass.	
Ix = (0.97, 0.24, -0.09)	Px = 1017087.31
Iy = (-0.24, 0.97, -0.08)	Py = 1021428.12
Iz = (0.07, 0.10, 0.99)	Pz = 1087594.85

Moments of inertia: (grams * square millimeters)		
Taken at the center of mass and aligned with the output coordinate system.		
Lxx = 1017659.45	Lxy = 563.52	Lxz = -4743.36
Lyx = 563.52	Lyy = 1021826.80	Lyz = -6571.77
Lzx = -4743.36	Lzy = -6571.77	Lzz = 1086624.03

Moments of inertia: (grams * square millimeters)		
Taken at the output coordinate system.		
Ixx = 7955832.38	Ixy = 1471885.70	Ixz = 1478037.59
Iyx = 1471885.70	Iyy = 5146727.20	Iyz = 3462410.31
Izx = 1478037.59	Izy = 3462410.31	Izz = 5157699.82

Table 3 Mass properties of CubeSat

The control of position for three axes (X-Y-Z) with reaction wheels needs some expressions for the simulation. The aim of the mass properties of the design is to calculate the effect of reaction wheels in the body frame. The mathematical model of system will be modelled automatically by Simscape.

3.2. Position Control Model Design

This chapter explains about development control algorithms. Due to the complex structure of the problem some of the terms are neglected. These terms are gravitational and friction force. The configuration of reaction wheels is mentioned in the figure (Figure 2.3).

3.2.1. Sensor Configurations and 3 DOF

Sensors are an essential component for designing the close-loop control algorithm. In this work, a close-loop control algorithm is developed in the Simscape environment. For doing that, a modelling sensor is important to measure position or angle. The below figure (Figure 3.8) shows the sensor modelling.
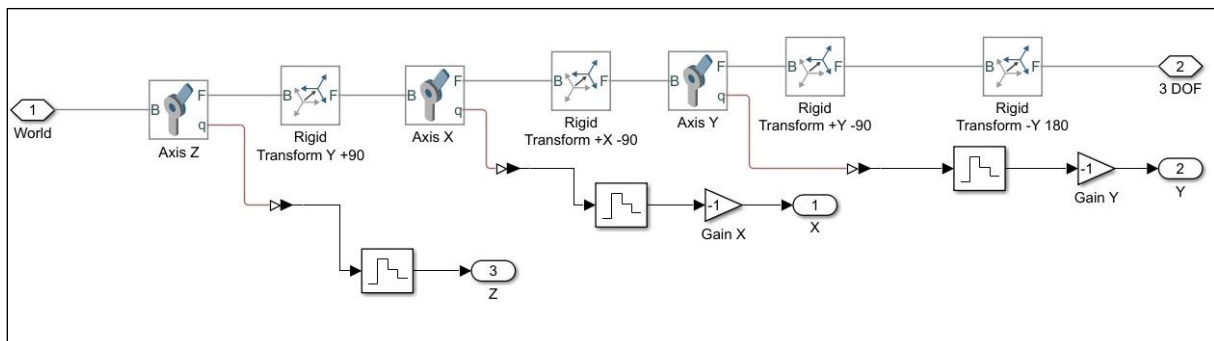
Figure 3.8 Configuration of the Sensor (3 Degree of Freedom)

Revolute joint provides a rotational degree around the Z axis. Rigid transform block translates the next port frame (F) with respect to the base port frame (B)[8]. The figure (Figure 3.9) shows the reference system of the revolute joint.

The revolute joint is rotated 90 degrees on the Y axis to obtain the rotation around X. The other revolute joint is to rotate 90 degrees as well on the X axis for getting the rotation around Y axis. As knows it is not necessary to do the same rotation about the Z axis because revolute joint has the feature of rotation around the Z-axis. Once all rotations are completed, it is possible to measure the position and angle on all axes. The figure (Figure 3.8) all connection between the blocks is represented 3 degrees of freedom. The below figure (Figure 3.9) shows feature of the revolute joint.

---

[8] Rigid Transform on the website of MathWorks

https://www.mathworks.com/help/physmod/sm/ref/rigidtransform.html
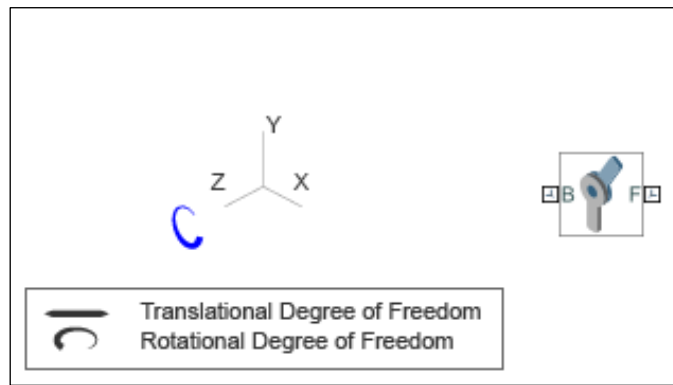
Figure 3.9 Revolute Joint and Joint Degrees of Freedom[9]

Revolute Joint measures angular position in radians. Input or sensor values convert radians with Radians to Degrees block.

3.2.2. DC Motor Modelling with Simscape

DC motor is a component for transforming electrical energy into mechanical energy. It is a common actuator for control system. In this work, Maxon EC Motor flat ∅32 mm (Appendix B.1) is chosen to simulate rotation of reaction wheels in simulation of Simscape.

Modelling DC motors with Simspace is different from Simulink. In Simulink it is necessary to calculate the transfer function for a mathematical model. However, some blocks are essential to model DC motors in the Simscape environment. In the below figure (Figure 3.10) is shown which kind of blocks are used for modeling DC motor in this work.
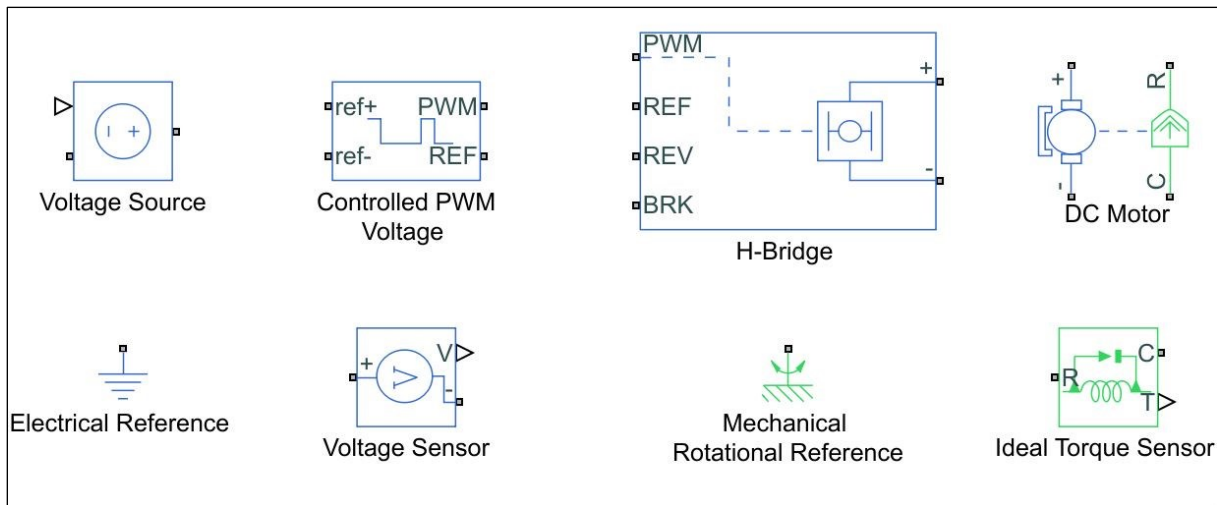
Figure 3.10 Simscape Motor Model Blocks

The below table (Table 4 Motor Data for Modelling with Simscape (Table 4) shows that motor's data is necessary to model in Simscape with DC Motor block.

Motor Data	Value	Units
Armature Inductance	1.61	mH
Stall Torque	68.3	mNm
No-Load Speed	3720	rpm

---

[9] Revolute Joint on the website of MathWorks

https://www.mathworks.com/help/physmod/sm/ref/revolutejoint.html

Nominal Voltage	9	V
No Load Current	74.7	mA
Rotor Inertia	35	gcm^2

Table 4 Motor Data for Modelling with Simscape

The electrical torque and mechanical parameters (Table 4) are be entered in DC Block that it shows on the below figure (Figure 3.11)
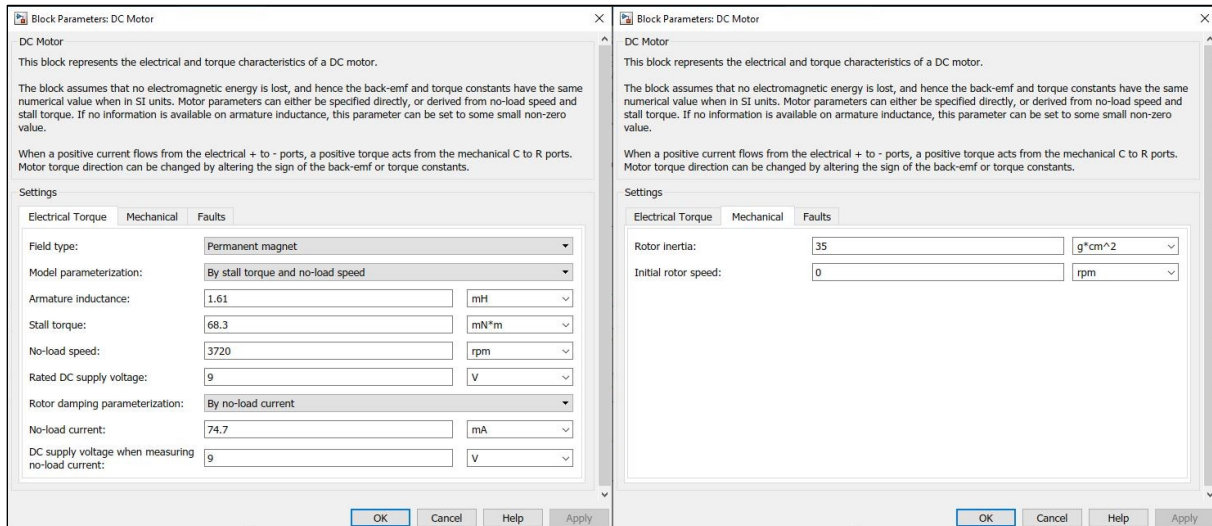
Figure 3.11 DC Motor Block Parameters

There are many ways to control DC Motor but one of the simplest ways is Pulse Width Modulation. In Simscape Controlled PWM Voltage is configured as below figure (Figure 3.12). PWM frequency of the PWM output signal is set to the default value (1000 Hz). Input voltage for %0 duty cycle is 0 V and output for %100 duty cycle is 9 V.
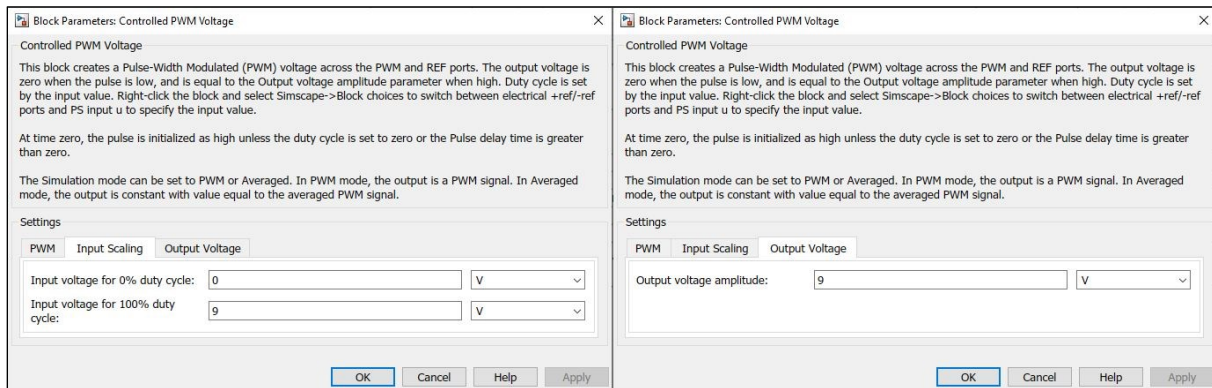
Figure 3.12 Controlled PWM Voltage

The H-bridge is an essential electronic circuit to control DC motor direction clockwise and anticlockwise. H-bridge parameters are configured according to nominal voltage (9V). Reverse threshold voltage is an important value for controlling the direction. If the input signal is higher than reverse threshold voltage (2.5V), H-bridge changes the switch, and the motor turns the opposite direction. All configurations are shown in the below figure (Figure 3.13).
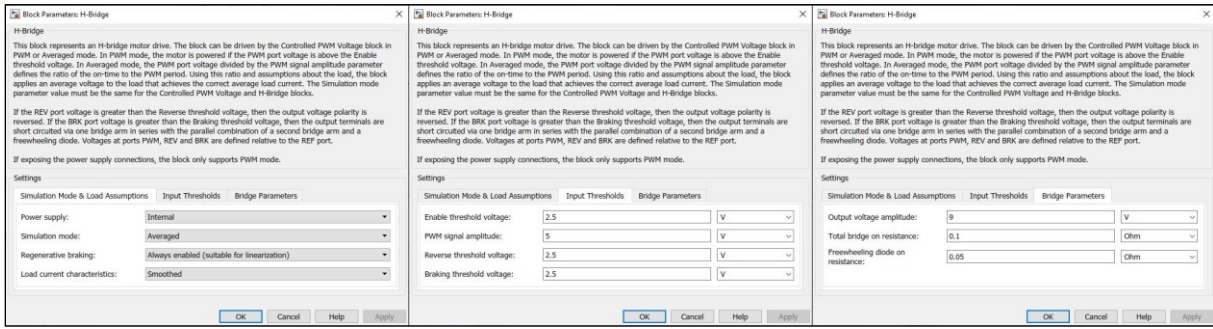
Figure 3.13 H-Bridge Configuration

Input and sensor signal are converted to signal voltage for controlling duty cycle and direction. When the control effort is between 0 V and 9 V, it is used to regulate duty cycle with the DUTY input port (Figure 3.14). The logic block is used to know if the control effort signal is less than 0 V. When the control effort is less than 0 V, the logic block gives "1". Then the control effort multiplies with 9 gain to send a signal to the REV input port for controlling the direction of the DC motor (Figure 3.14) [4].
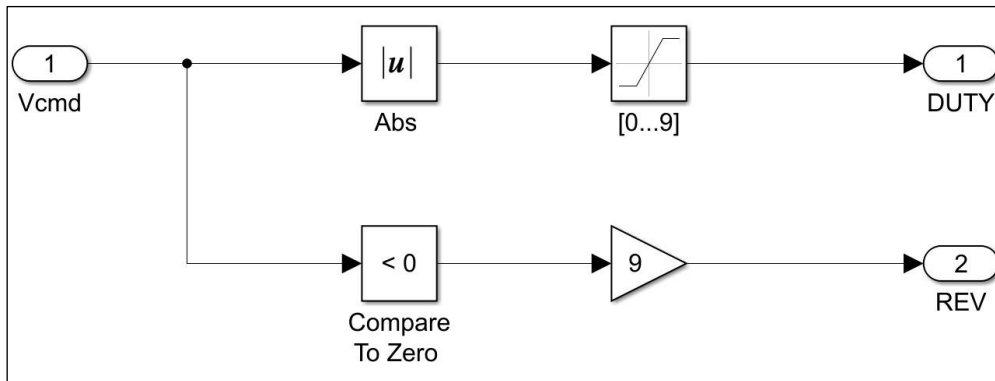
Figure 3.14 Voltage Signal for Duty and Reverse

Two main ports are used for designing the control algorithm for the DC Motor in Simscape. The DUTY input is connected to ref+ port (Controlled PWM Voltage) (Figure 3.15) for controlling the duty cycle. The REV input port is connected to the H-Bridge REV port for controlling the direction (Figure 3.15). It is necessary to convert electric energy to mechanical energy with the Ideal Torque Sensor to spin the reaction wheel (Figure 3.15).
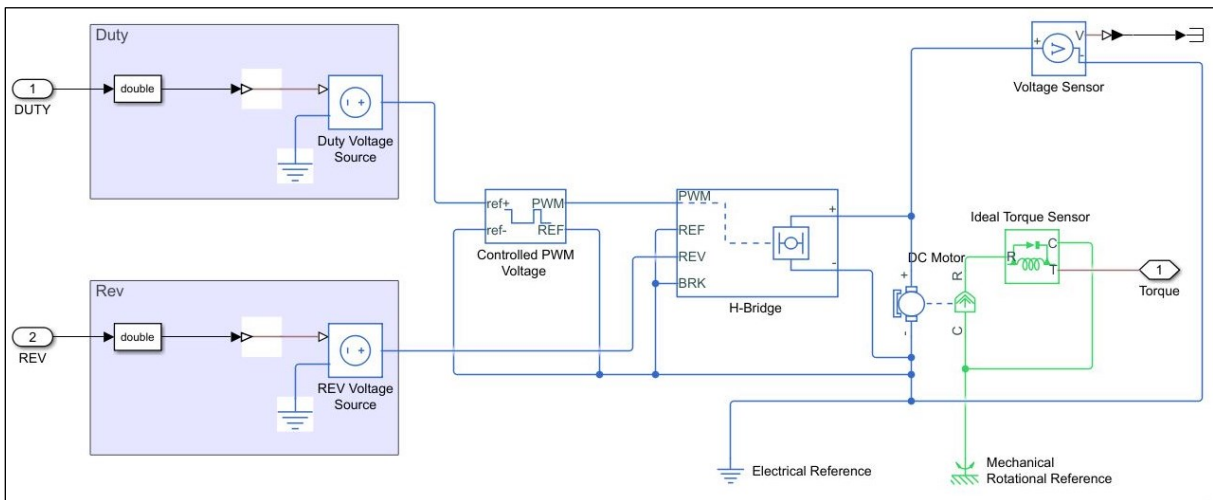
Figure 3.15 Modelling DC Motor

The torque of the DC Motor has to be connected to the three-dimension model. The revolute Joint is a Simscape block for modeling the degree of freedom. The Revolute Joint has torque input to use for the spinning reaction wheel (Figure 3.16).
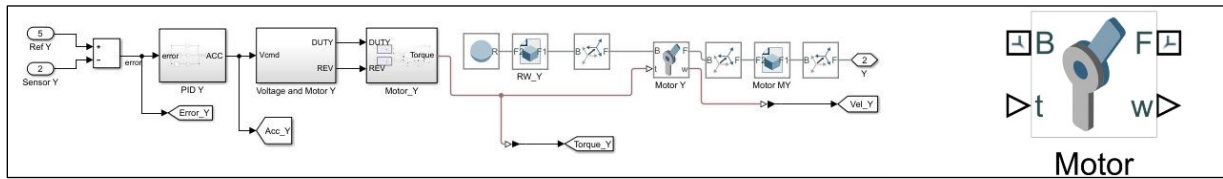
Figure 3.16 Connection to Reaction Wheel and Revolute Joint

Finally, the control algorithm design shows the above figure (Figure 3.16). The DC motor modelling and three-dimension model are connected to each other for control position.

3.2.3. PID Design

In the simulation PID proportional-Integral-Derivative (PID) controller is used for controlling the angles of the multibody system.

Controller	Axes		
	X	**Y**	**Z**
Proportional - Kp	0.3	0.5	0.6
Integral - Ki	0.1	0.215	0.4
Derivative - Kd	0	0.1	0

Table 5 PID Configuration of Simulation

The PID control design is made according to the observation of the system. After a few testing's PID, it is configured final PID values. The above table (Table 5) shows the final PID values.

3.2.4. Simulation with MATLAB Simulink/Simscape

This chapter covers the results of the simulation. Once the sensor modelling and the DC motor modelling are completed. The next process is to obtain the data of systems' behavior. Different desired angles are simulated which are 45º degrees, 60º degrees and 75º degrees. Finally, all desired angles are compared to analyze the system.

3.2.4.1. Step Input 45º degrees

Controlling the single axis would be more stable than three degrees of freedom. While controlling one position, it is important to see how other axes are affected. The below figure (Figure 3.17) represents the controlling X axis. Calculating for the settling point of the X is to seek the constant time which corresponds to 63% of the final values. This value is 28.35º degrees. The constant time is 16.681 seconds for 45º degree angles. The settling time (98%) is 60.482 seconds. The form of response of the X axis is overdamped. The end of the response shows that the systems is reached the reference input.

The control effort for X axes is similar to the error graph. And the other axes keep their position which is represented in the below figure (Figure 3.18).
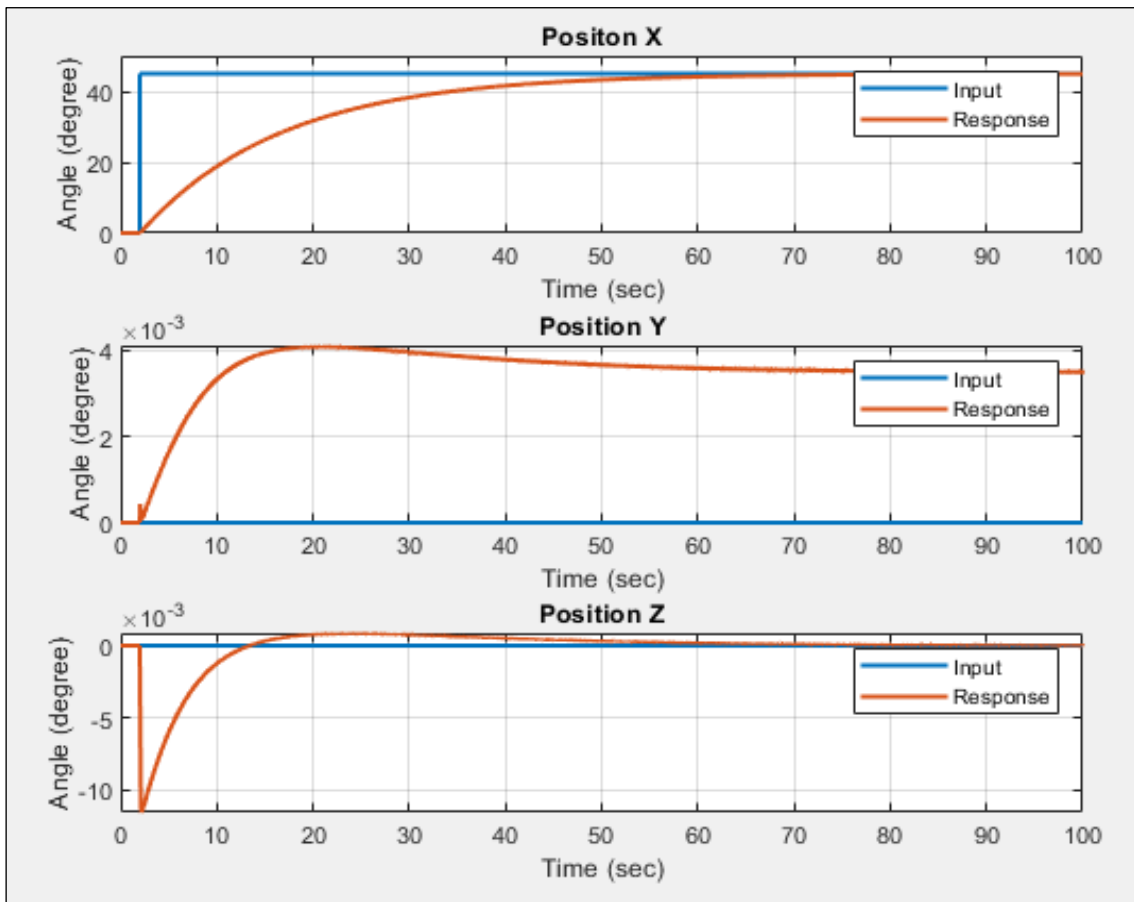
Figure 3.17 Step Input Position X, 45º degrees (X Axis)
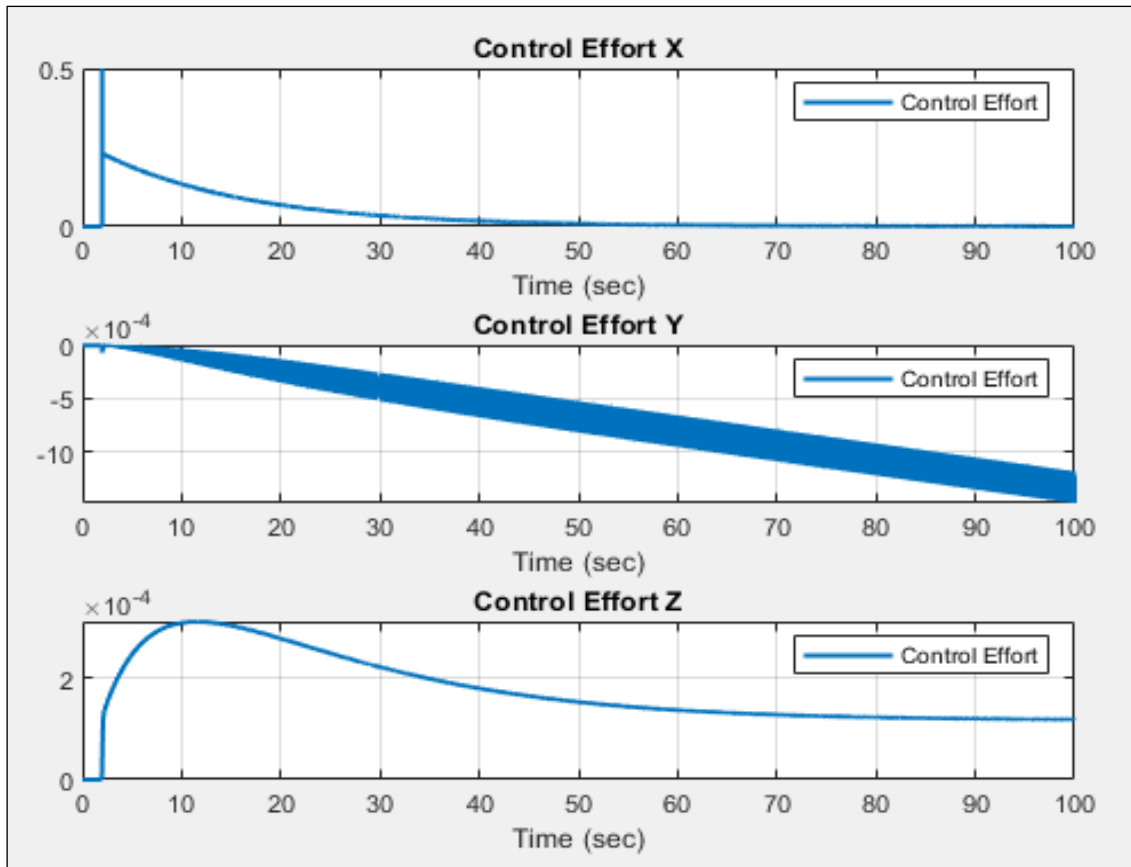
Figure 3.18 Control Effort for all axes, 45 degrees (X Axis)
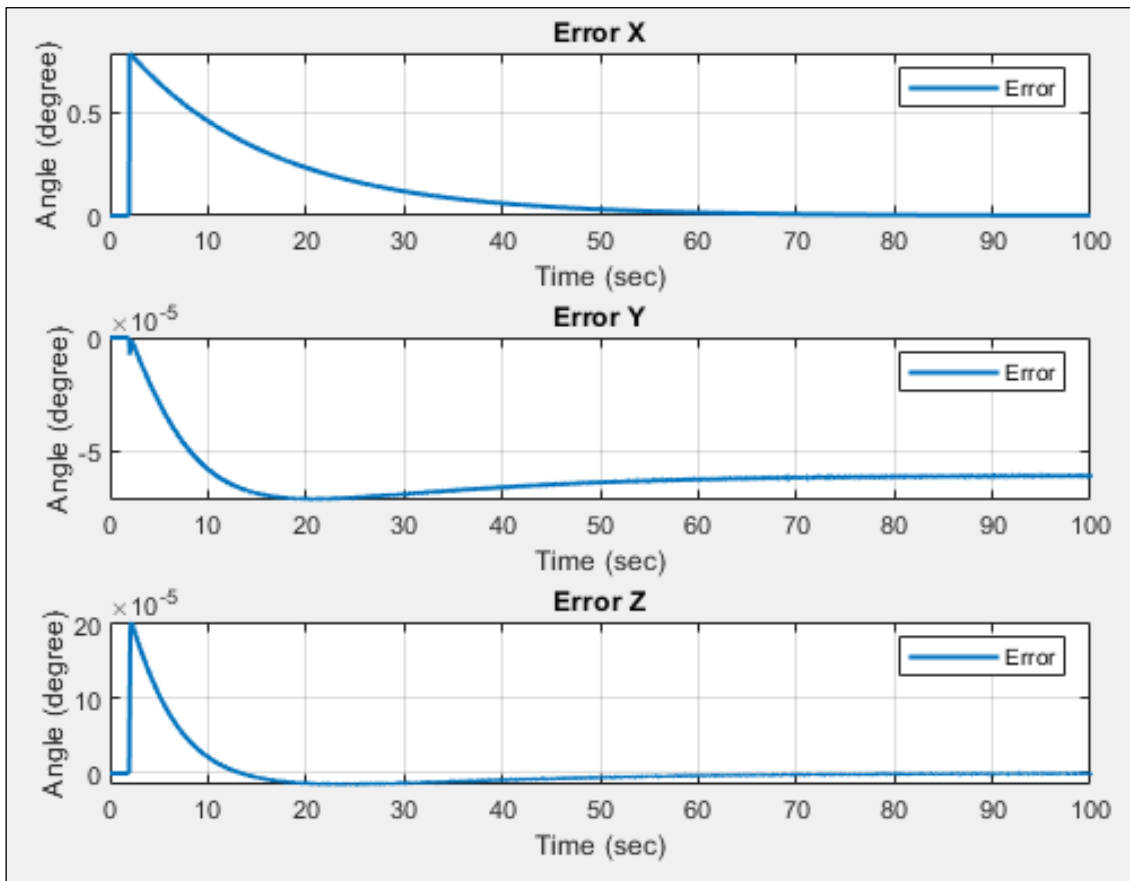
Figure 3.19 Errors 45º degrees (X Axis)

The same reference input is applied each axis. At this point it is simulated on the Y axis. Clearly it is seen (Figure 3.20) that the behavior of the response is almost the same. However, the response is a bit slower than the X axis. So, it can be seen that the settling time (%98) of the Y axis is around 95.58 seconds. The control effort for Y axes is similar to the error graph as the graphs of X axis. The control effort figure shows (Figure 3.21) that the controller of each axis controls the position as it is expected. The form of the response' graph is overdamped. The error figure (Figure 3.22) of the Y position of the peak point is 1 degree.
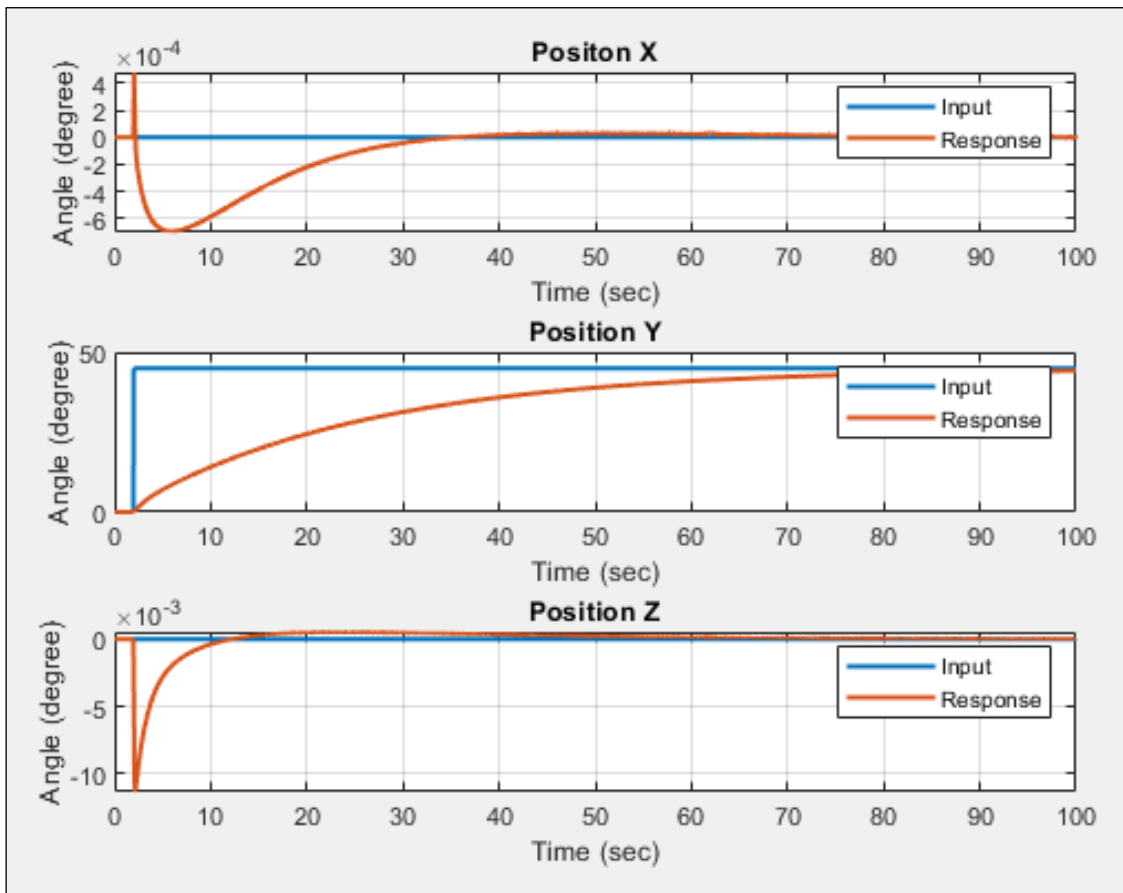
Figure 3.20 Step Input Position Y, 45º degrees (Y Axis)
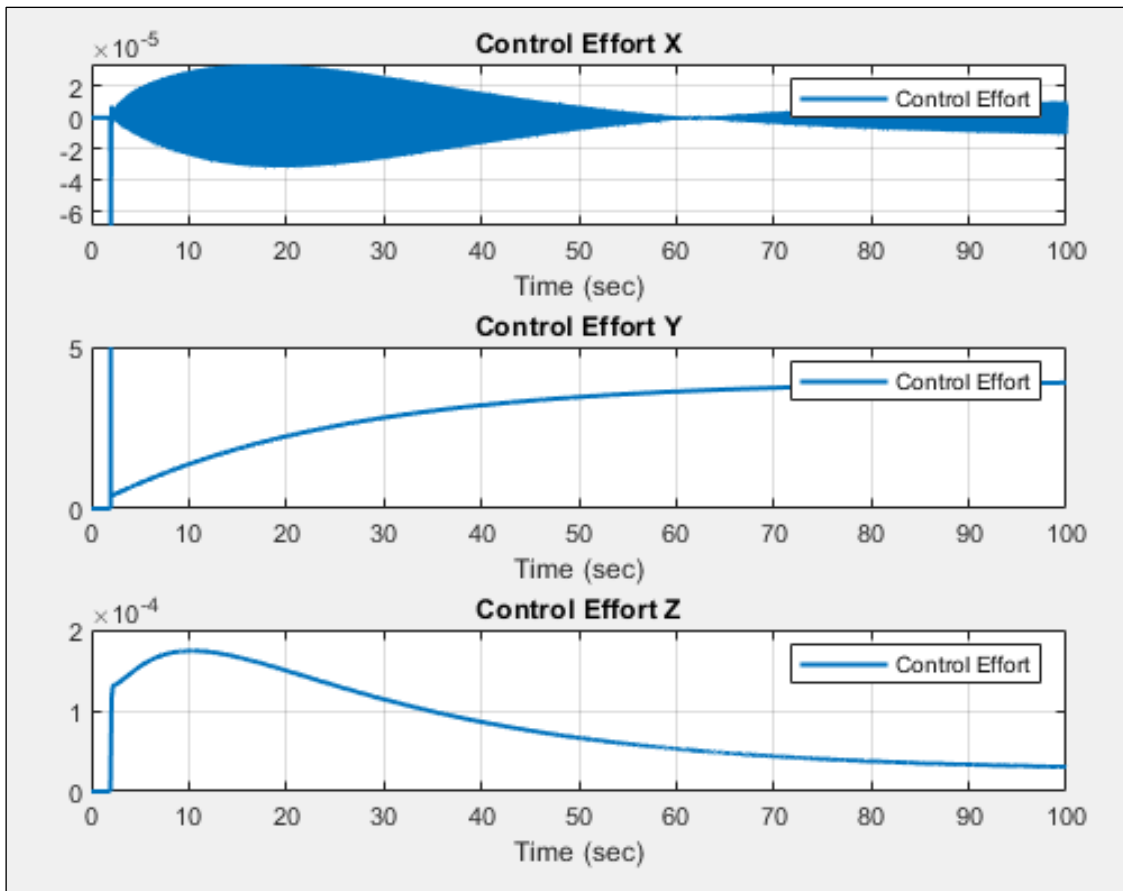
Figure 3.21 Control Effort for all axes, 45 degrees (Y Axis)
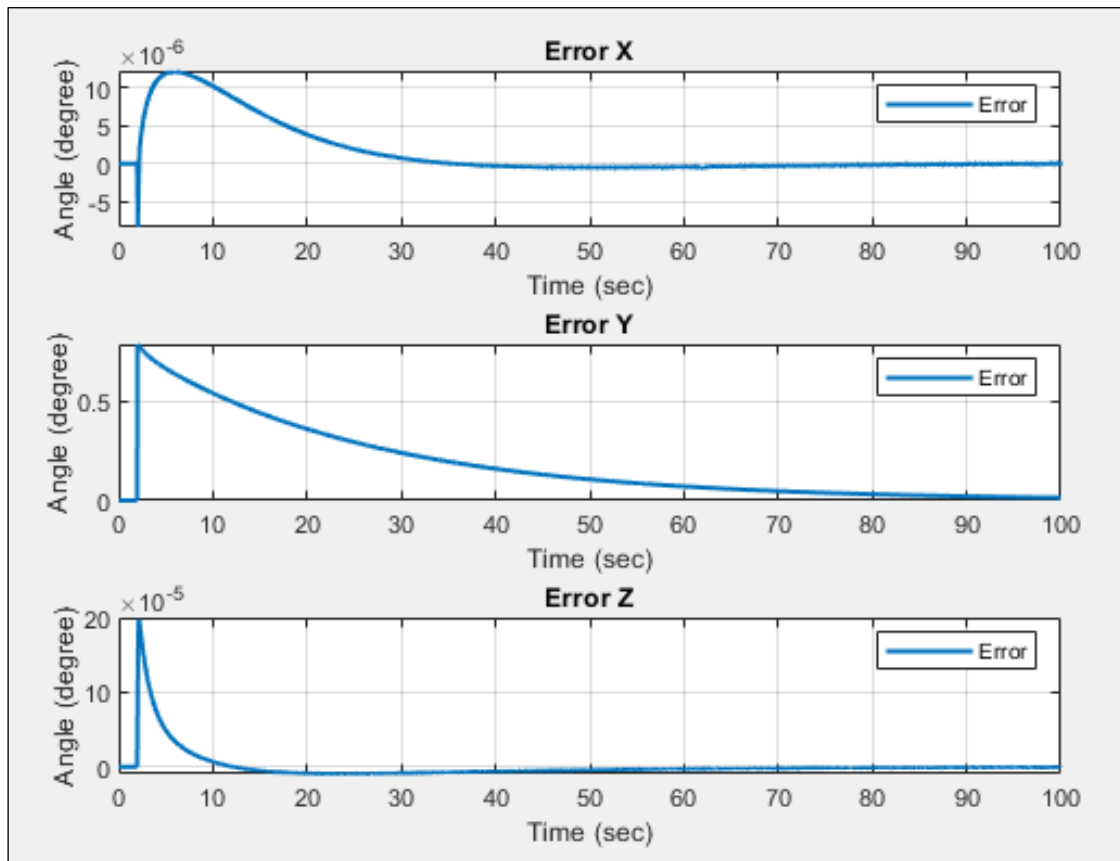
Figure 3.22 Errors 45º degrees (Y Axis)

The last simulation of 45º degrees is for the Z axis. There is a significant difference when it is compared with the other axis. While the Z axis is rotated, the X and Y axis are affected slightly. The other simulation is about 45º degrees, while the one is rotated, the others are kept the position as zero. In this simulation the X and Y axes reach around 0.02º degrees. The X axis is returned to the initial position, but the Y axis is settled around 0.02º degrees. The form of the response' graph is critically damped.

The settling time (%98) of the Z axis is 25.612 seconds. Clearly, it seems that the rotation of the Z axis is faster than the others. The control effort of Z axis efforts to fix the position error. The control effort of the other axis is almost zero.

Figure 3.23 Step Input Position Z, 45º degrees (Z Axis)
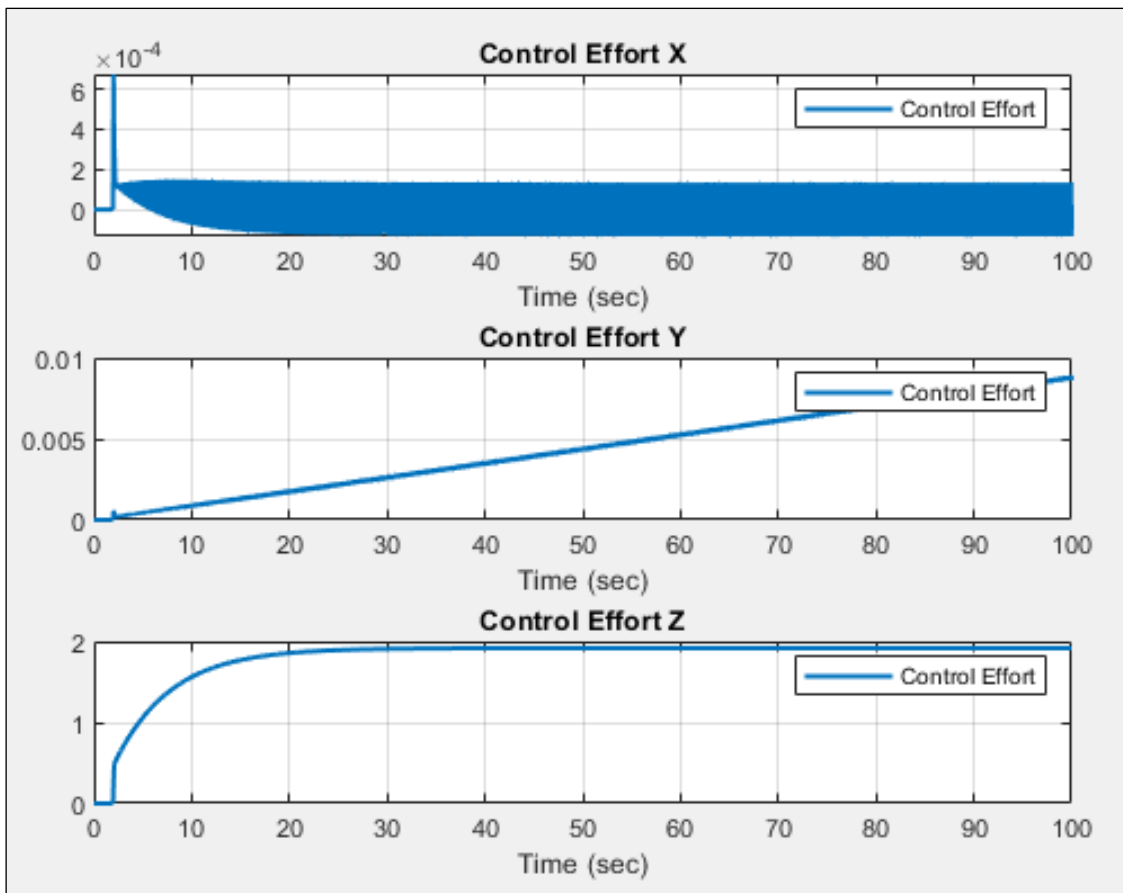
Figure 3.24 Control Effort for all axes, 45 degrees (Z Axis)
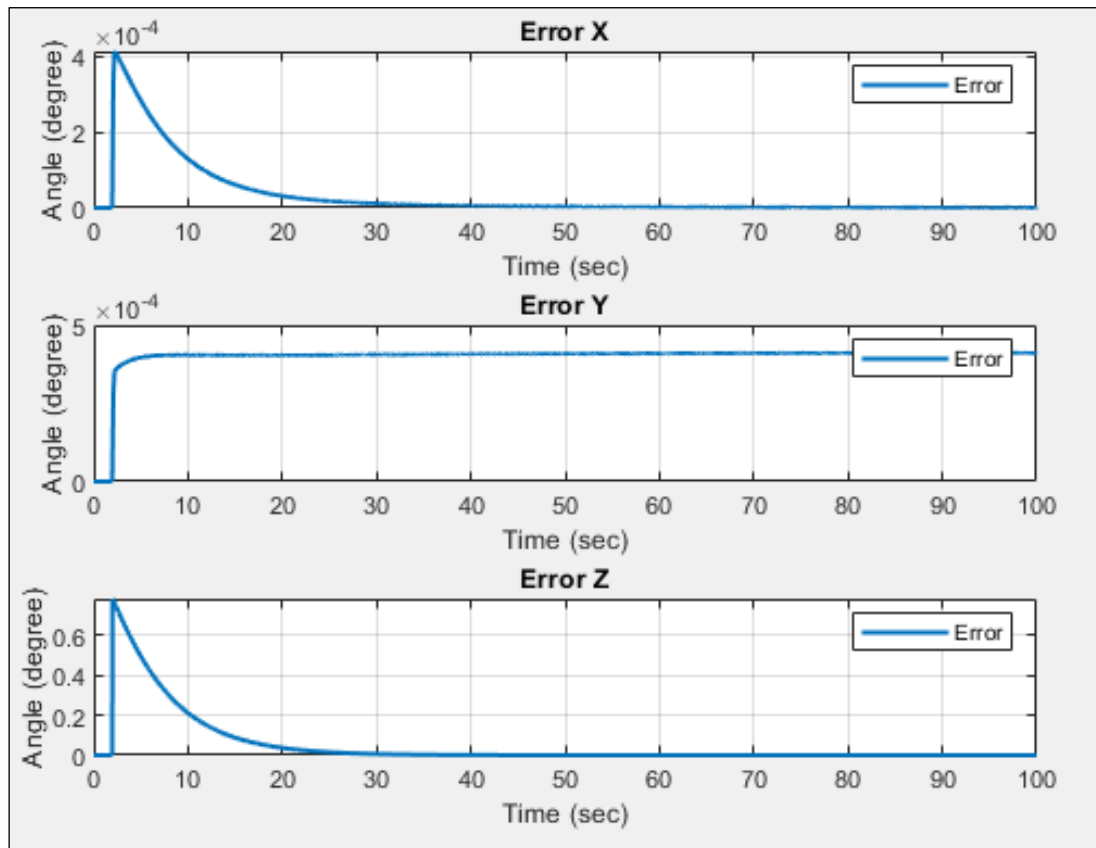
Figure 3.25 Errors 45º degrees (Z Axis)

The below figures (Figure 3.26, Figure 3.27 and Figure 3.28) show that the responses of all axes correspond to the negative angle input. All responses are the same as the positive reference input.
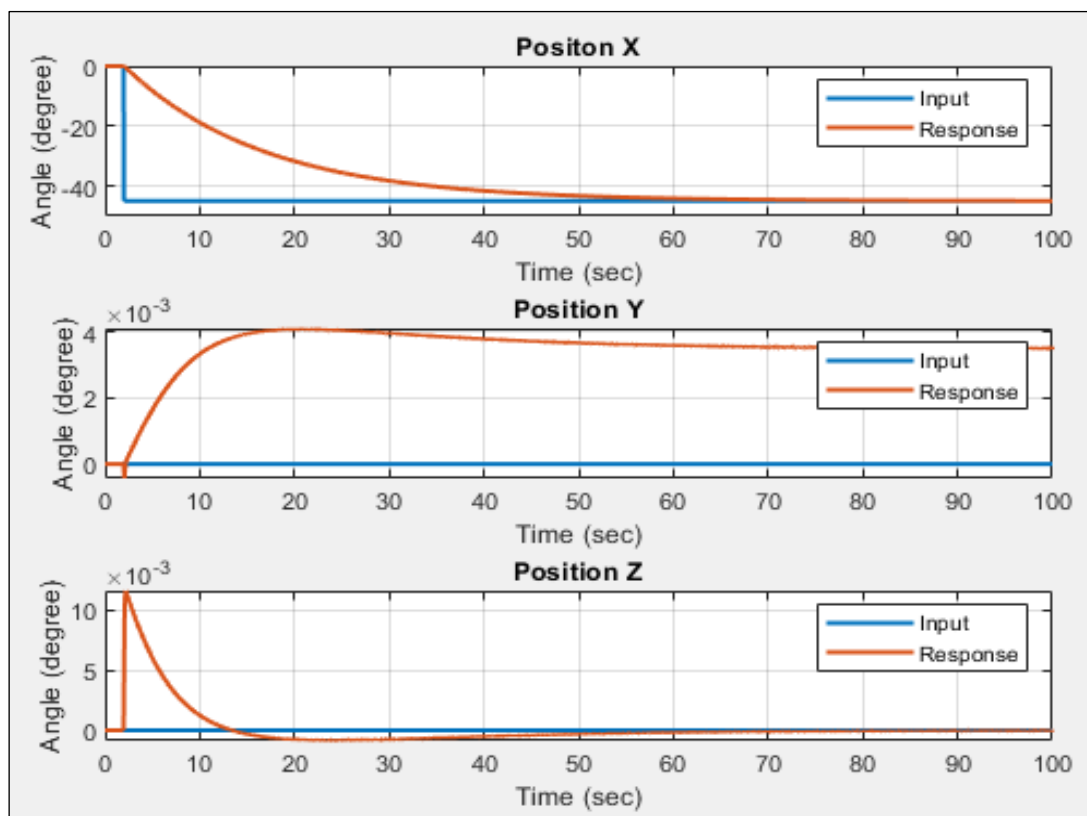
Figure 3.26 Step Input Position Y, -45º degrees (X Axis)
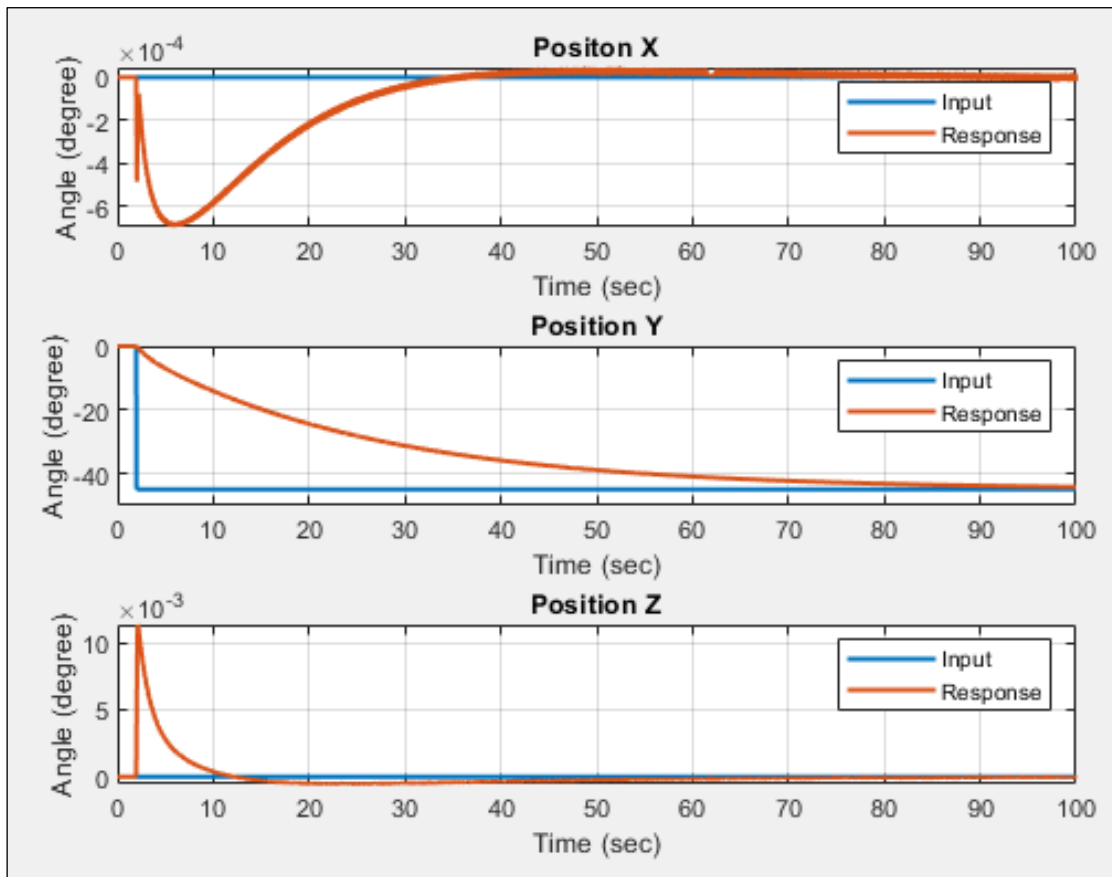
Figure 3.27 Step Input Position Y, -45º degrees (Y Axis)
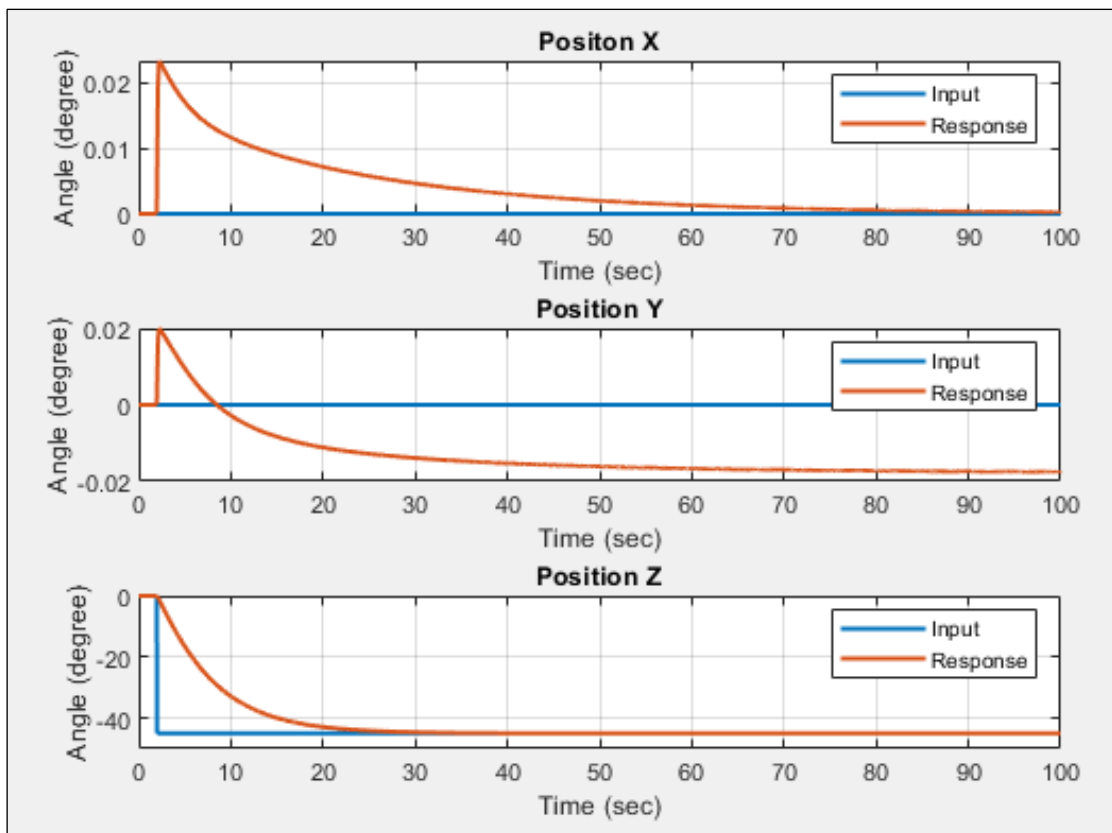
Figure 3.28 Step Input Position Y, -45º degrees (Z Axis)

3.2.4.2. Step Input 60º degrees

The input of 45º degrees results are satisfied to simulate the bigger angle. In this chapter 60º degrees is simulated for the model.

The below figures (Figure 3.29, Figure 3.30 and Figure 3.31) show that the simulation results of 60º degrees for the X axis.
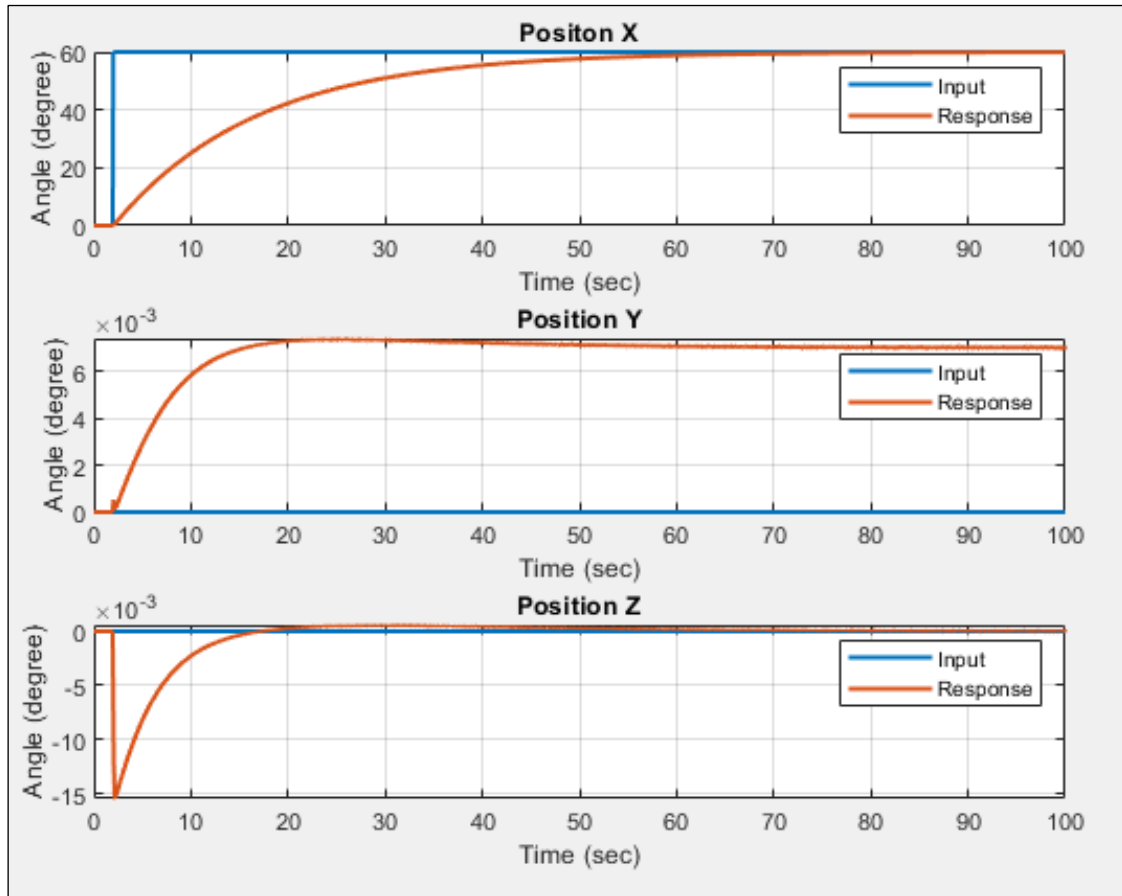
Figure 3.29 Step Input Position X, 60º degrees (X Axis)

As it is seen that the result of X position is about 60 degrees, the response is reached in the same time as 45º degrees. Clearly, the response of the system demonstrates the same behavior as 45º degrees.

The settling time for 60º degrees is 60.482 seconds. The control effort fixes the error as it is expected. The other angle positions are stable in zero as demonstrated in the figure (Figure 3.29). The error of the X axis is fluctuated between 0 and 1. The error is acceptable for controlling the system.

The figure (Figure 3.32) shows rotation about the Y axis. The behavior of the system is the same as the previous simulation. The settling time (98%) of Y axis is around 95.58 seconds. The other axis keeps the position in zero as it is expected. In the figure (Figure 3.33) the control effort of X and Y are zero because the position is not changed.

Lastly, while the axis Z is rotated, the position of X and Y axis changes significantly. In the figure (Figure 3.35) shows that the controllers correct to the position error and the two positions are backed in zero.

Figure 3.30 Control Effort for all axes, 60º degrees (X Axis)


Figure 3.31 Errors 45º degrees (X Axis)

Figure 3.32 Step Input Position Y, 60º degrees (Y Axis)

Figure 3.33 Control Effort for all axes, 60º degrees (Y Axis)

Figure 3.34 Errors 60º degrees (Y Axis)
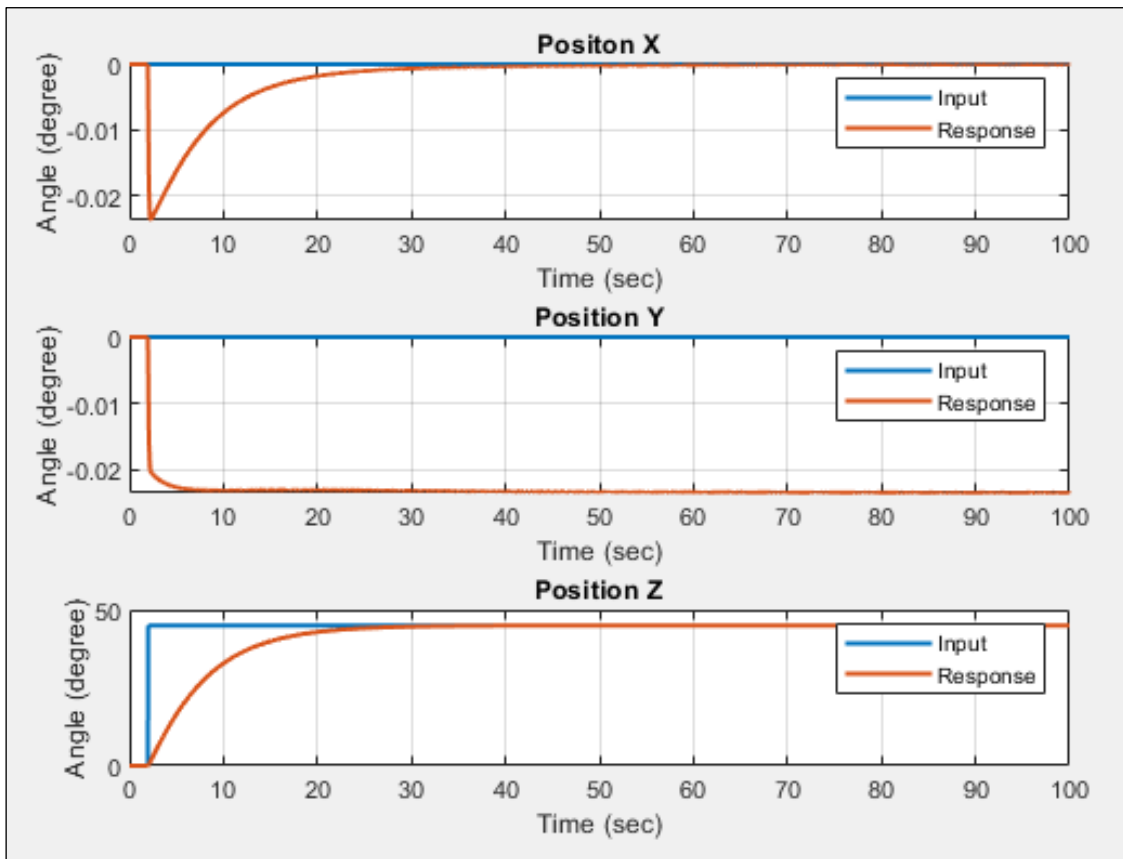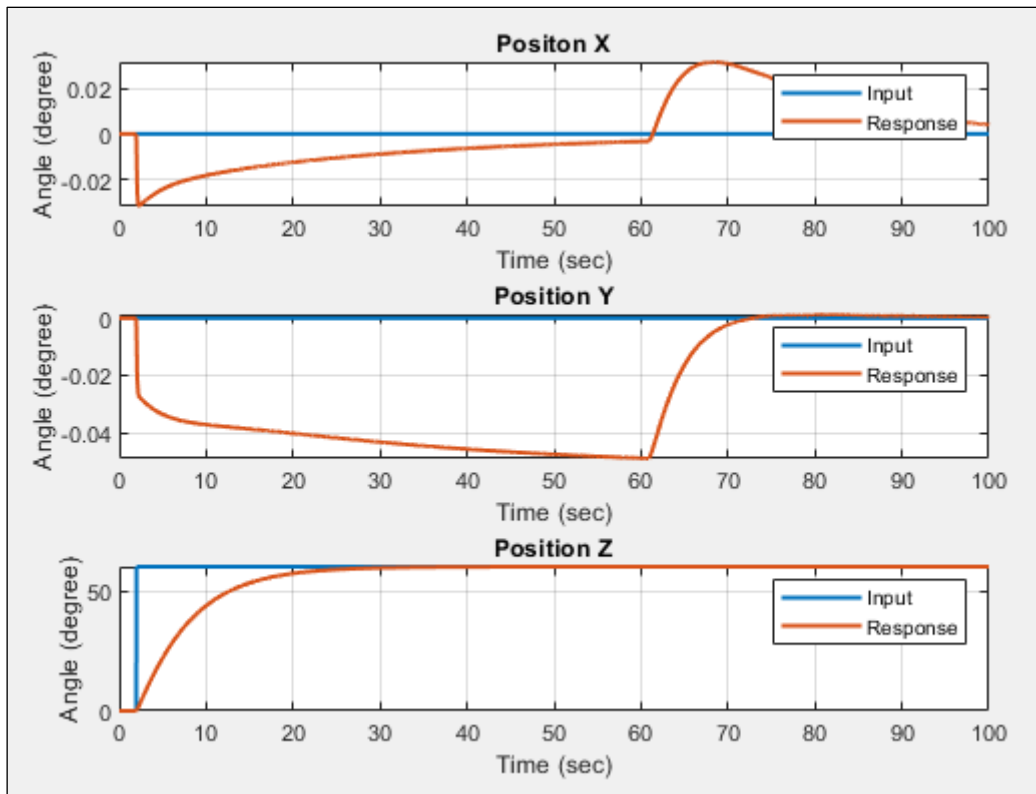

Figure 3.35 Step Input Position Z, 60º degrees (Z Axis)
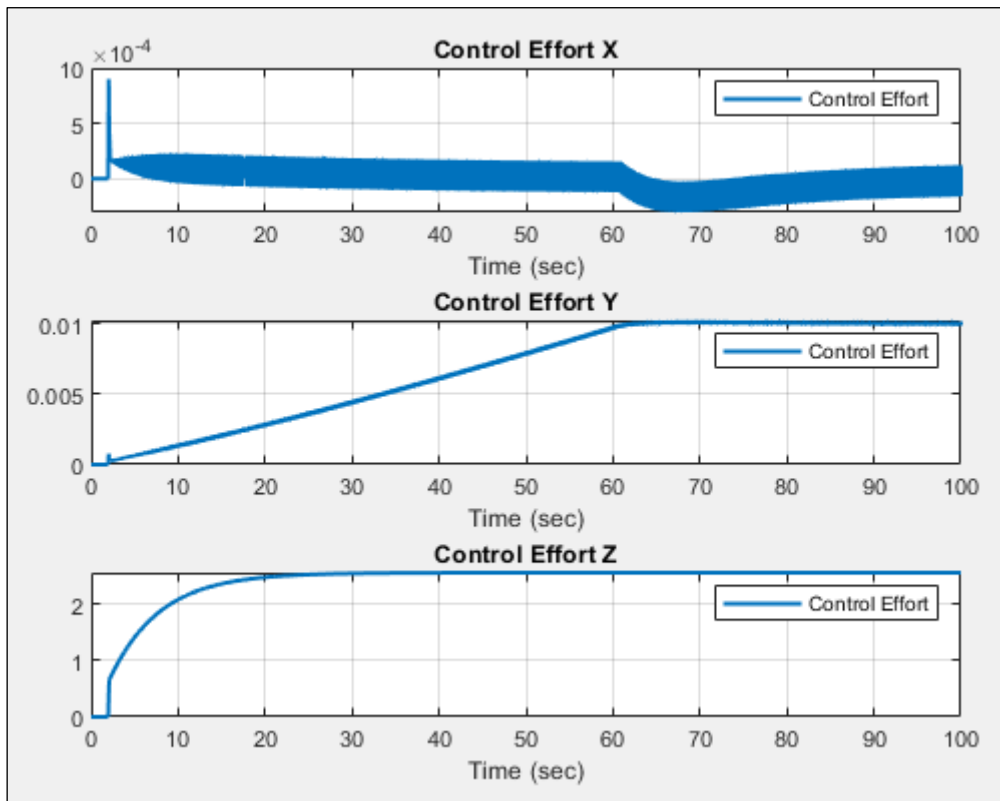
Figure 3.36 Control Effort for all axes, 60º degrees (Z Axis)
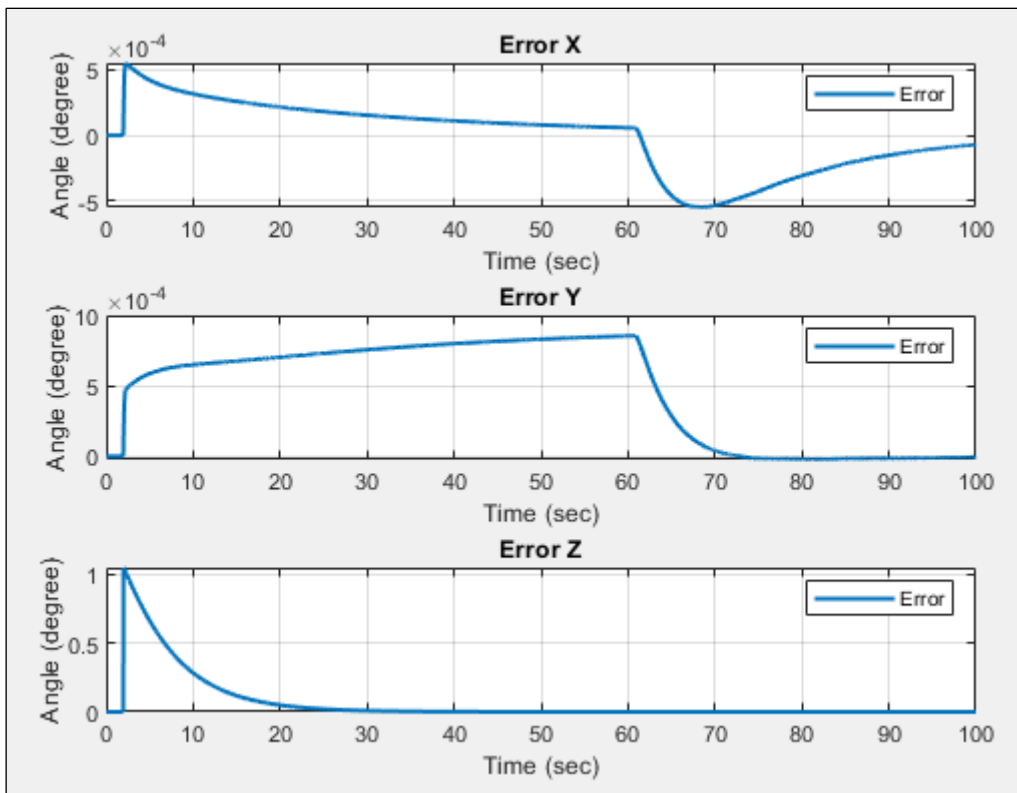
Figure 3.37 Errors 60º degrees (Z Axis)

3.2.4.3. Step Input 75º degrees

The last reference input is 75º degrees. It is the big reference angle for the simulation. The figures (Figure 3.38, Figure 3.39 and Figure 3.40) show the result of the rotation around the X axis. The settling time is the same as the previous simulation. The control effort and the error figures show similar responses.

The result of the Y axis (Figure 3.41,Figure 3.42 and Figure 3.43) gives the same response as the previous simulation. The control effort of X and Z axes are zero while the Y axis rotates. The error peak point is 1º degree.
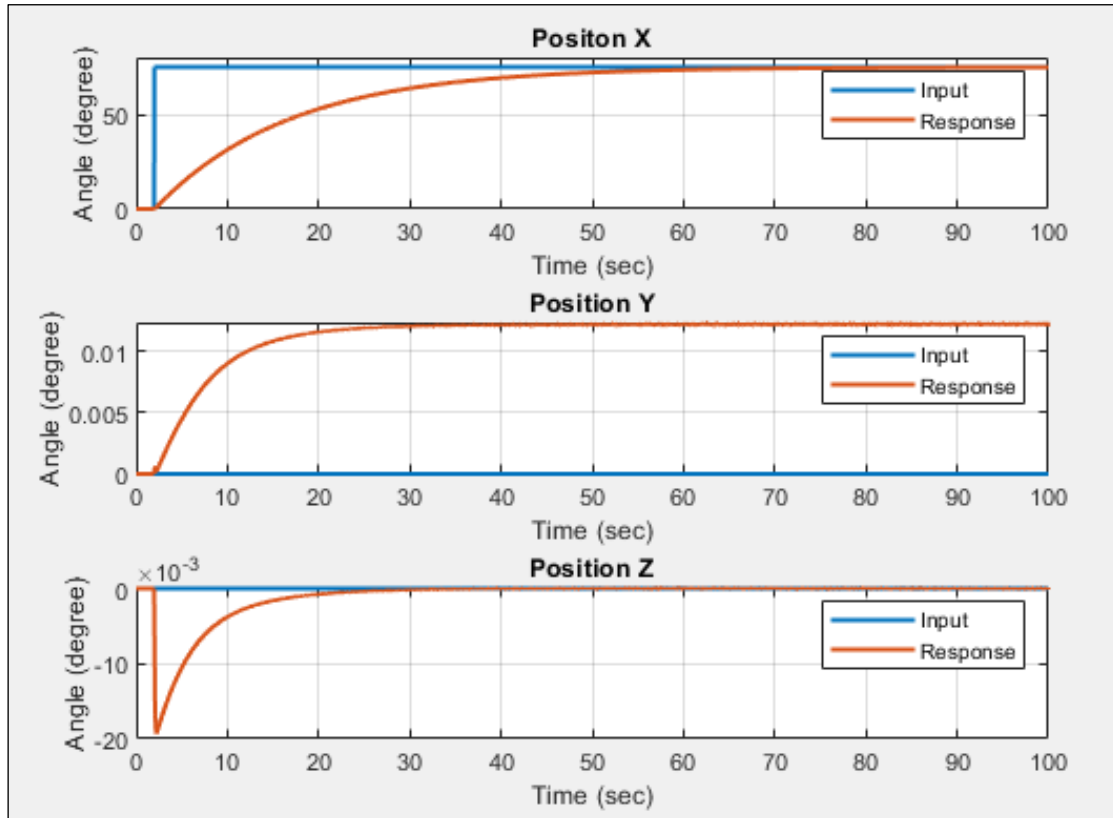
Figure 3.38 Step Input Position X, 75º degrees (X Axis)

The final simulation of the thesis is the Z axis for 75 degrees. The figures (Figure 3.44, Figure 3.45 and Figure 3.46) are represented the result of the Z axis. The significant effect is that while the Z axis rotates, the response of the X and Y positions have disturbances, but these effects are fixed by the controllers.
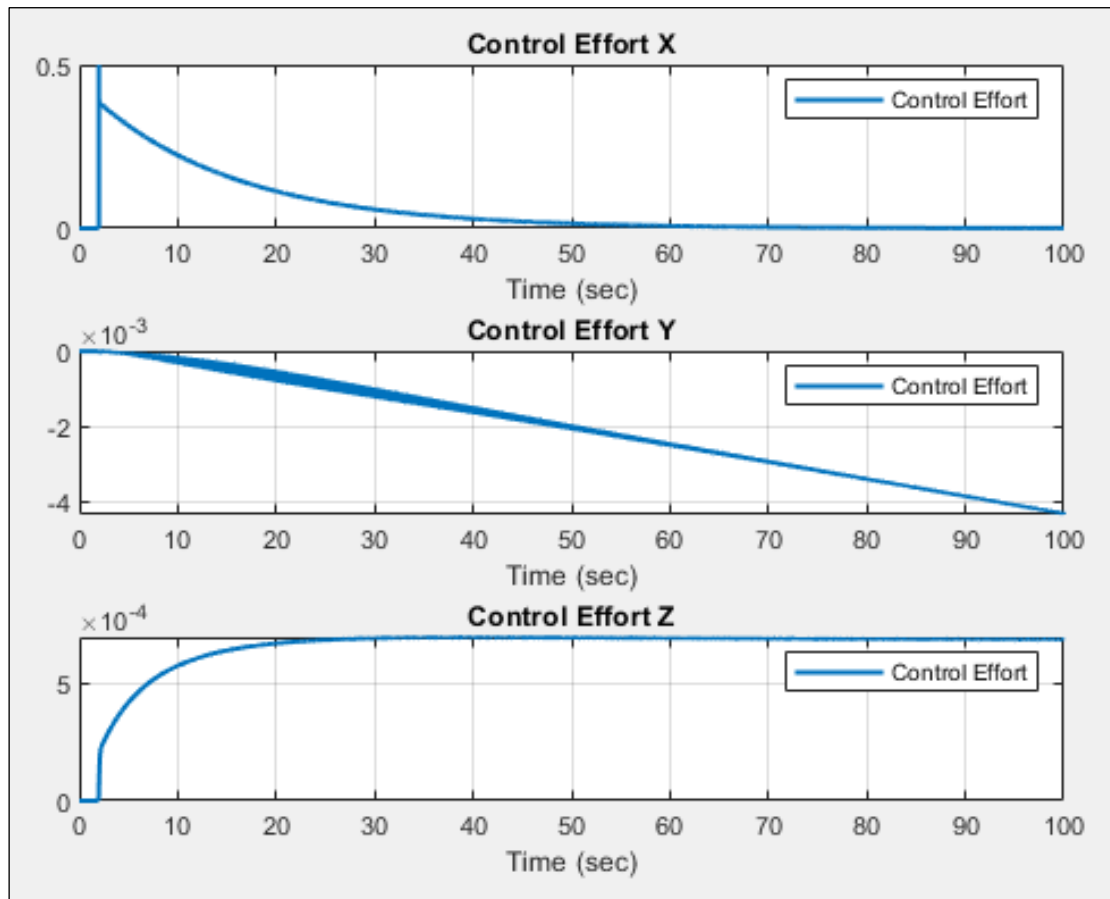
Figure 3.39 Control Effort for all axes, 75º degrees (X Axis)
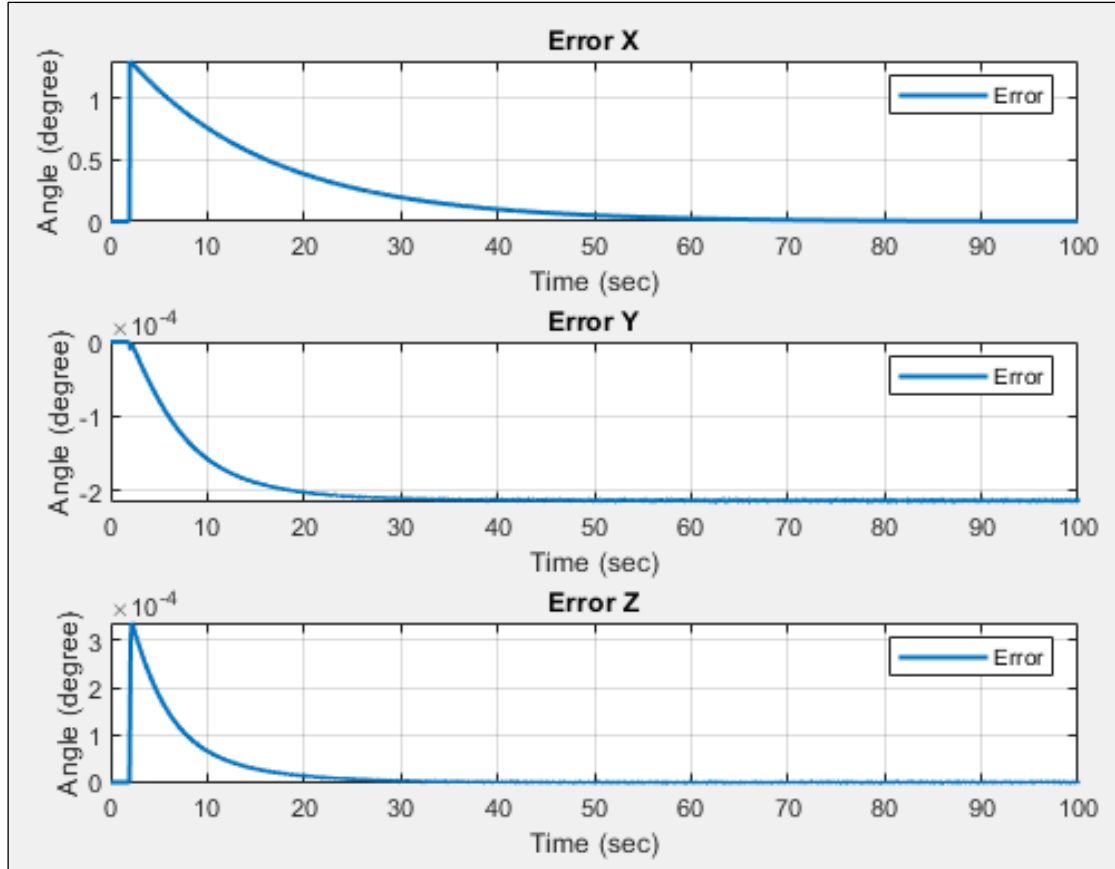
Figure 3.40 Errors 75º degrees (X Axis)
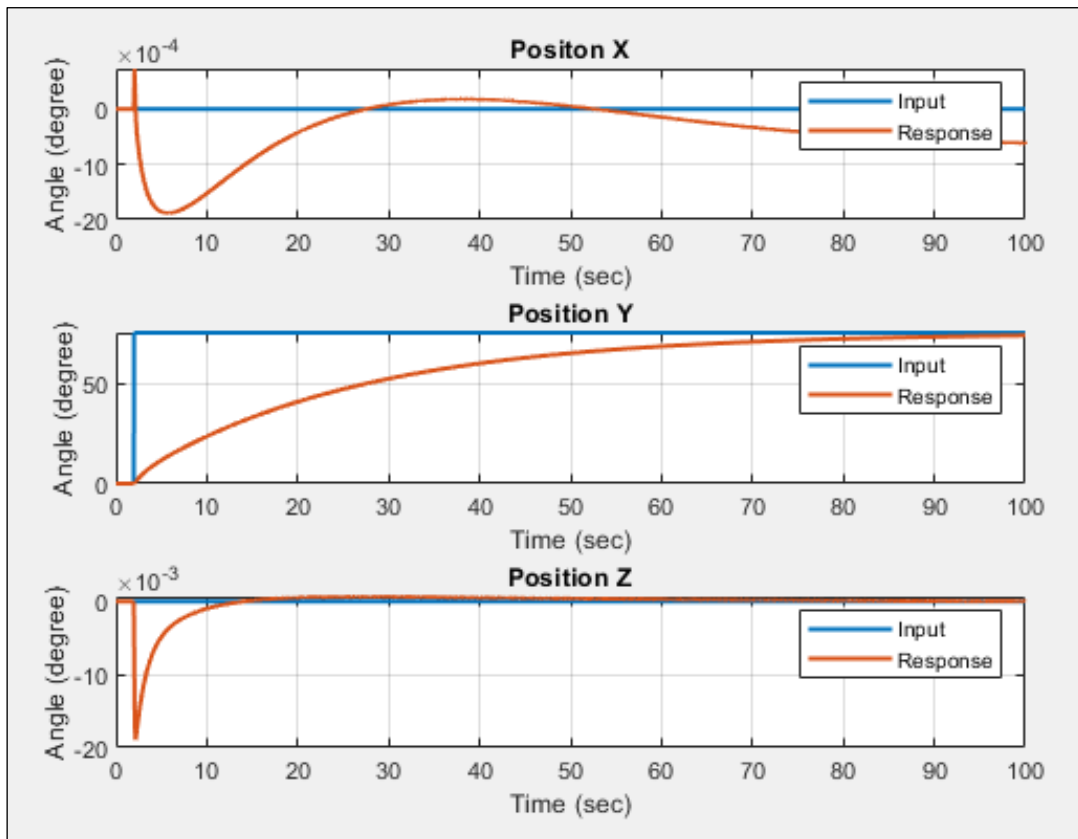
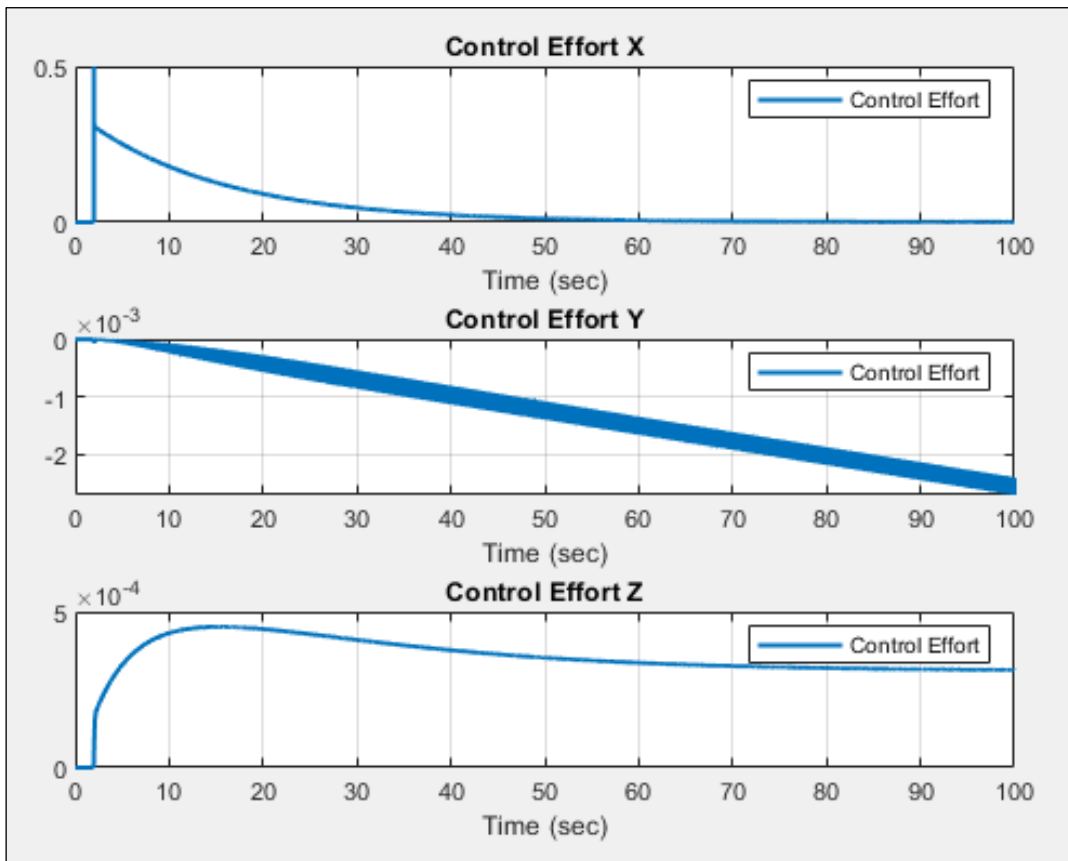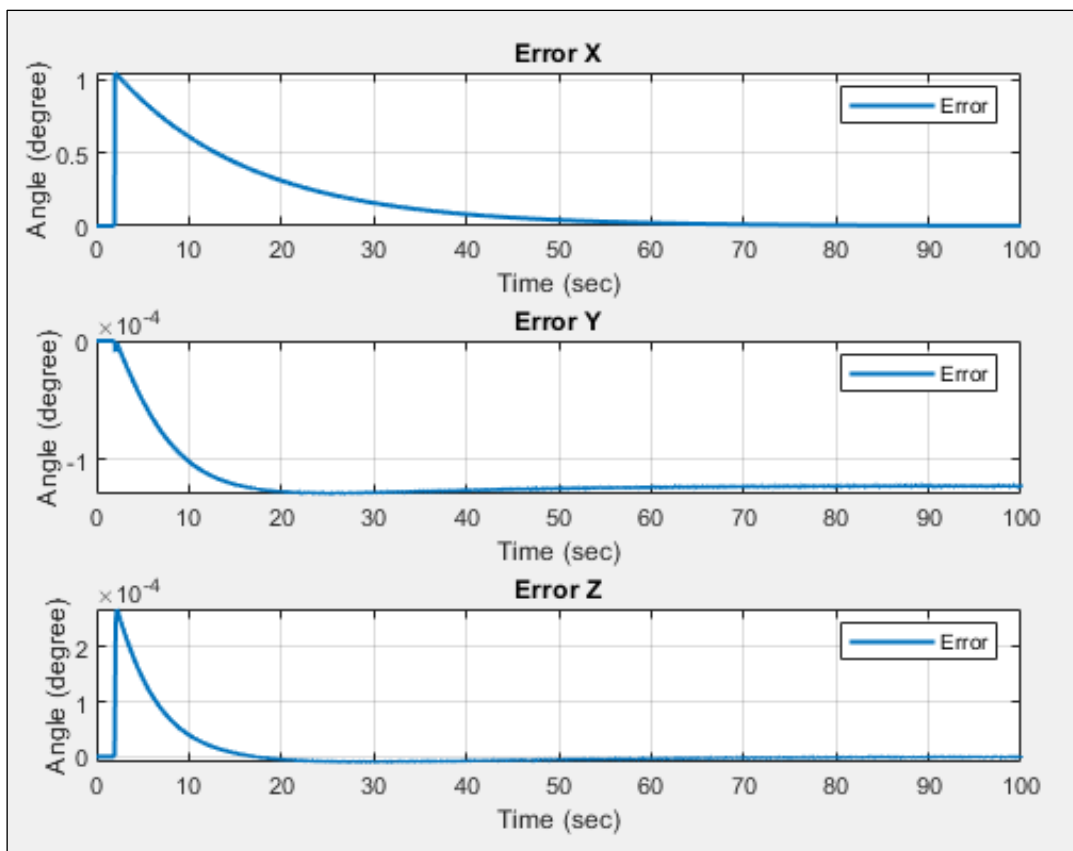Figure 3.41 Step Input Position Y, 75º degrees (Y Axis)
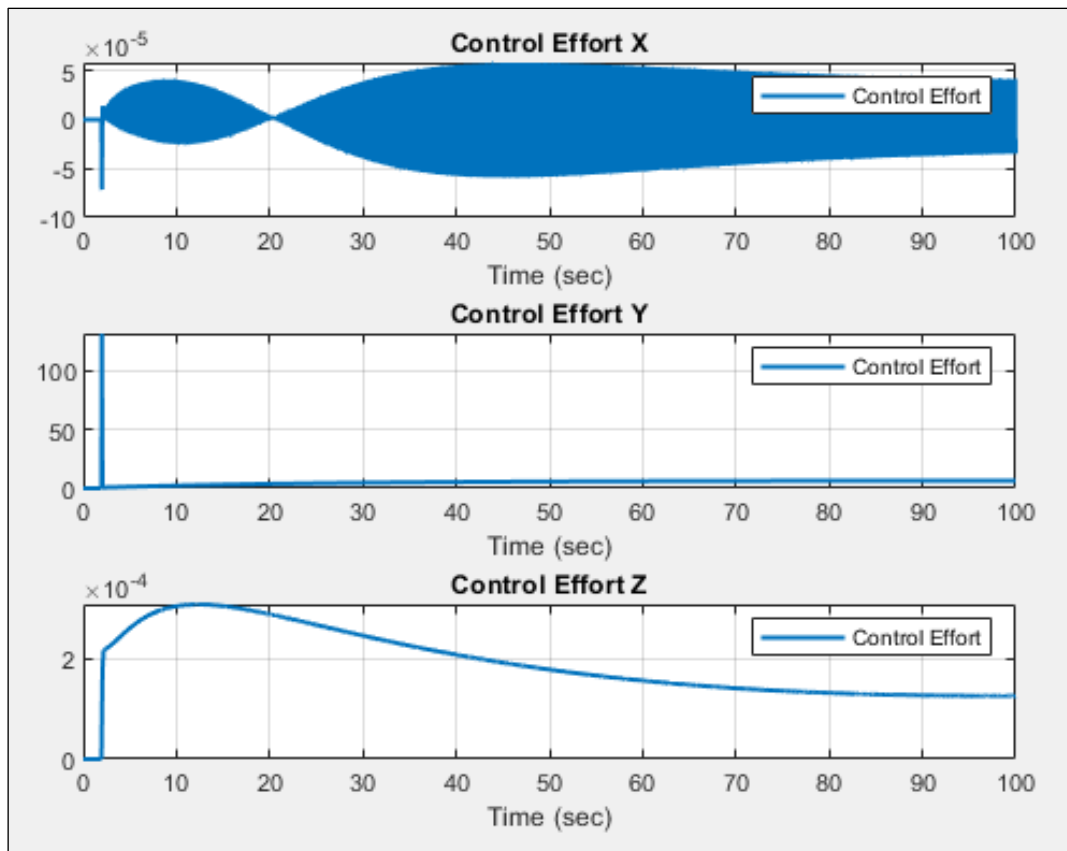
Figure 3.42 Control Effort for all axes, 75º degrees (Y Axis)

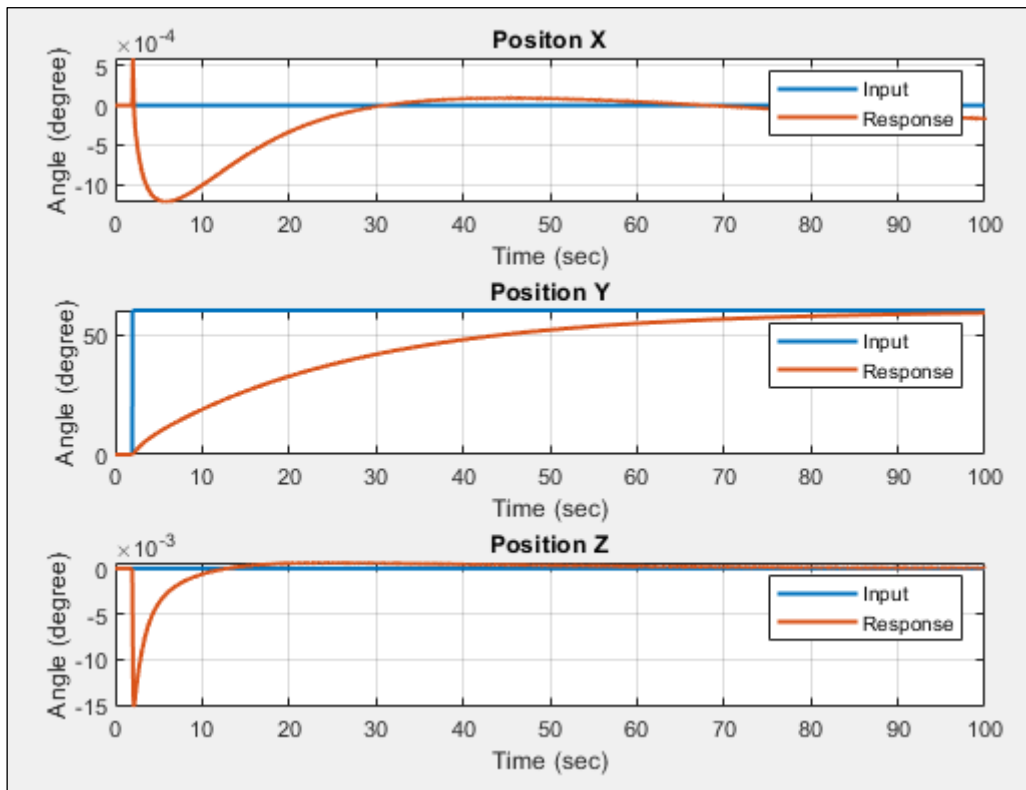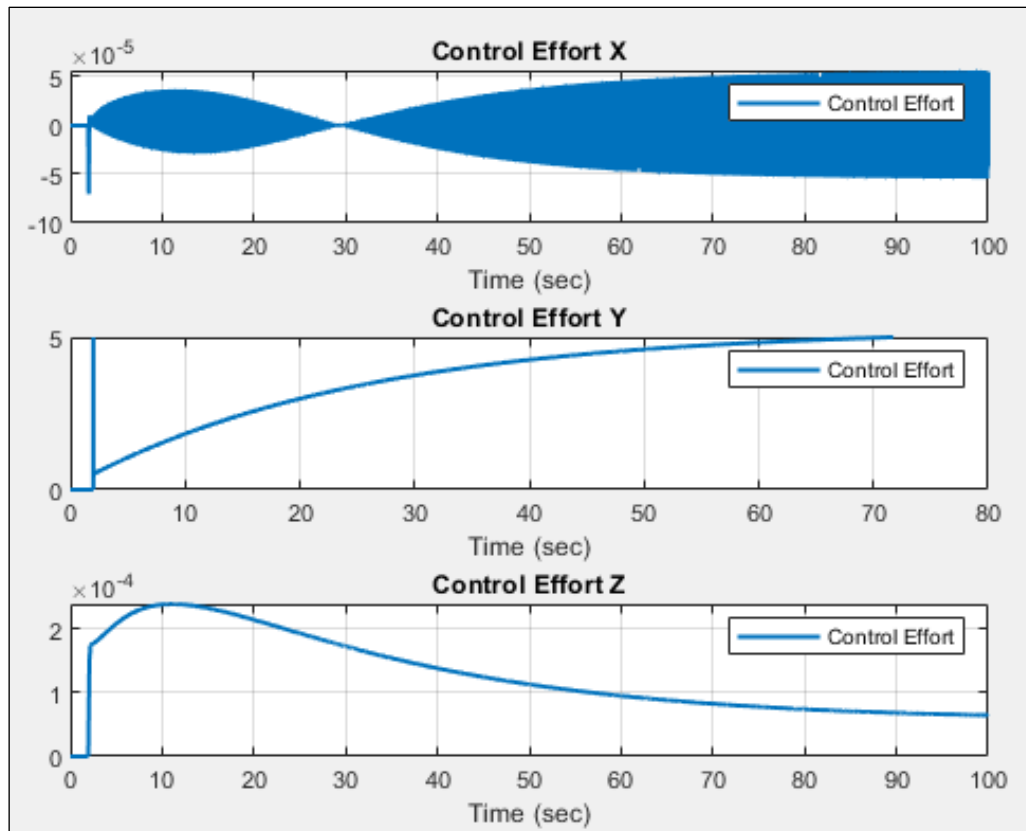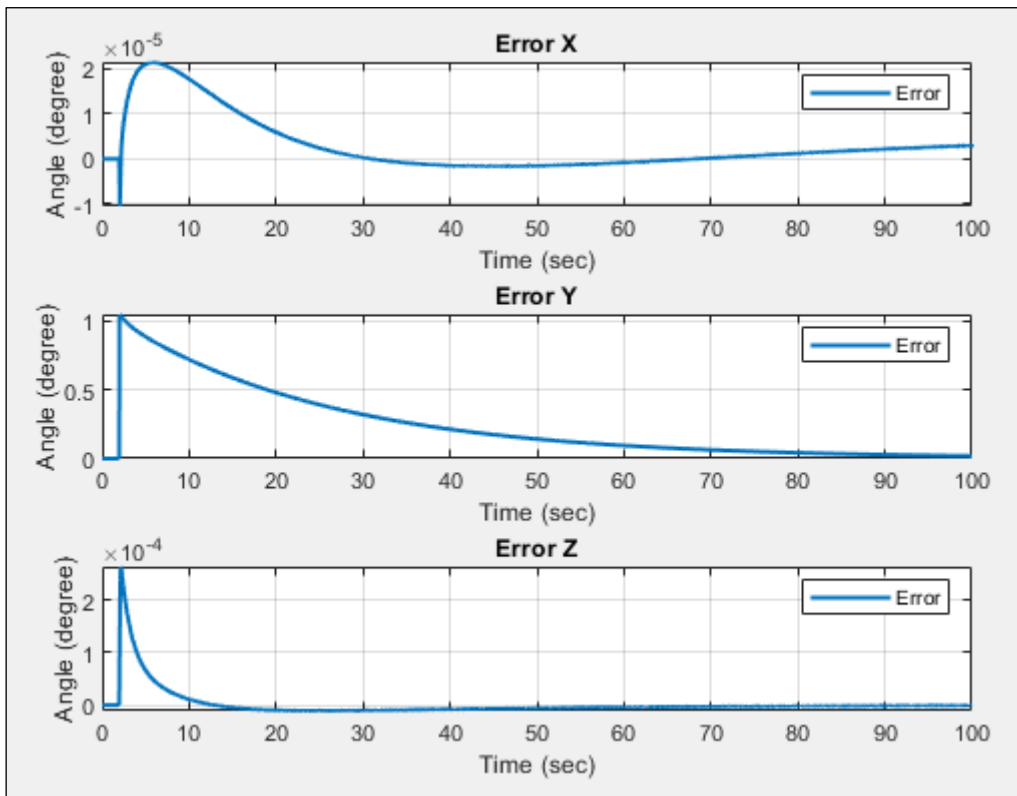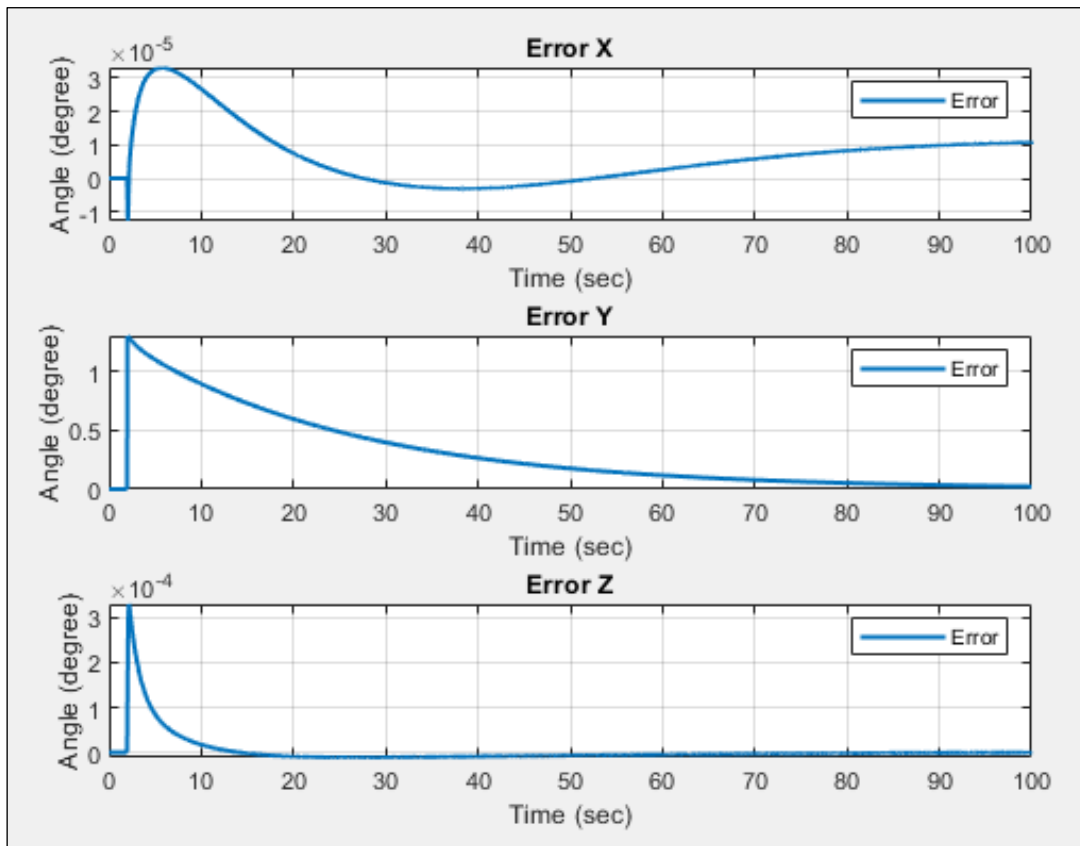Figure 3.43 Errors 75º degrees (Y Axis)
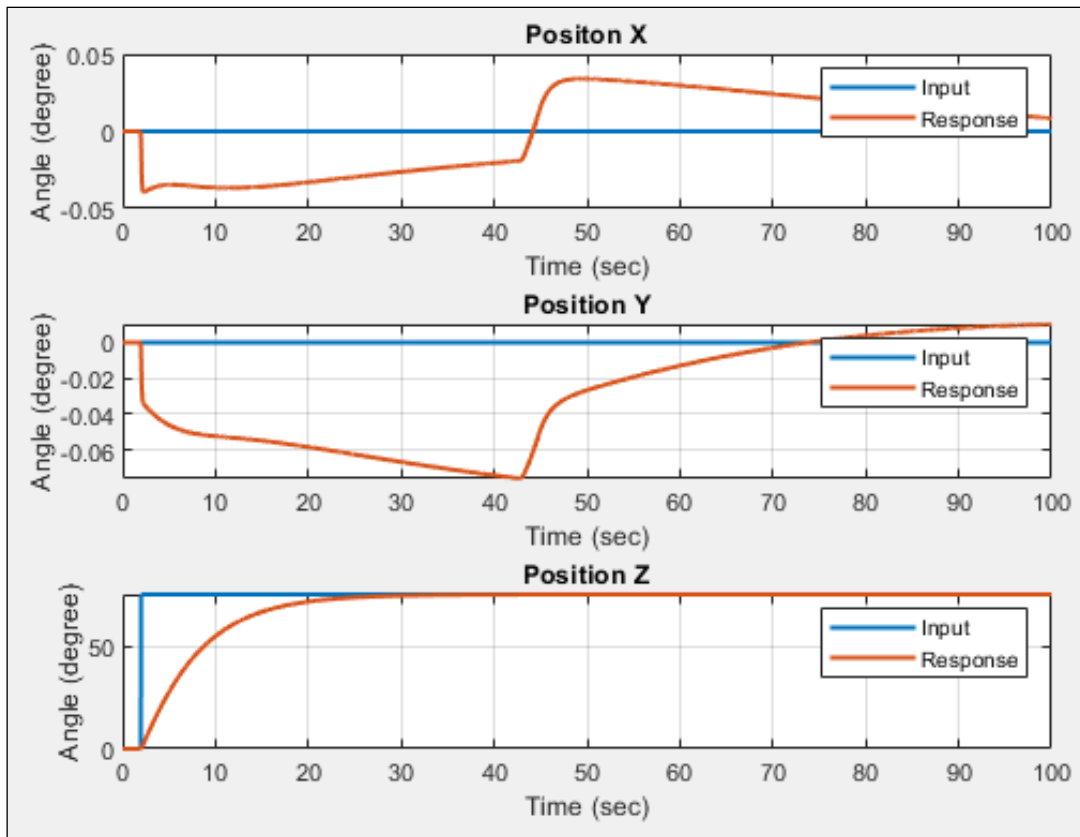
Figure 3.44 Step Input Position Z, 75º degrees (Z Axis)
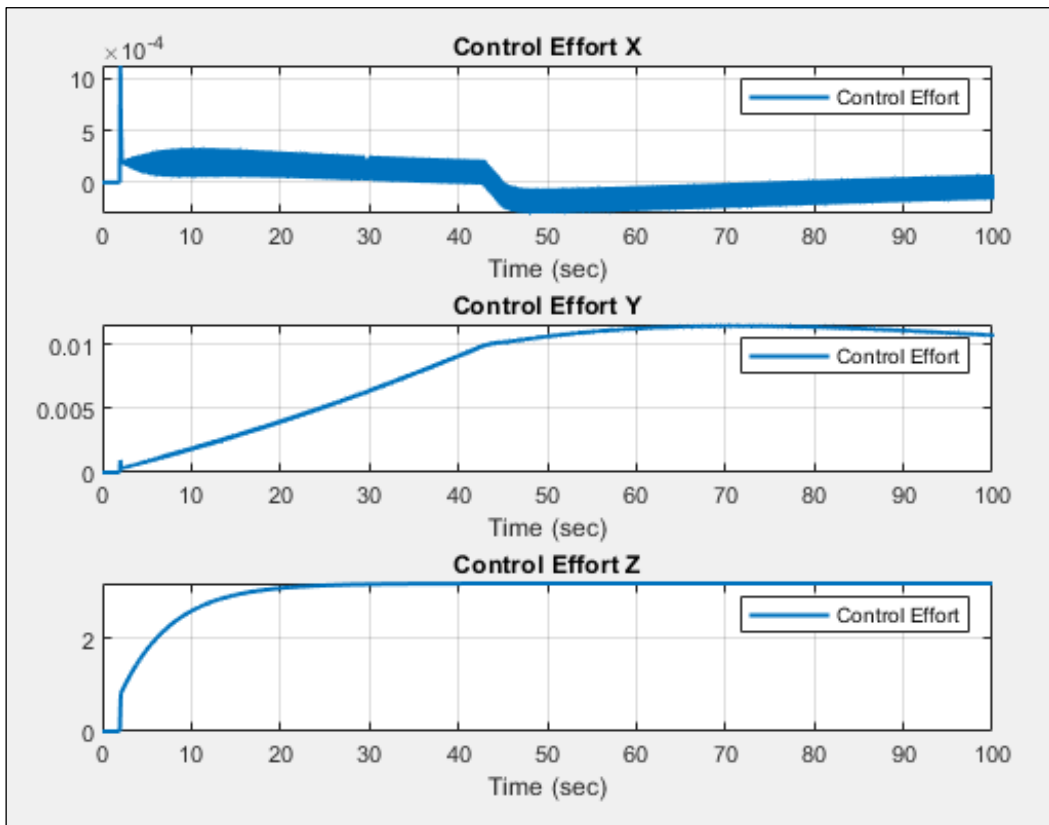
Figure 3.45 Control Effort for all axes, 75º degrees (Z Axis)
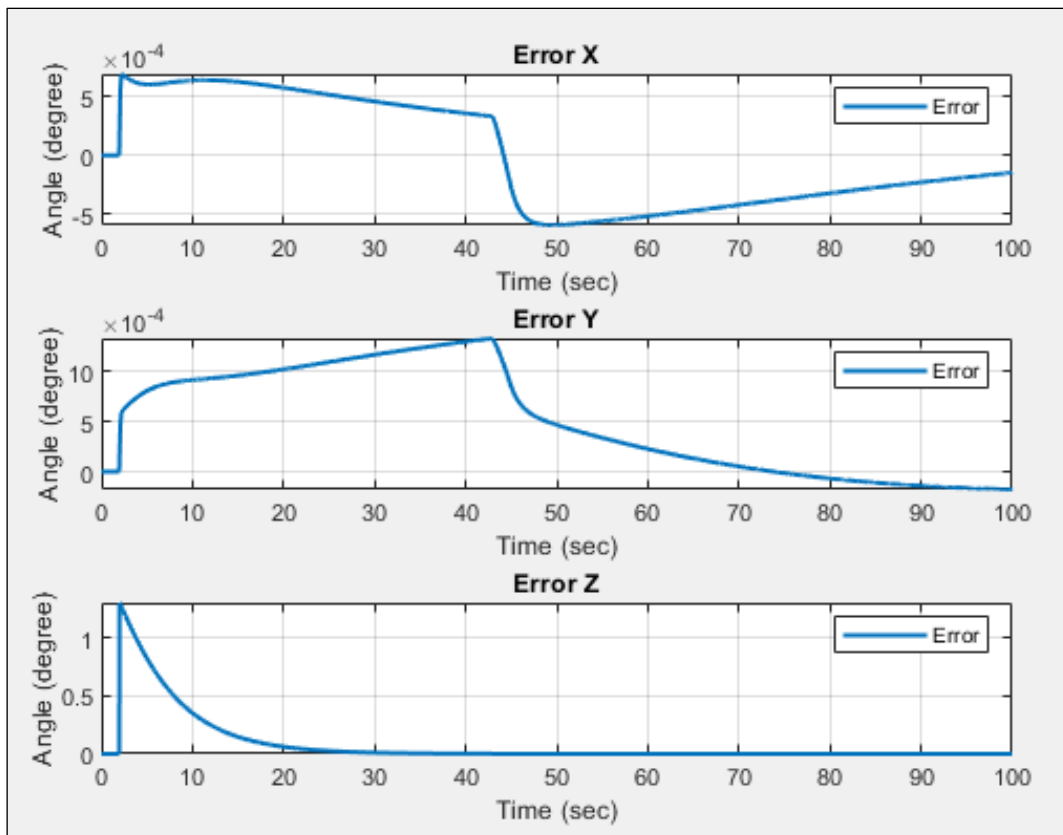
Figure 3.46 Errors 75º degrees (Z Axis)

3.2.4.4. Comparison the Results

All results of simulations with Simscape are acceptable for development of control algorithms. It is known that being stable is a vital feature for the pointing or orbiting process. For this reason, obtaining settling time is necessary part of the knowing behavior of the systems. The below table shows the settling time with different angles for each axis.

Settling Times (seconds)			
Axes	**45º degrees**	**60º degrees**	**75º degrees**
X	60.482	60.482	60.482
Y	95.58	95.58	95.58
Z	25.612	25.612	25.612

Table 6 Settling Times

As it is observed, the settling time is the same for each axis even at different reference angles. The importance of knowing these times does not make a request for another axis without completing the other rotation.

3.2.4.5. Rotation Around All Axes in the Same Simulation

After the completion of the simulation for each axis, the next process is rotation of all axes in the same simulation. For doing that the previous chapter is calculated the settling time for all axes. It is important to obtain the settling time due to the balance of the system. The step inputs of the time set are 2 seconds, 30 seconds and 130 seconds Z, Y and X, respectively.
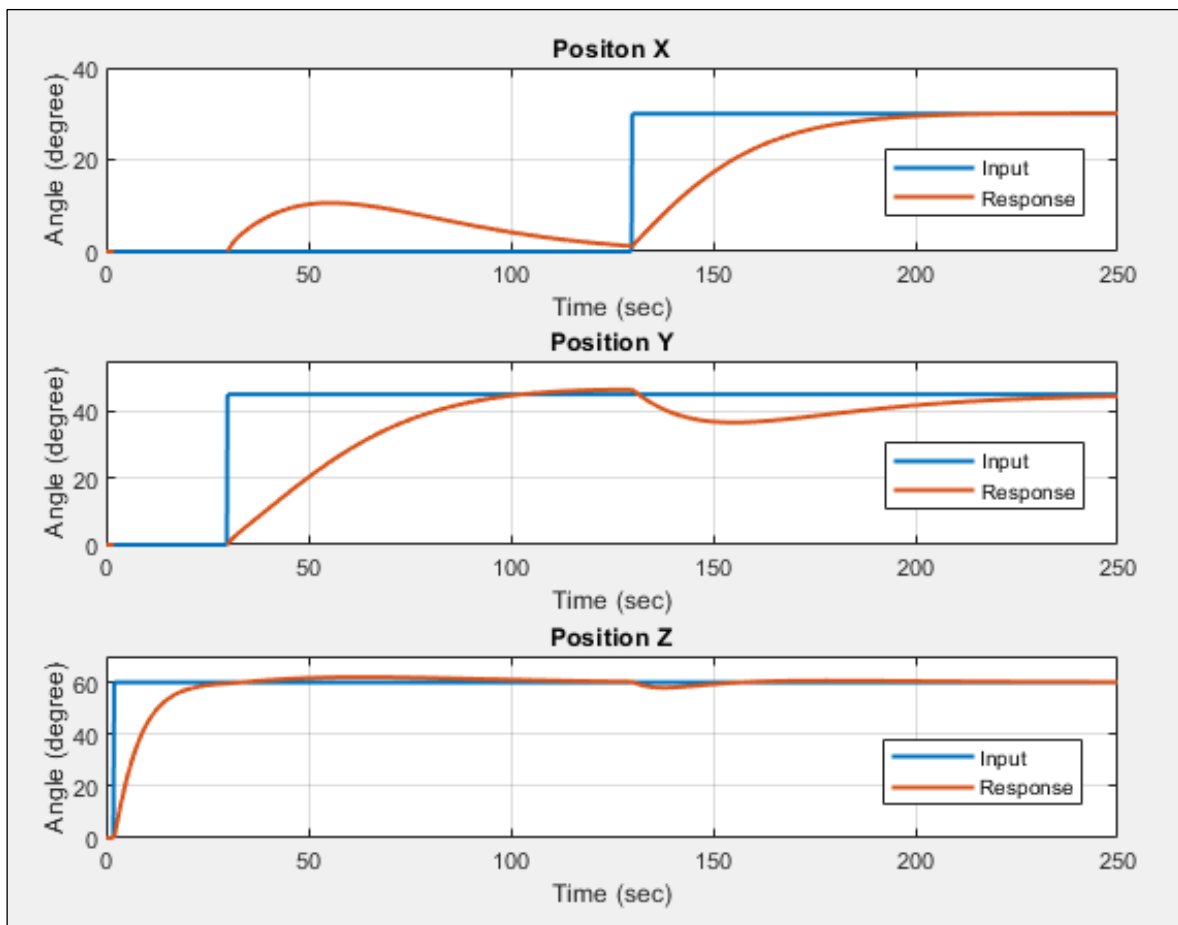
Figure 3.47 Rotation around all axes (X axis 30º degrees, Y axis 45º degrees, Z axis 60º degrees)

The above figure (Figure 3.47Figure 3.47) shows the effect between the axes. As it is seen, while the Z axis rotates, X and Y are unaffected. Then, the position of the X axis is affected because the Y axis starts to rotate. The X controller fixes this error around 130 seconds. After that point, the X axis begins to rotate, and the Y axis is affected significantly meantime the Z axis position slightly deviates from the reference point. The controller of Z corrects the deviation.
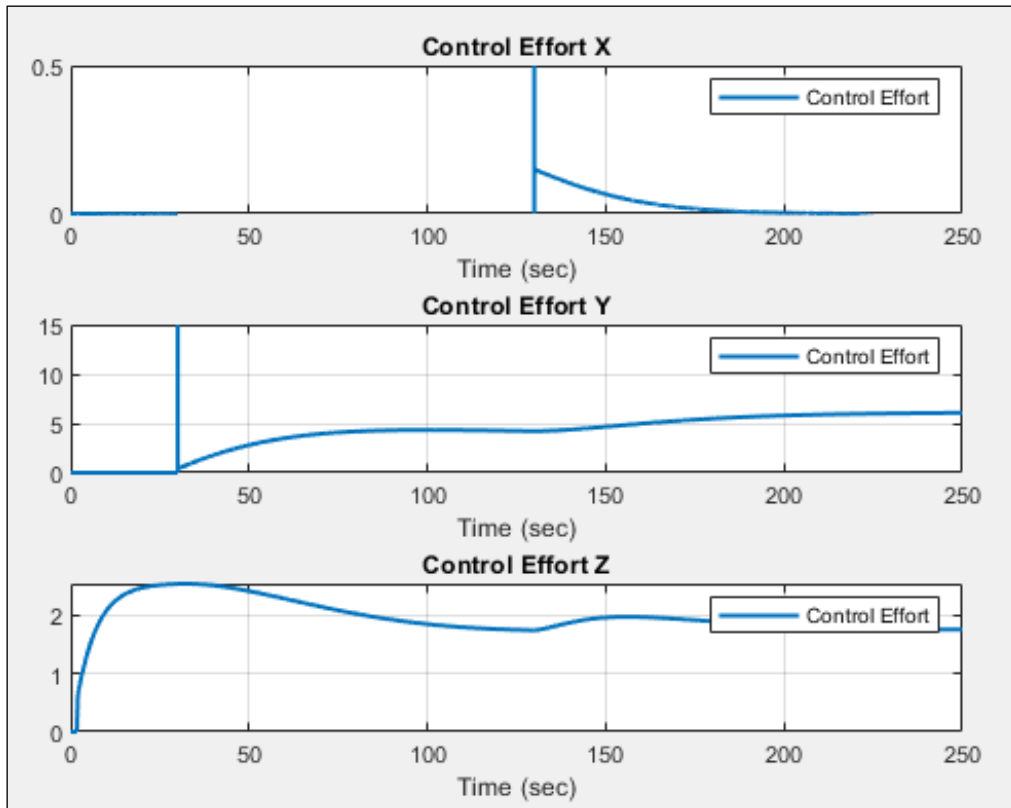
Figure 3.48 Control Effort for all axes (X axis 30º degrees, Y axis 45º degrees, Z axis 60º degrees)
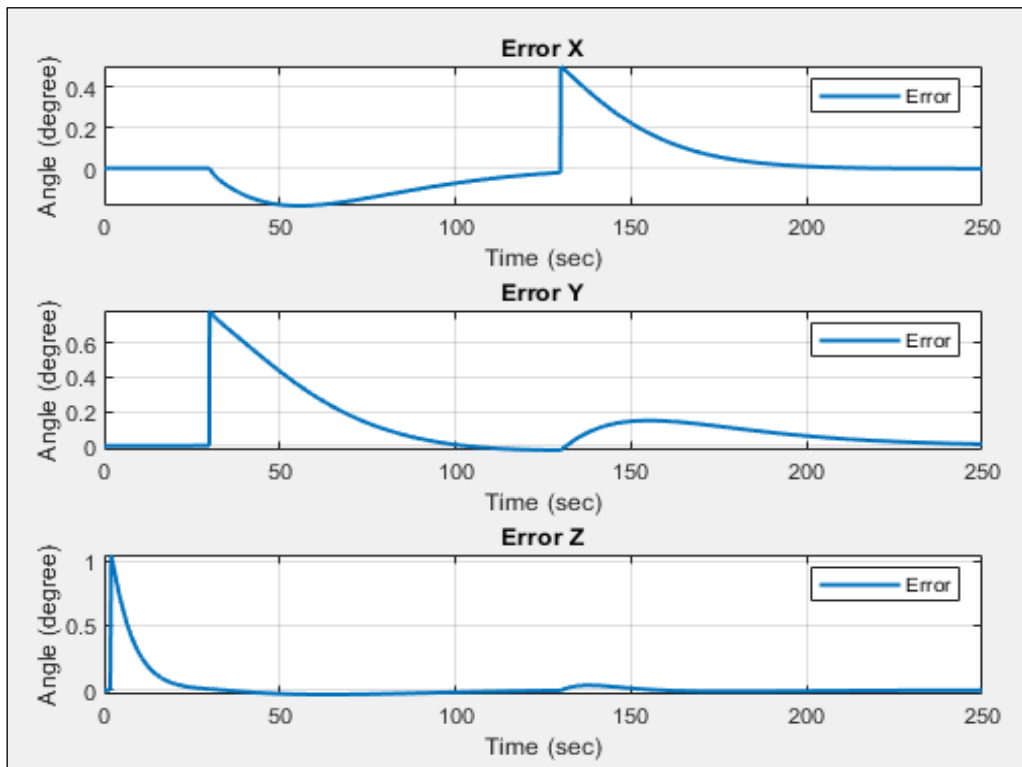
Figure 3.49 Errors (X axis 30º degrees, Y axis 45º degrees, Z axis 60º degrees)
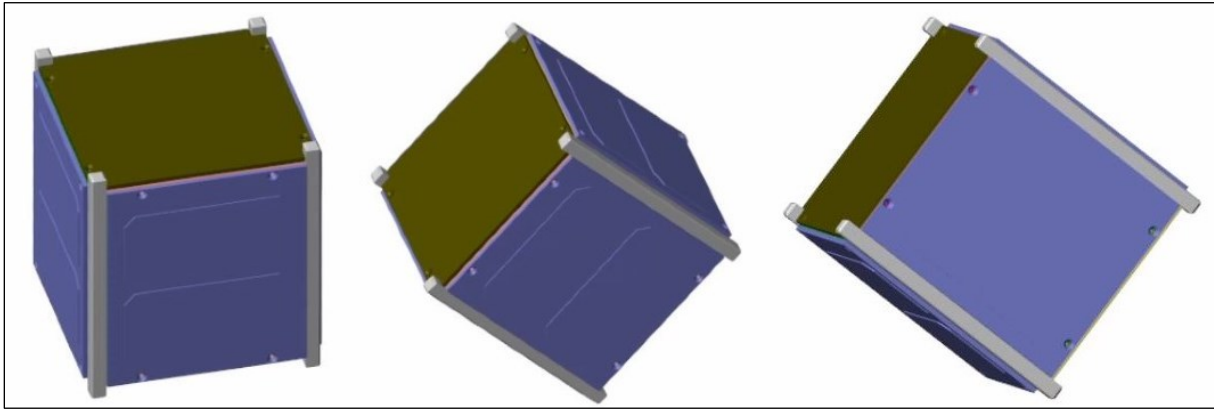
Figure 3.50 Z axis 60º degrees, Y axis 45º degrees and X axis 30º degrees respectively

The above figure (Figure 3.50) shows the simulation of 3D about the position of Z 60º degree, the position of Y 45º degrees and the position of X 30º degrees, respectively.

4. Implementation

Once the simulation part is finished, it is necessary to verify the simulation results through real implementation. The controlling of the Z axis is tested in the real world because of the complex nature of controlling 3 degrees of freedom. It knows that the gravitational effect is another problem of controls of X and Y axes.

These two reasons make the problem more complex and difficult. The controlling of the gravitational effect needs different mechanical components for development of control algorithms for all axes.

Finally, the Z axis was chosen for controlling with Simulink (Hardware in the Loop). Neglecting the gravitational effect is the strategy of the implementation during the controlling of the Z axis. Doing this, the gravitational effect does not affect the Z axis because of the assembly of mechanical design. The control algorithm is developed with Simulink.

4.1. Mechanical and Electronic Components

The main aim of the mechanical design is to know the angle of the mechanism between initial position and final position. The design concept is that there are 90 holes (Figure 4.1) above the cylinder. These 90 holes provide accuracy of 4 degrees. Moreover, considering the sensor sensibility the diameter of the holes is 4 mm (Appendix A.7). The distance between two holes is 4 mm. The sensor (Appendix B.4) can detect the holes and the surface of the cylinder easily while the holes are inside the sensor reading slot (Figure 4.1).
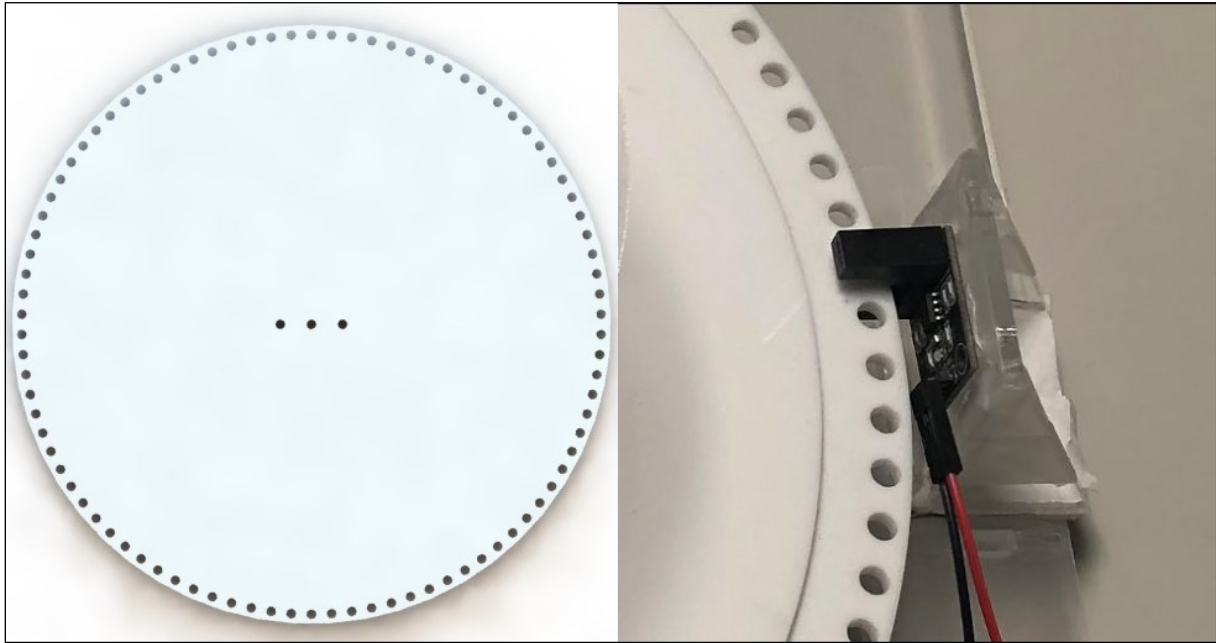
Figure 4.1 Holes, Cylinder and Sensor

Controlling the only single axis is necessary to have articulation (joint). This articulation is assembled between the base and the cylinder for rotating the mechanics. The main principle of the rotating is that when the reaction wheel produces the force, the mechanism turns the opposite side.

The chosen articulation is a slip ring which is made by SENRING (Figure 4.2). Slip ring has several advantages for this kind of work. Slip ring provides cable for connection between DC motor and control unit (Arduino DUE). The other advantage is that while the mechanism rotates around the axis, the cables of connection (DC motor, power supply etc.) are avoided to twist.

The model of slip ring is SENRING H2042 (Appendix B.5) which has six cables and the articulation around the Z axis.
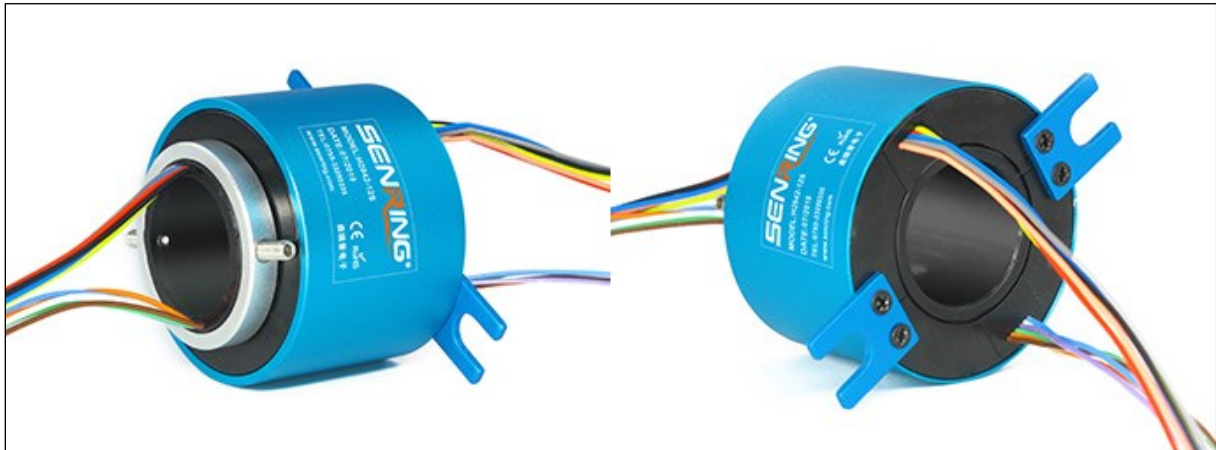
Figure 4.2 SENRING Slip Ring H2042[10]

The reaction wheel is an essential component for controlling the position. It provides high pointing accuracy. The material of the reaction wheel is methacrylate. The diameter of the reaction wheel is 14 cm (Appendix A.8).

---

[10] The photos of the slip ring https://www.senring.com/through-hole-slip-ring/small-hole/h2042.html
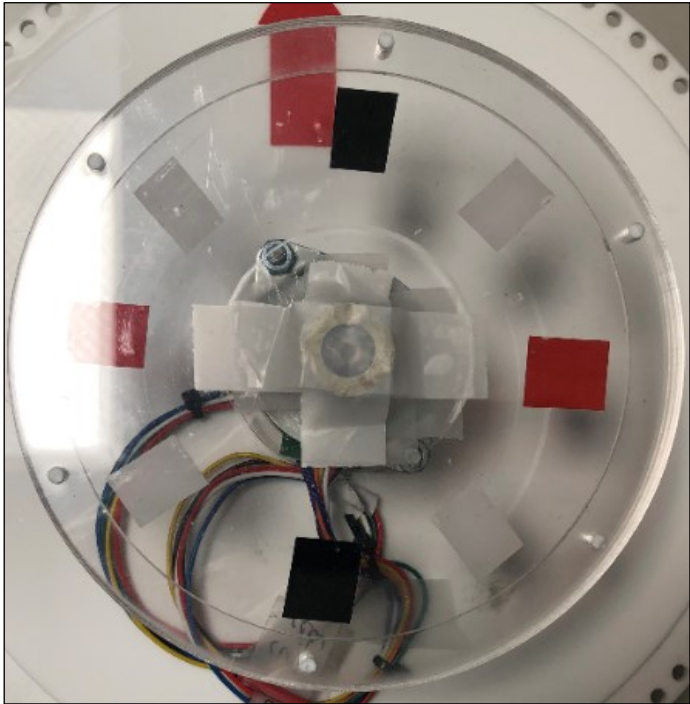
Figure 4.3 Reaction Wheel

NIDEC 24H677 (Appendix B.2) motor is used for the implementation. This motor has its own motor driver and encoder for the velocity of the motor. NIDEC 24H677 has eight connections which are CHA, CHB, 5V, CW/CCW, PWM, Brake, GND, Vm (24V) (Figure 4.4). CHA and CHB are for the velocity. Encoder has 100 pulses per revolution. CW/CCW is for controlling the direction of the motor. PWM pins have to connect with PWM cable for controlling the motor with Arduino DUE.

Figure 4.4 Nidec 24H677

The model of SENRING Slip Ring H2042 has six connections. Therefore, it is not suitable for using all motor connections. Brake and CHB connections were not used during the implementation part. All used connections between Slip Ring and Motor are shown on the below table (Table 7).

Cable Number	Connections

1	CHA
2	5V
3	CW/CCW
4	PWM
5	GND
6	Vm (24V)

Table 7 Connections between Slip Ring and Arduino DUE

The Arduino DUE (Appendix B.3) has been chosen to simulate Hardware-in-the-loop and control with Simulink.

Using Arduino DUE has different benefits. One of them is that MATLAB/Simulink has Open Block Library for Arduino Hardware (Figure 4.7). This library provides to develop control algorithms with blocks. While the control algorithm runs into the hardware, Simulink supports data acquisition in the real time.

There are some fundamental features of Arduino DUE (Figure 4.5) support to control the motor and data acquisition. Some pins of Arduino DUE have Pulse-width Modulation (PWM) which is an essential feature for controlling the duty cycle of the motor. In addition to this digital pins and interrupter pins support reading data for evaluating the response of the mechanism.
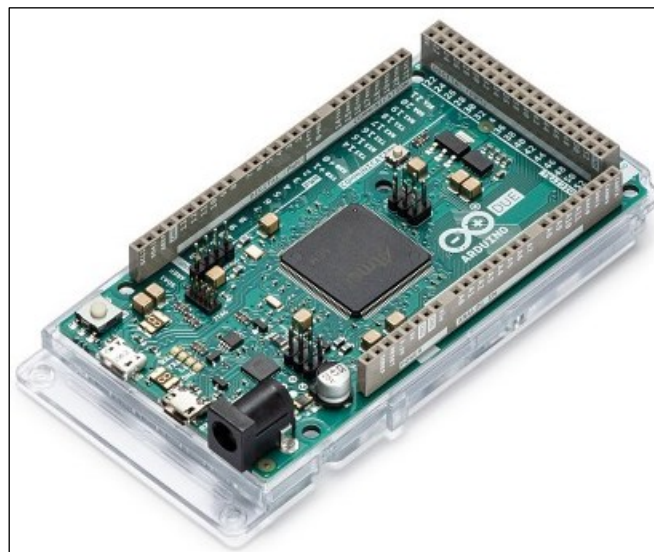
Figure 4.5 Arduino DUE

Once collecting all the components for assembly, the software development should be begun to control the motor and data acquisition.
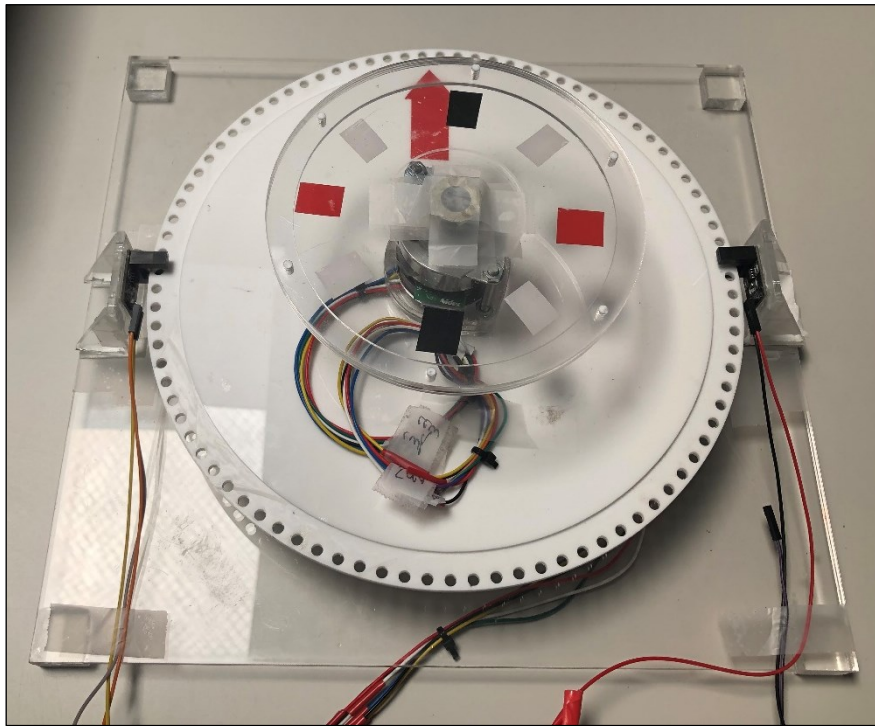
Figure 4.6 Assembly

Finally, the above figure (Figure 4.6) shows the final assembly of the mechanism. There are two sensors on the right and left side. The cables are connected with the Slip Ring on the below. The Slip Ring is between the cylinder and the base of the mechanism.

4.2. Hardware-in-the-loop (HIL)

Hardware-in-the-loop (HIL) is a method for development and test of complex simulation model real time. It provides a platform for testing the control algorithm. In this study Hardware-in-the-loop (HIL) is chosen because while the software runs in the hardware to observe the data of the mechanism with real time. The process of the development of the Simulink model benefits from Simulink Open Block Library for Arduino Hardware[11]. The below figure (Figure 4.7) shows the common blocks of the Arduino's library.

---

[11] The website of MathWorks/Simulink https://www.mathworks.com/help/supportpkg/arduino/ug/open-block-library-for-arduino-hardware.html
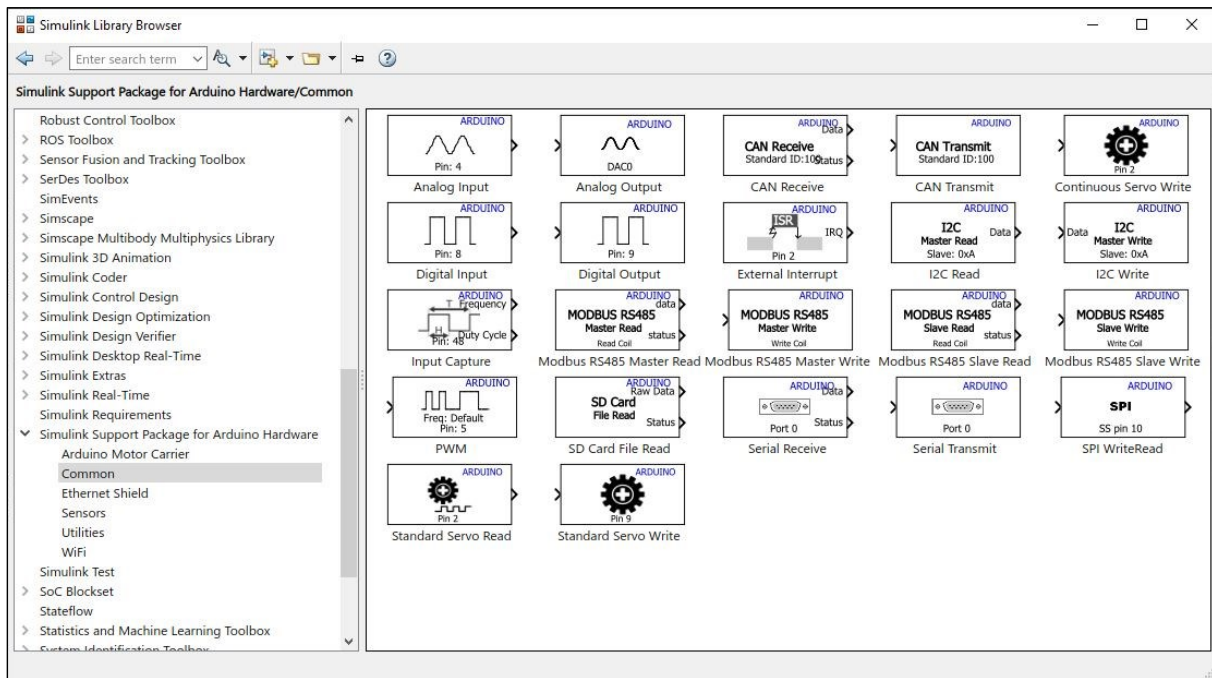
Figure 4.7 Simulink's Open Block Library for Arduino Hardware (Common Blocks)

Mainly four keys feature of Arduino library are used in the Simulink. These are Digital Input, Digital Output, External Interrupt and PWM as show in the below figure (Figure 4.8).
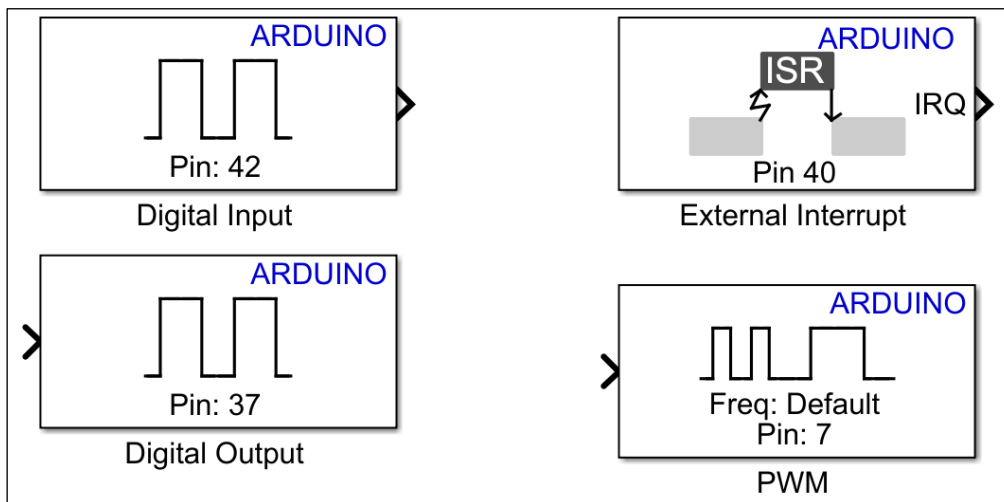
Figure 4.8 The blocks of Arduino DUE

These main features provide for reading data, sending desired input, and controlling duty cycle. After installing the library, the software development can be started. In this work firstly it is focused on reading the sensor and controlling the motor. When the two essentials control logic work properly, after this, the next logic is the sending desired angle and controlling the angle with the reaction wheel.

4.2.1. Configuration of Sensors

The configurations of hardware and software should be different to control the position and direction of the mechanism. The logic of the configurations is that using two interrupt pins and digital input pins. The below table (Table 8) shows hardware configuration for each sensor.

Hardware Connections				
	Configuration Pins			**Configuration Pins**
Right Sensor	40 Interrupt	**Left Sensor**		41 Interrupt
	42			44
	44			43

Table 8 Hardware Connections

The digital pin of the sensors is connected with one female jumper wire cable and the connection of Arduino is connected with three male jumper wire cables to the pins of Arduino. The below figure (Figure 4.9) shows that how to connection of Arduino.
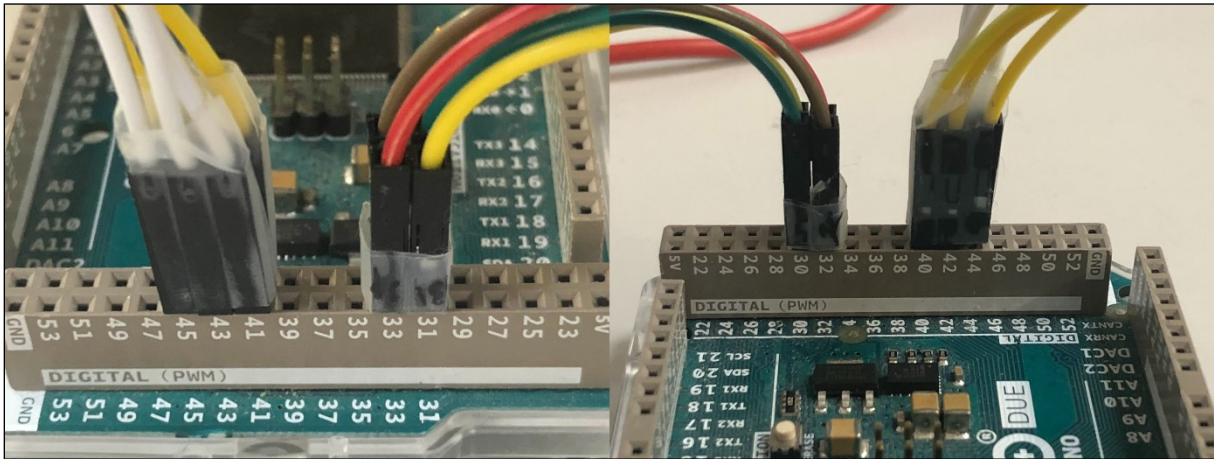
Figure 4.9 Hardware Connection of Sensors

The logic of encoder provides a specified number of pulses in one rotation of the encoder. In this work there are two sensors and 90 holes (number of pulses). The output of sensors provides two output signals when the sensors read the holes (pulses). The right sensor can be an "A" channel while the left sensor can be a "B" channel. These two channels of signals are offset for determining the rotation. The direction of the mechanism can be determined according to which channel leads the other. The below figure (Figure 4.10) shows the configuration of sensors which is measured by oscilloscope. As it can see (Figure 4.10), there is phase difference between the two sensors. For doing that the position of the sensors needs to be adjusted by checking at the oscilloscope. Once the position of the sensors is the correct position on the mechanism, the next process is to develop the Simulink model.
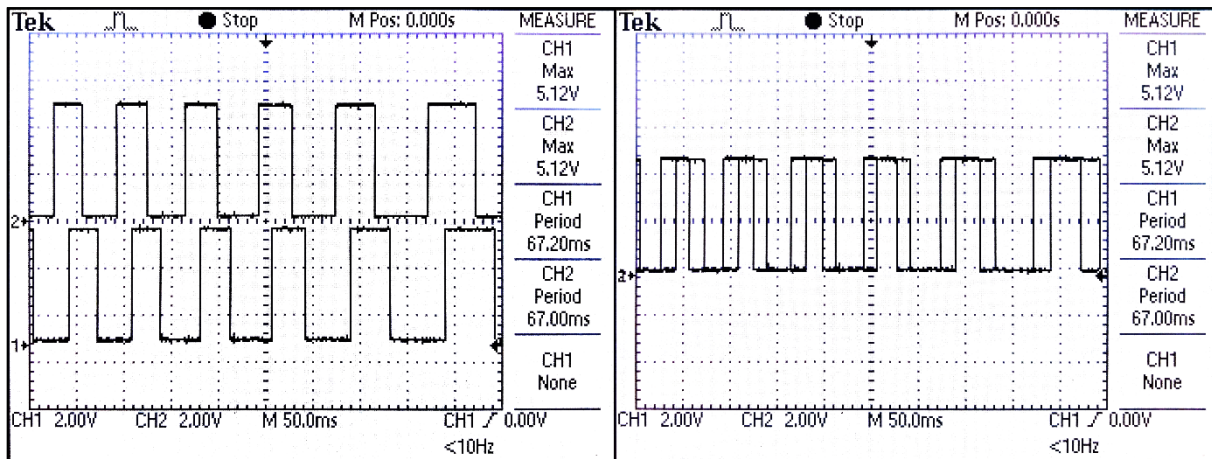
Figure 4.10 Signals of Sensors with Oscilloscope (Signal 1: Right Sensor – Signal 2: Left Sensor)

As it is mentioned above the configuration of the model of Simulink is unlike the configuration of the hardware. The logic of software is to be used two external interrupts[12] pins and four digital pins to compare both signals. The interrupt trigger condition is CHANGE so the software evaluates the signal when it is rising edge and it is failing edge. This condition provides 4X decoding.

As mentioned in this chapter (4.1 Mechanical and Electronic Components) the cylinder has 90º holes. Considering this with 4X CHANGE condition of the external interrupts, the software will be able to measure 360º degrees full rotation with a precision of four degrees.

Software Configurations				
Right Sensor	**Configuration Pins**	**Left Sensor**	**Configuration Pins**	
	40 External Interrupt (4X Change)		41 External Interrupt (4X Change)	
	42		45	
	43 Left Sensor		44 Right Sensor	

Table 9 Software Configurations

The above table (Table 9) shows the configuration of the Simulink model. The outputs of the sensor compare to each other in the Simulink model.

It is used as a relational operator block to compare the outputs of the sensors. When the external interrupt blocks trigger the subsystem (Figure 4.11 and Figure 4.12) (right and left), digital input blocks send the signal to the relational operator. If the signal edges the same level, the right sensor subsystem counts up the degree and the left sensor subsystem counts down.

As shown in the figure (Figure 4.10) when the signal is rotating specific direction, one of these sensors leads to the other sensor to determine the direction. The same logic can be considered for counter direction.

The below figures (Figure 4.11 and Figure 4.12) show the modelling of both sensors. If the output of the relational operator is the same level, the switch block sends '1' after the comparison. If it is not the same level, the switch block sends '-1'.

---

[12] The website of MathWorks of External Interrupt

https://www.mathworks.com/help/supportpkg/arduino/ref/externalinterrupt.html
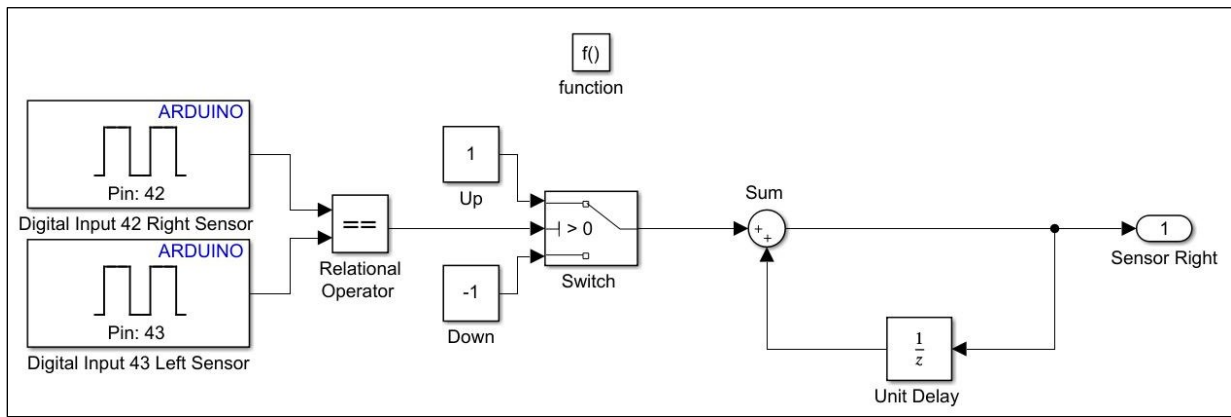
Figure 4.11 Simulink Configuration of Right Sensor Subsystem

After the switch block, the signal merges the sum block. Unit delay[13] block should be used for designing basic counters.
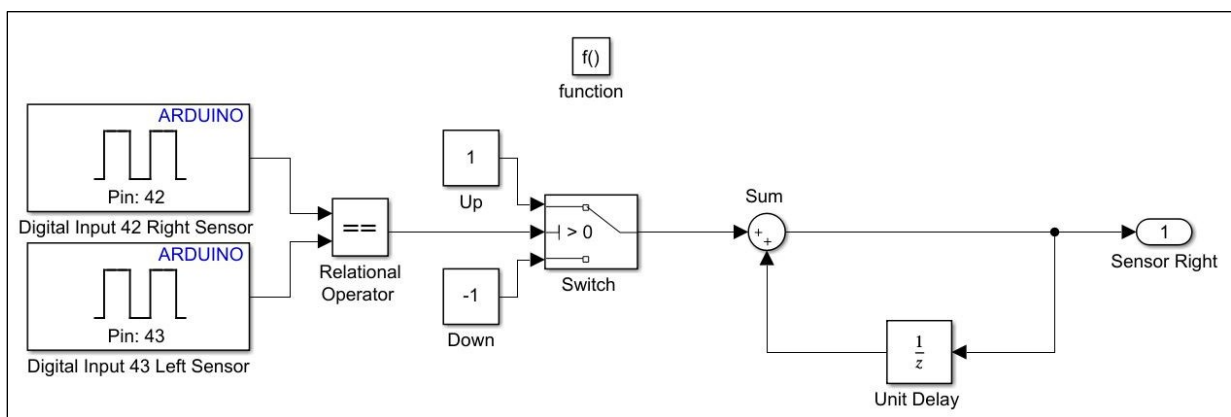
Figure 4.12 Simulink Configuration of Right Sensor Subsystem

The unit delay block holds and delays the signal by the same sample period. It returns the signal to the sum block after hold the signal. The sum block sums all signals which come from the input side and the unit delay block.
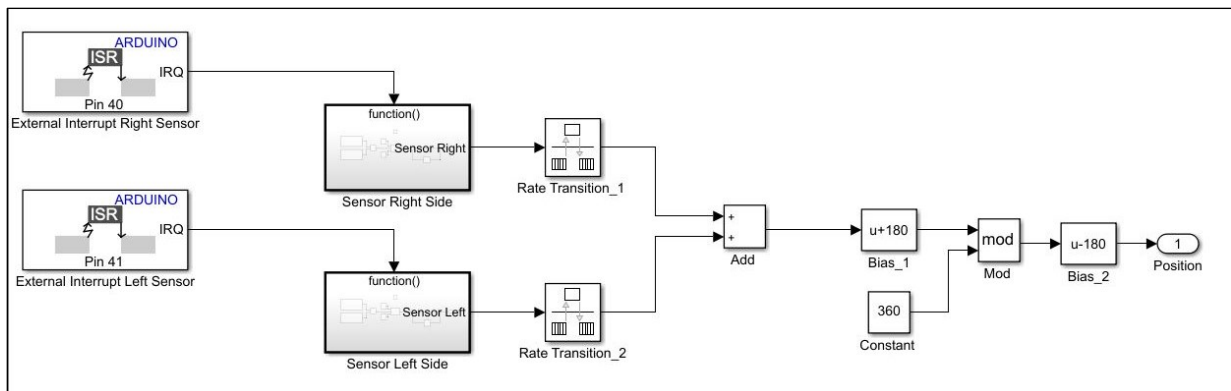
Figure 4.13 Sensors Configuration of Simulink (Position Subsystem)

The design of the counter should be set to a maximum point to avoid counting infinitely. For doing that it should be made some mathematical adjustments.

Bias_1 and Bias_2 set the limit of position between -180º degrees and 180º degrees. The mechanism cannot rotate bigger than these values. Mod block is used for setting maximum degree for avoiding the counting error. The maximum degree is 360º degrees.

---

[13] The MathWorks website about Unit Delay https://www.mathworks.com/help/simulink/slref/unitdelay.html
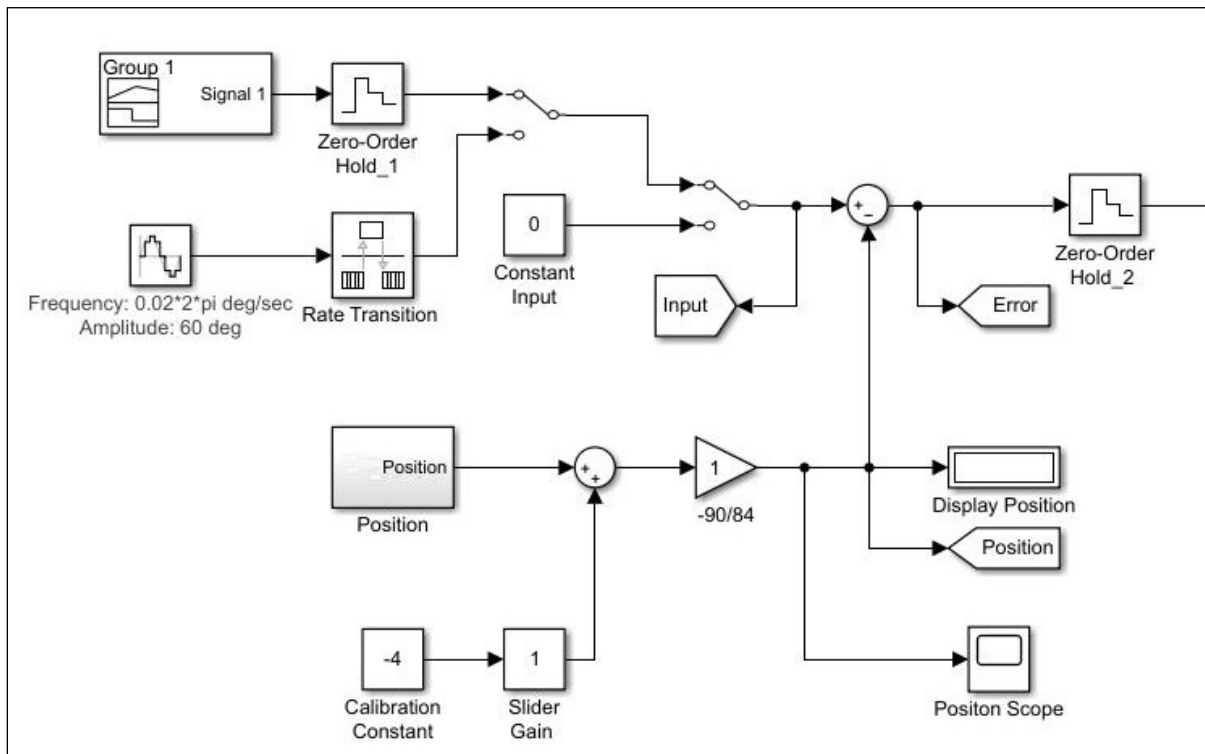
Figure 4.14 Position Subsystem

When the Simulink model executes into the Arduino DUE, the Simulink measures initial position error. After the observation, a 4º degrees error is determined. The calibration constant is added to the model of Simulink to fix the error. The second calibration should be done for 90º degrees. The mechanism is rotated 90º degrees for observing the value of position. It is observed that 90º degrees is measured as 84º degrees. So for that reason, the measured position multiplied with gain (-90/84) to fix the error. The above figure (Figure 4.14) shows the final model.

4.2.2. PID Design

In the implementation PID proportional-Integral-Derivative (PID) controller is used for controlling the position of the mechanism.
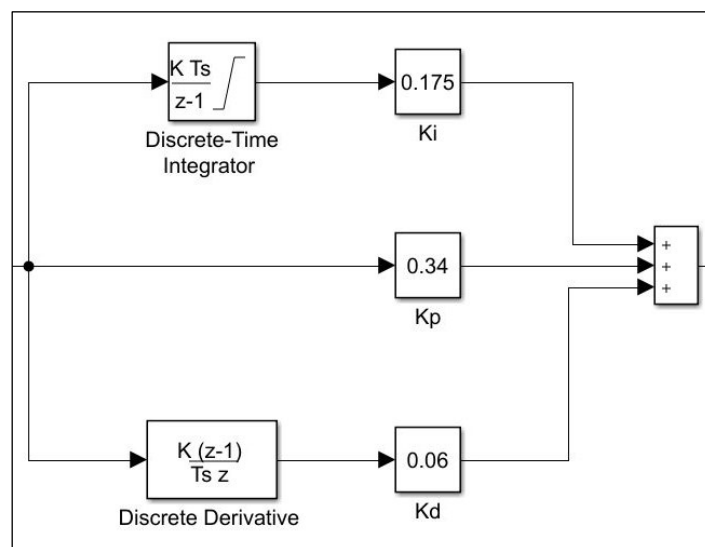
Figure 4.15 PID Design

The PID control design is made according to the response of the system. After a few testing's PID, it is configured final PID values. The below table (Table 10) shows the final PID values.

PID Values	
Proportional - Kp	0.34
Integral - Ki	0.175
Derivative - Kd	0.06

Table 10 PID Values

4.2.3. Controlling The Motor with Simulink

The motor NIDEC 24H677 is selected for implementation. Controlling this motor with Arduino DUE can be with Arduino library blocks. As it known that controlling duty cycle is essential way to control the velocity of motor
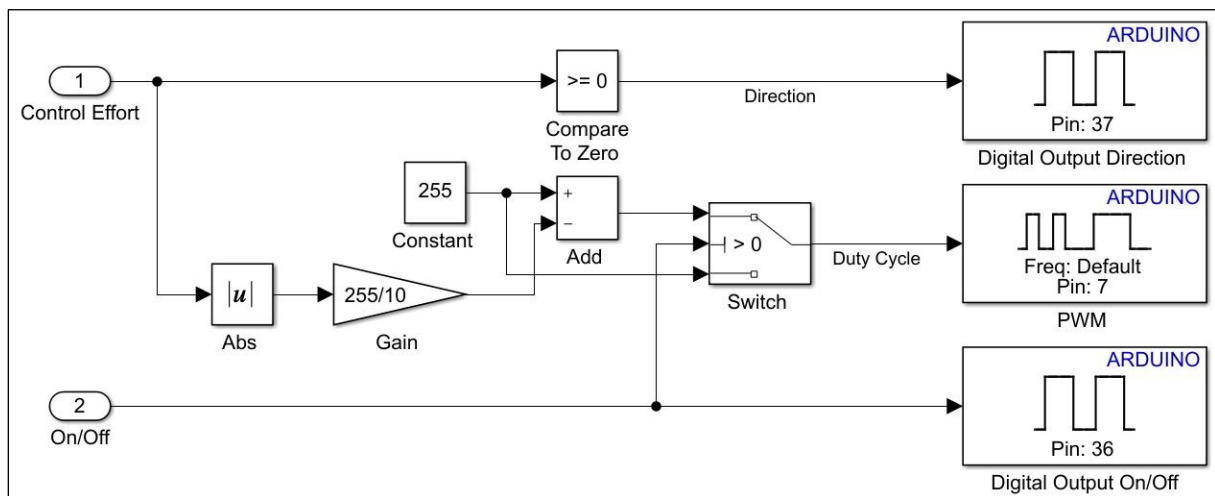
Figure 4.16 Nidec Motor Control Subsystem

The above figure shows that 100% duty cycle is 0 and 0% duty cycle is 255. The control logic of NIDEC 24H677 is different than normal logic. In addition to this, there is a limitation of the control effort. The limit is between -10 and 10. However controlling duty cycle of PWM is always between 0 and 10 because of Abs block.

There is a comparison block which is called Compare to Zero for controlling the direction of the motor. When the control effort is bigger than zero, it sends a logic level high '1' to change the direction of the motor.

The other controlling configuration is On/Off. The below figure (Figure 4.17) shows that there is a manual switch which send '1' and '0' for On and Off the motor

After the PID blocks (Figure 4.15) there are two blocks which are Dead Zone block and Saturation block. If the control effort is between -0.1 and 0.1, Dead Zone block sends zero to the duty cycle. Saturation block is as a limiter for minimum value and maximum value. The control effort cannot be lower and higher than -10 and 10. Once control motor logic is done, it should be controlled the velocity of the reaction wheel and motor. Doing this, the motor's own encoder is used to control the speed of the motor and reaction wheel. While the mechanism is at the desired angle, the motor should be stopped.
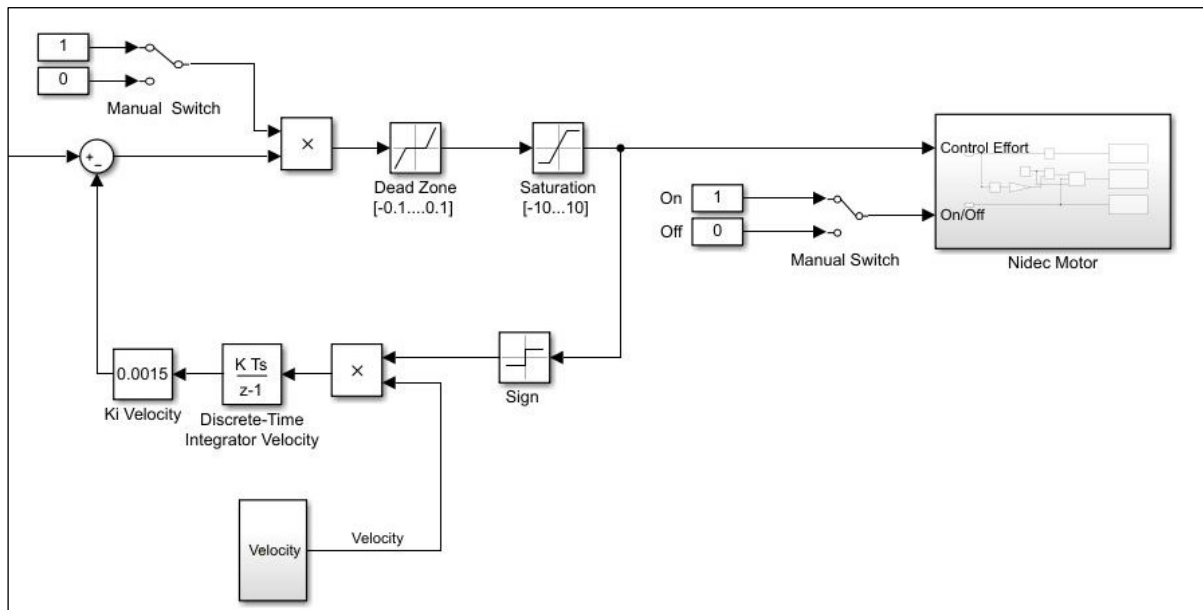
Figure 4.17 Motor Control

The encoder of motor has two channels. Channel A has 100 pulses and channel B has 100 pulses. There are six cables of Slip Ring. So that it is only possible to use Channel A. Channel A is connected to pin 32. When the digital pins send rising edge, the counter counts up otherwise the counter counts down.
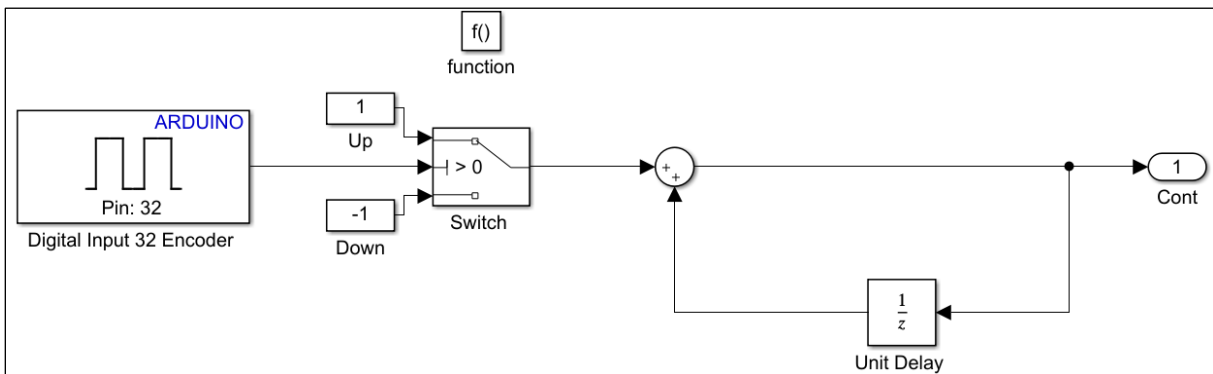
Figure 4.18 Motor's Encoder

The configuration of the external interrupt block is RISING. The block triggers the encoder subsystem when the digital output signal is at the rising edge.
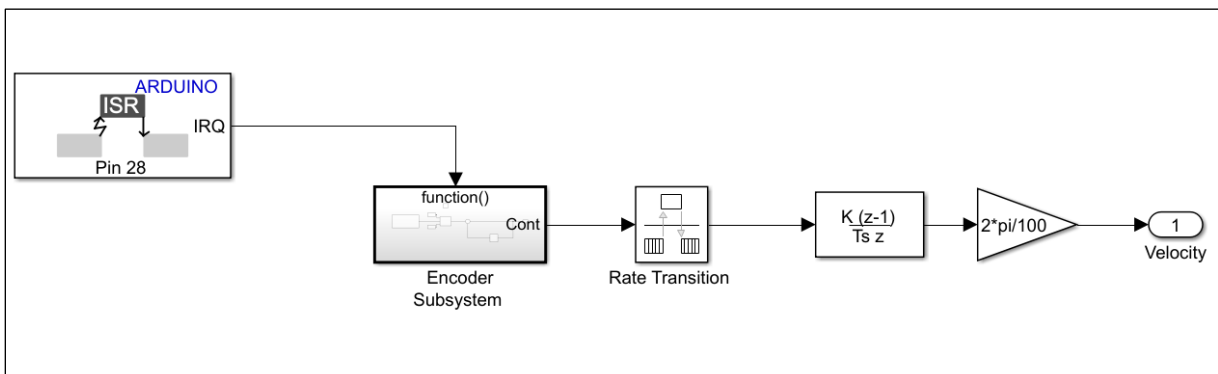
Figure 4.19 Encoder Model

Finally, the output of the counter has to be calibrate with gain. This gain depends on encoder pulses. Channel A has 100 pulses, the counter multiplies 2*pi/100. Because of 100 pulses per revolution.

4.3. Implementation (HIL) Results

Once the Simulink model is completed for Hardware in the Loop, the next process of the implementation is to obtain the response of the system. For doing that three-input waves are experimented for the implementation in order to get different results. These waves are step input, sine waves input and triangle input. In addition to this, the direction of the mechanism are considered for experiments.

4.3.1. Step Input Between 0º degree and 90º degrees

The step input is chosen for the first experiment of the implementation. The direction of the step input is positive angle. And the step input is between 0º degree and 90º degrees. The below figure (Figure 4.20) shows the reference input and the response.
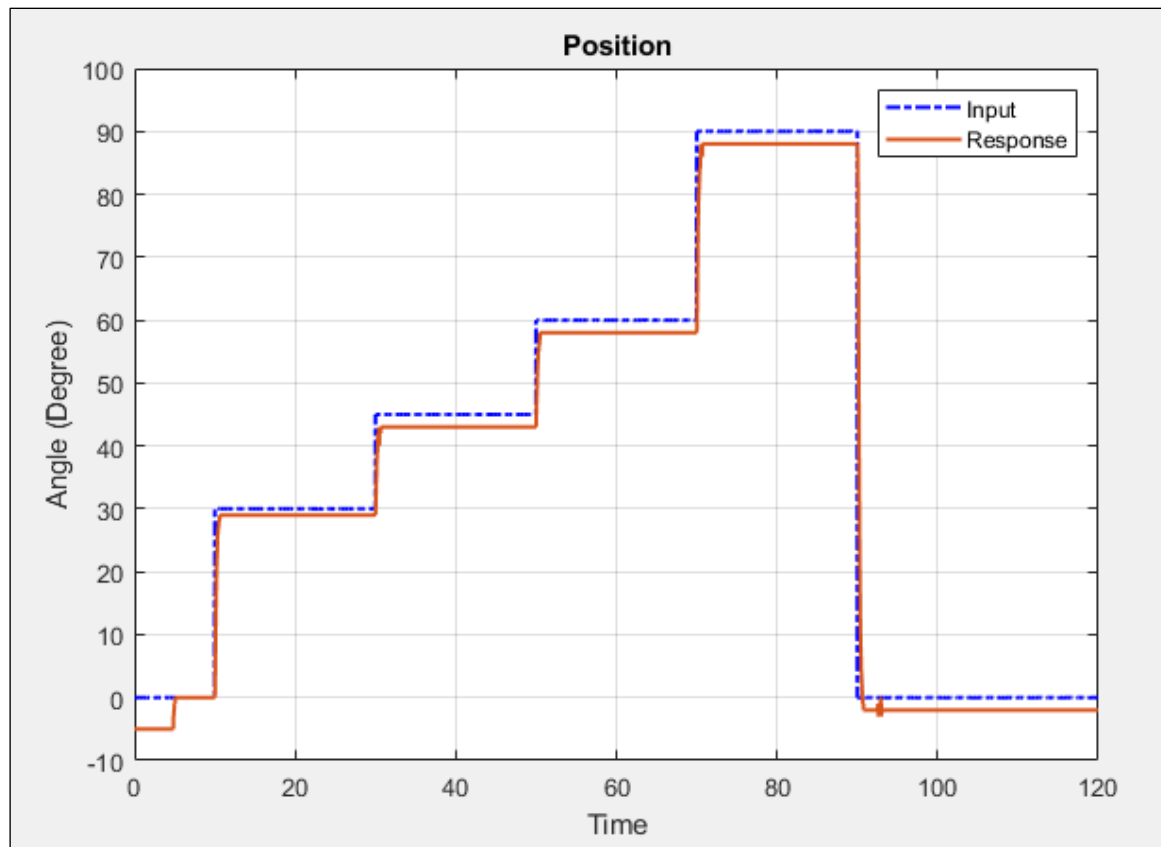
Figure 4.20 Input (0º degree and 90º degree) and Response

There is a position error the beginning of the implementation. The system immediately corrects this error and follows the reference input signal. The figure (Figure 4.21) shows that the time of the error correction is less than 1 seconds to find the reference signal. The correction process is started around 5 seconds. Probably the problem is electric connections of the motor. Nevertheless, the response of the system is satisfied for the first experiment.

After that when the time is 10 seconds, reference signal is 30º degree (Figure 4.21). As it can see, the response of the system follows the reference signal. However, there is an error which is just 1º degree. In sum, the response of the system is satisfied for first experimental. The other important step of the response is between 90º degrees and 0º degree (Figure 4.22). Before 90 seconds the position of the system is 88º degrees. In 90 seconds, the system responds to the desired position. The response follows the reference signal, and it is stopped -2º degrees with 2º degrees errors. This error is negligible because of initial position error 2º degrees.
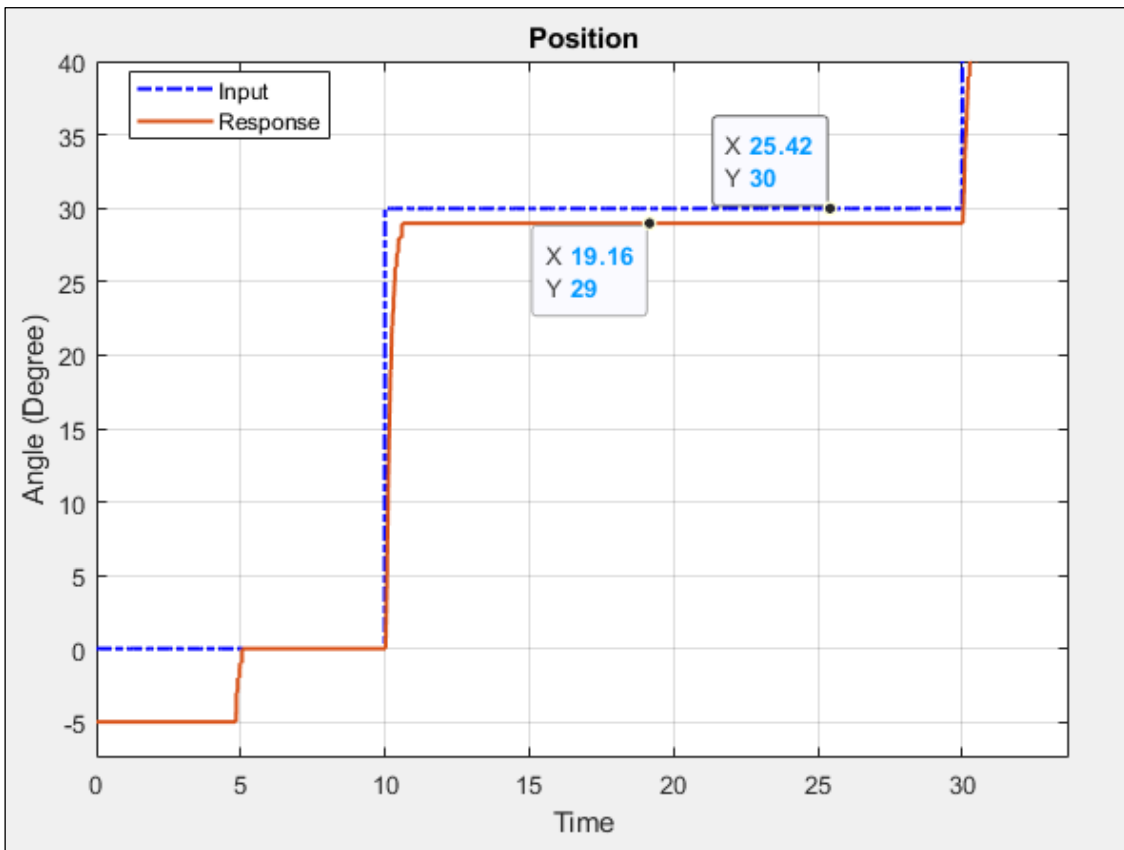
Figure 4.21 Initially Error Correction with labels
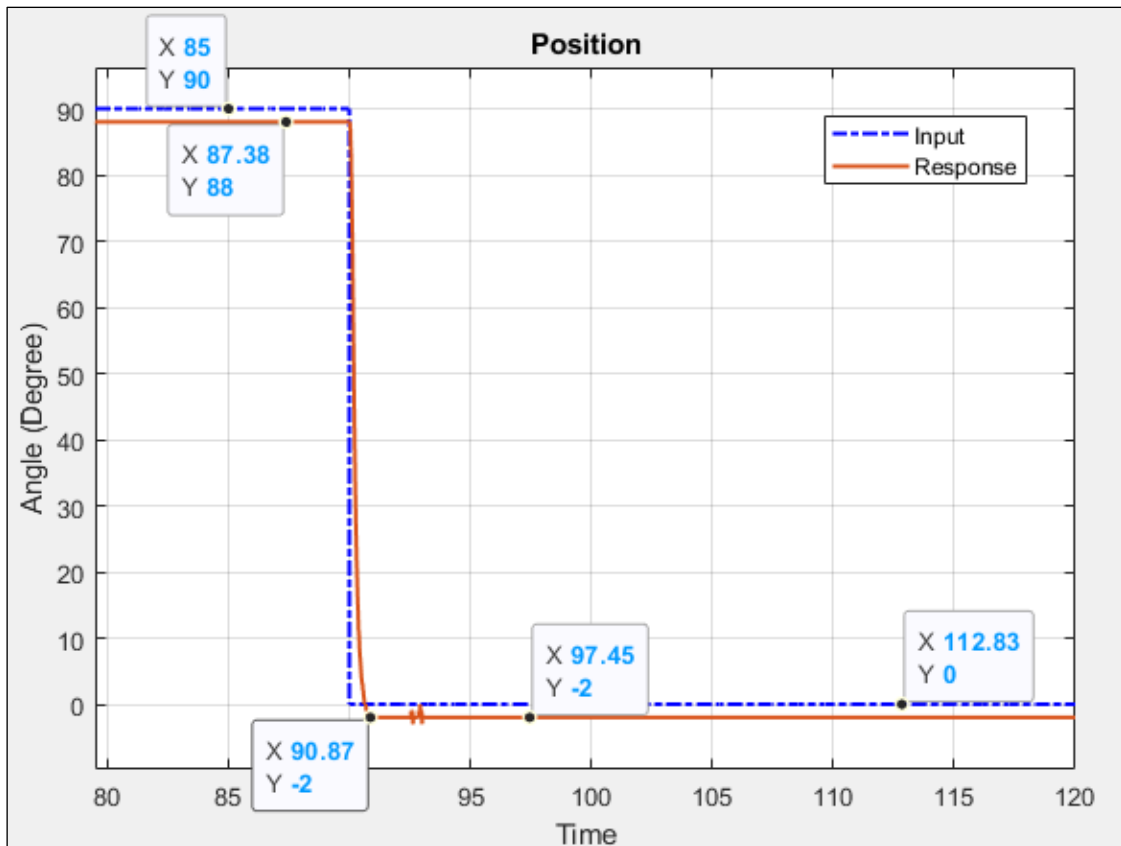
Figure 4.22 The response between 90º degree and 0º degree with labels
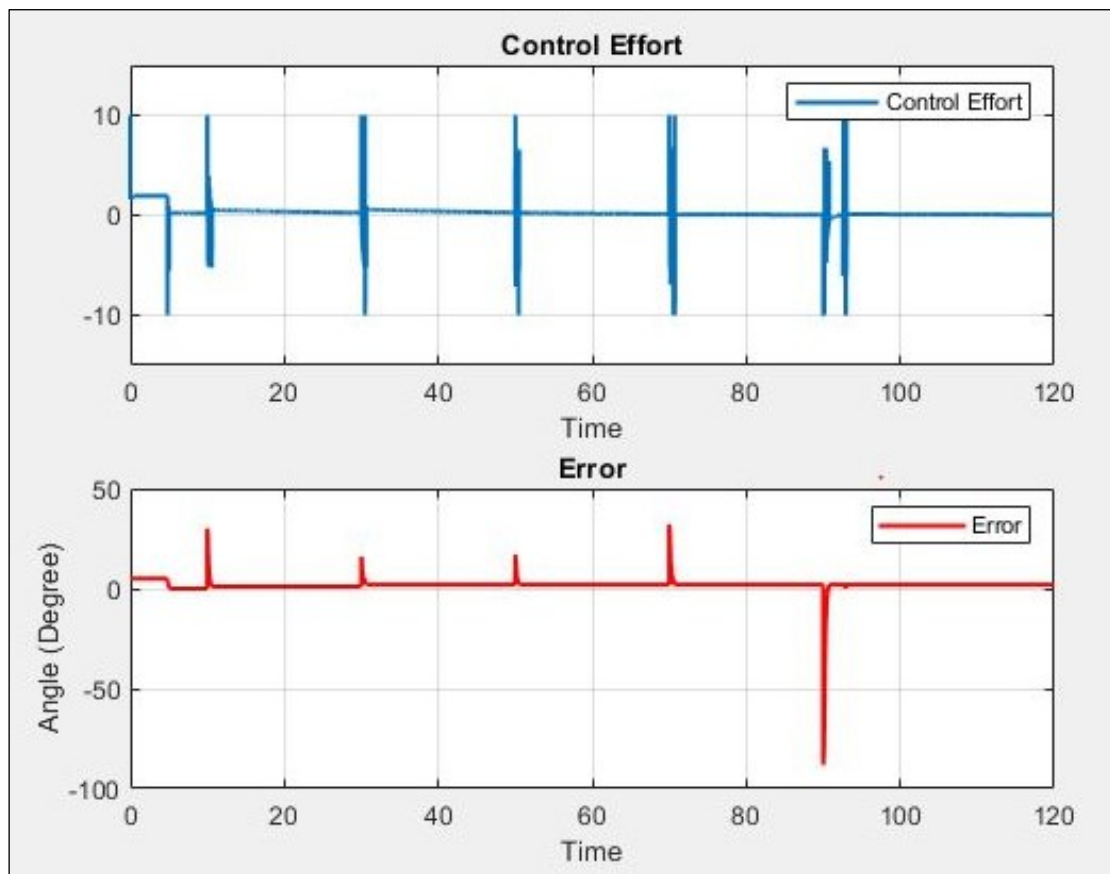
Figure 4.23 Control Effort and Error
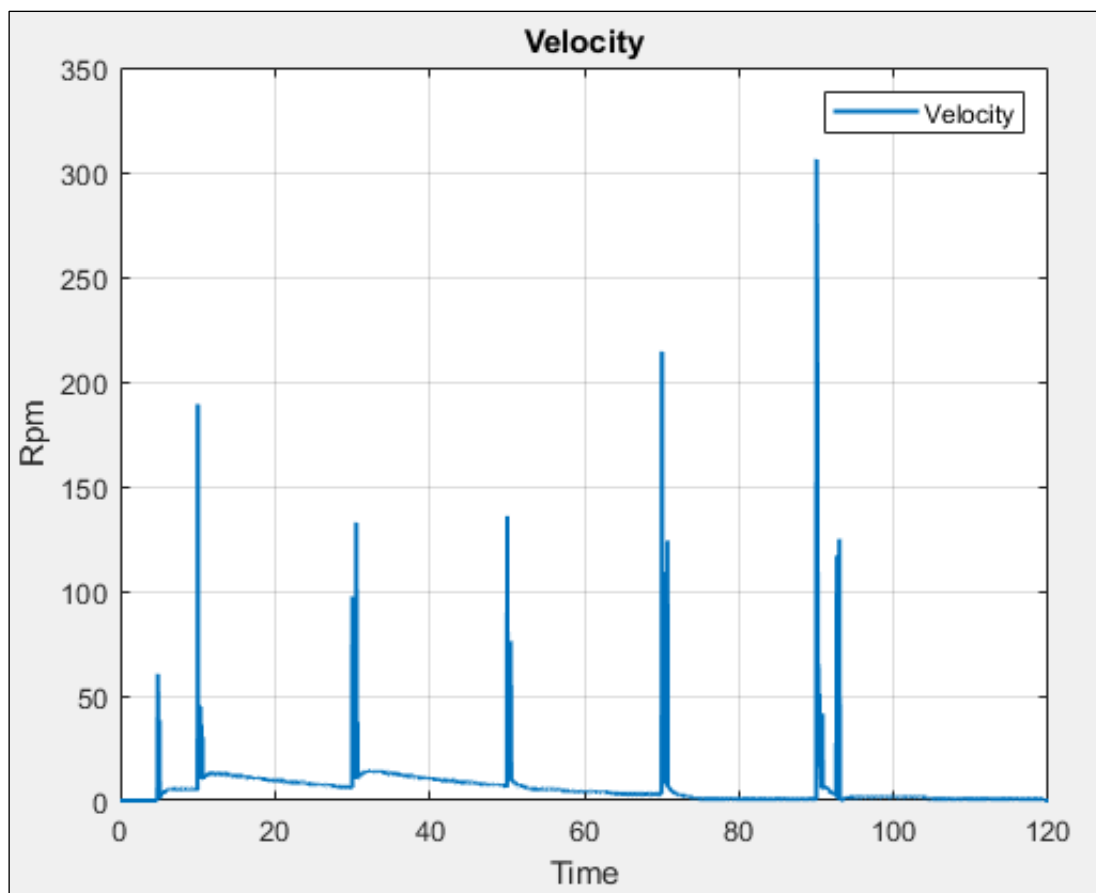
Figure 4.24 Velocity of Motor

The graph of the control effort and error is represented in the above figure (Figure 4.23). Predictably, the control effort is fluctuating between -10 and 10. Regarding this, the form of error graph is similar to the control effort. When the error is unacceptable, the control effort is higher to reach the reference angle. Meanwhile the velocity of the motor graph is shown above figure (Figure 4.24) As it can be seen, when the system is at the desired angle, the motor reduces the velocity to be stable at the desired angle.

4.3.2. Step Input Between 0º degree and -90º degrees

After the first experiment the direction of the rotation should be changed, and negative angles are tested. The reference angle of the second experiment is between 0º degree and -90º degrees.
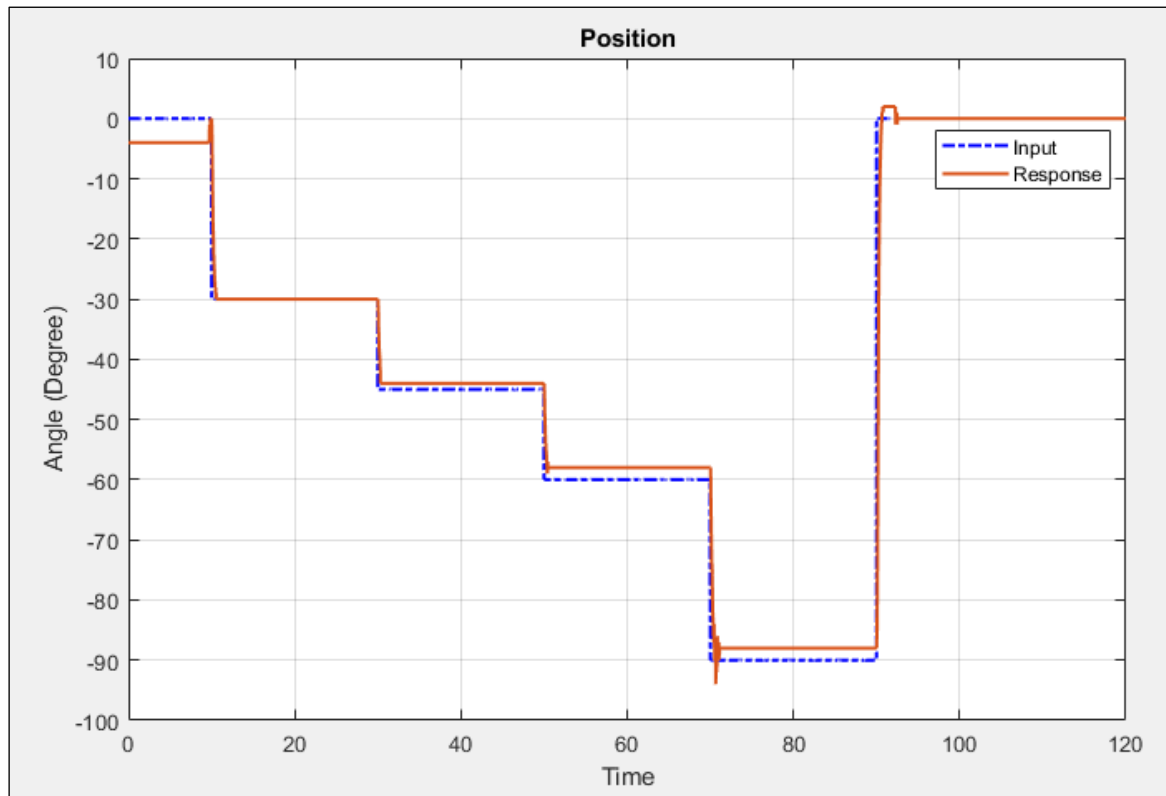
Figure 4.25 Input (0º degree and -90º degree) and Response

As it is seen in the above figure (Figure 4.25) the response of the mechanism follows the reference input. At the beginning of the second experiment there is an initial error as the first experiment. However, the system corrects the error to follow the reference input. The different sides of the graph are angles of -60º degrees, -90º degrees, 0º degree. The below figure (Figure 4.26) shows the difference.

The reference input (Figure 4.26) changes from the -60º degrees to -90º degrees. The response of the system exceeds -90º degrees and stops at -93º degrees. After that point, the system fixes the error, and it is stopped at -88º degrees. When the reference point is 0º degree, there is a peak point which is 2º degrees and it passes over 0º degree. The controller corrects the error, and the system of response catches the reference input.

As it is expected, the control effort is fluctuated between -10 and 10 with each error correction as the first experiment (Figure 4.27). The velocity of the motor always is low speed when the system is the desired angle as designed (Figure 4.28).
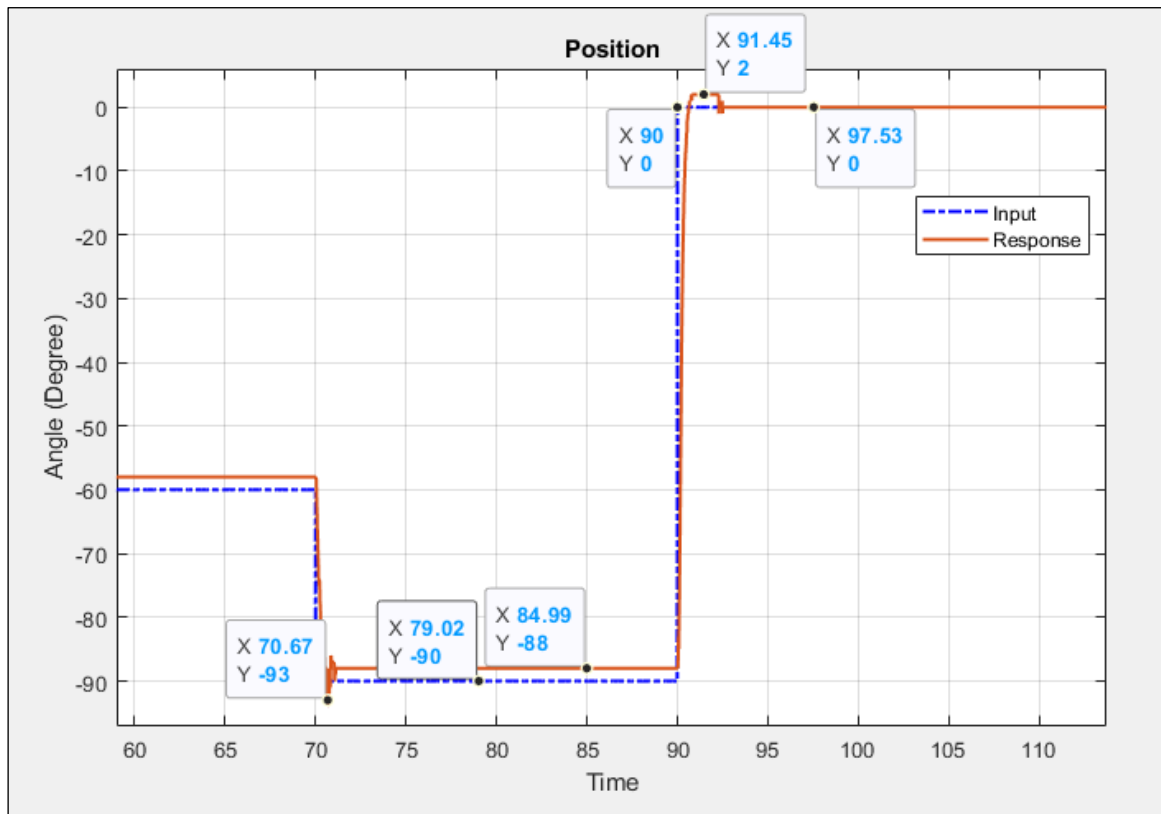
Figure 4.26 The response between -60º degree and 0º degree with labels
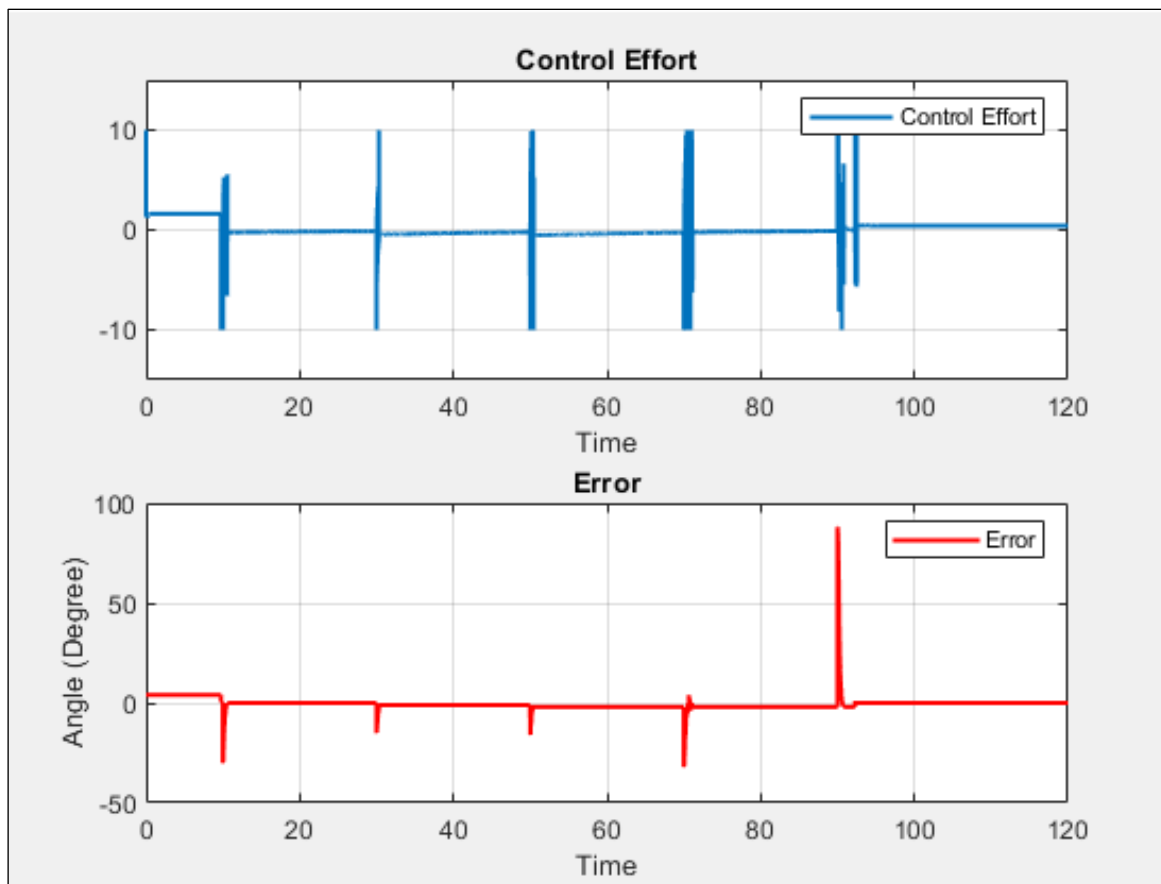
Figure 4.27 Control Effort and Error between -60º degree and 0º degree
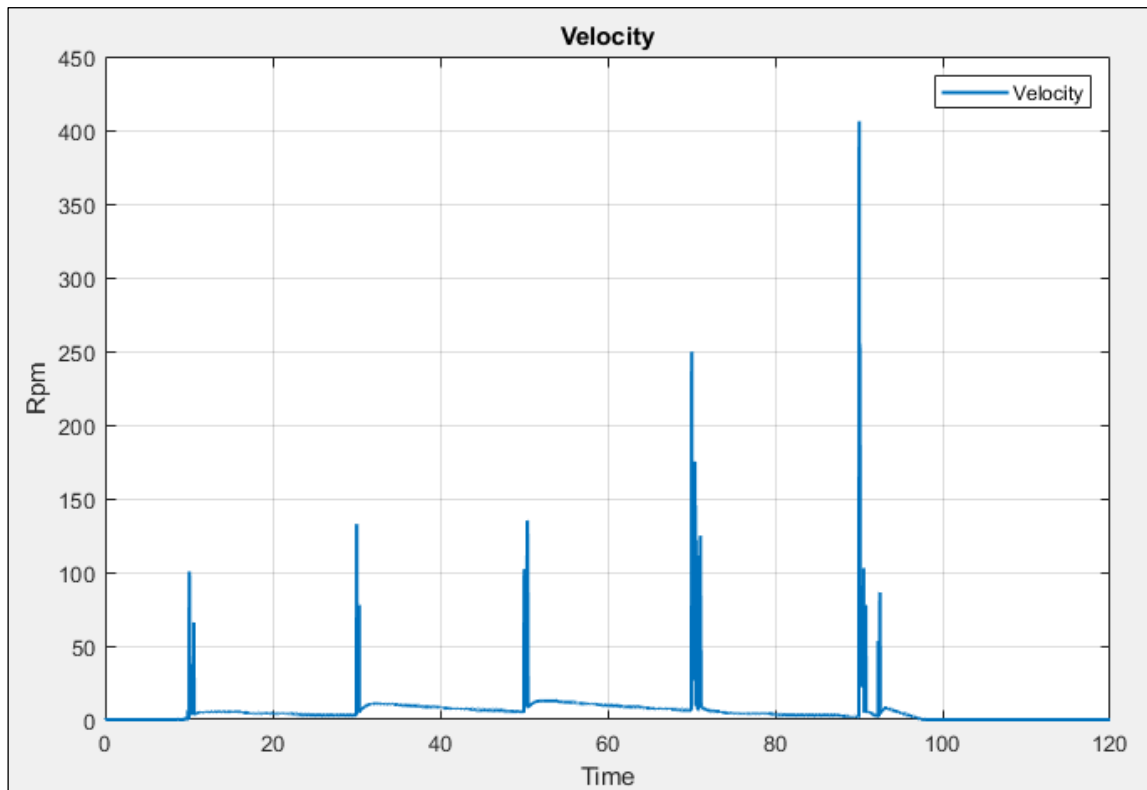
Figure 4.28 Velocity of Motor between -60º degree and 0º degree

4.3.3. Step Input -120º degrees, 0º degree, 120º degrees

First two experiments have a limitation of the angle. This limitation is about not more than 90º degrees. As seen in the results of experiments, the results are satisfied to test a bigger angle more than 90º degrees. The figure (Figure 4.29) shows the response of the system. As it is seen, there is not a big difference (almost the same) between the response and the reference input even with major changes.

The error of the system is functioned between 0º degree and 2º degree. This error can be a measurement error which can be negligible. The control effort and the error (Figure 4.31) are the same as previous experiments. Also, the behavior of the velocity is similar as before (Figure 4.32).

Consequently, the behavior of the system with step inputs with even higher values is acceptable. As it is seen, the controller performs its duty as expected.
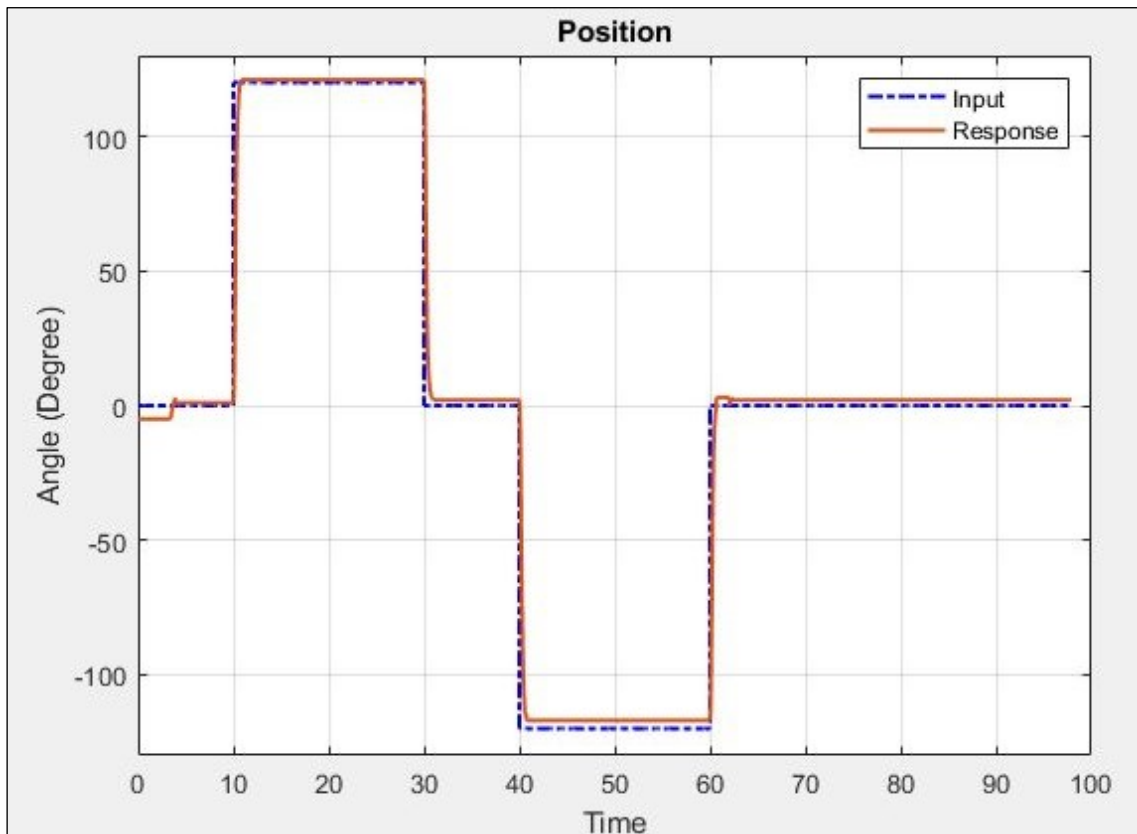
Figure 4.29 Input (-120º degrees, 0º degree, 120º degrees) and Response
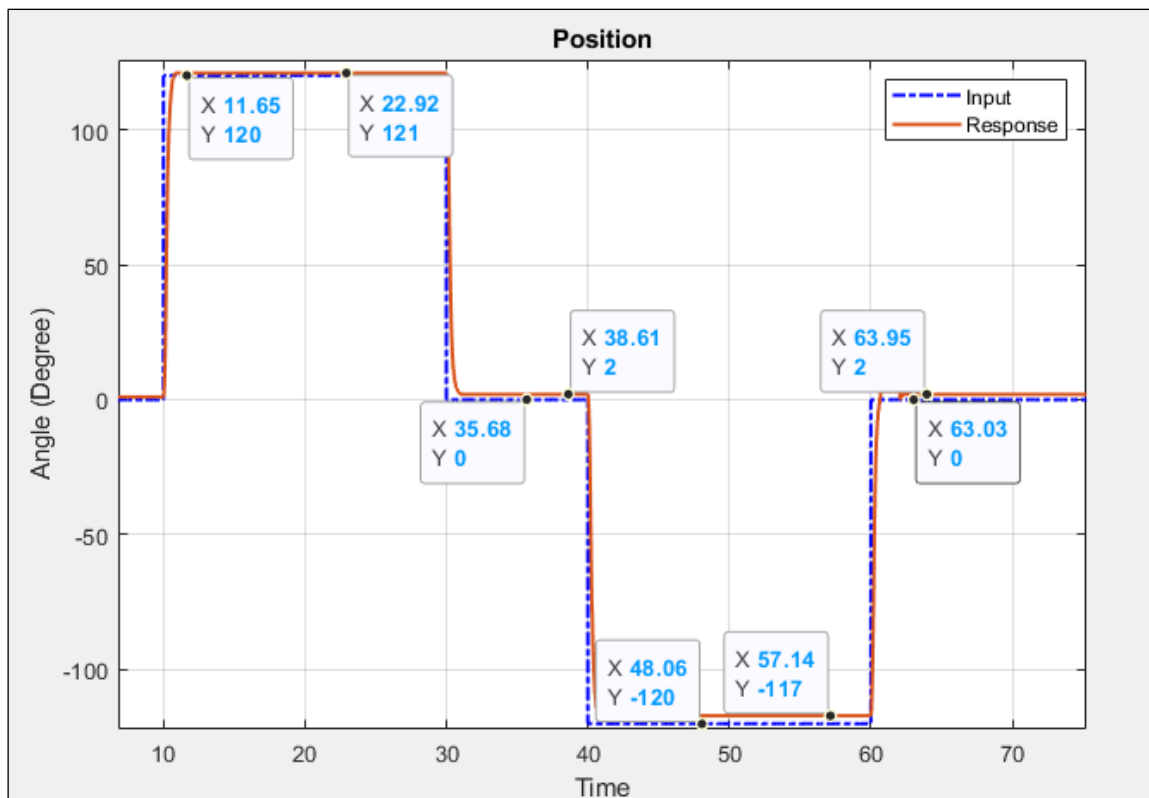
Figure 4.30 The response between 120º degrees, 0º degree, -120º degrees with labels
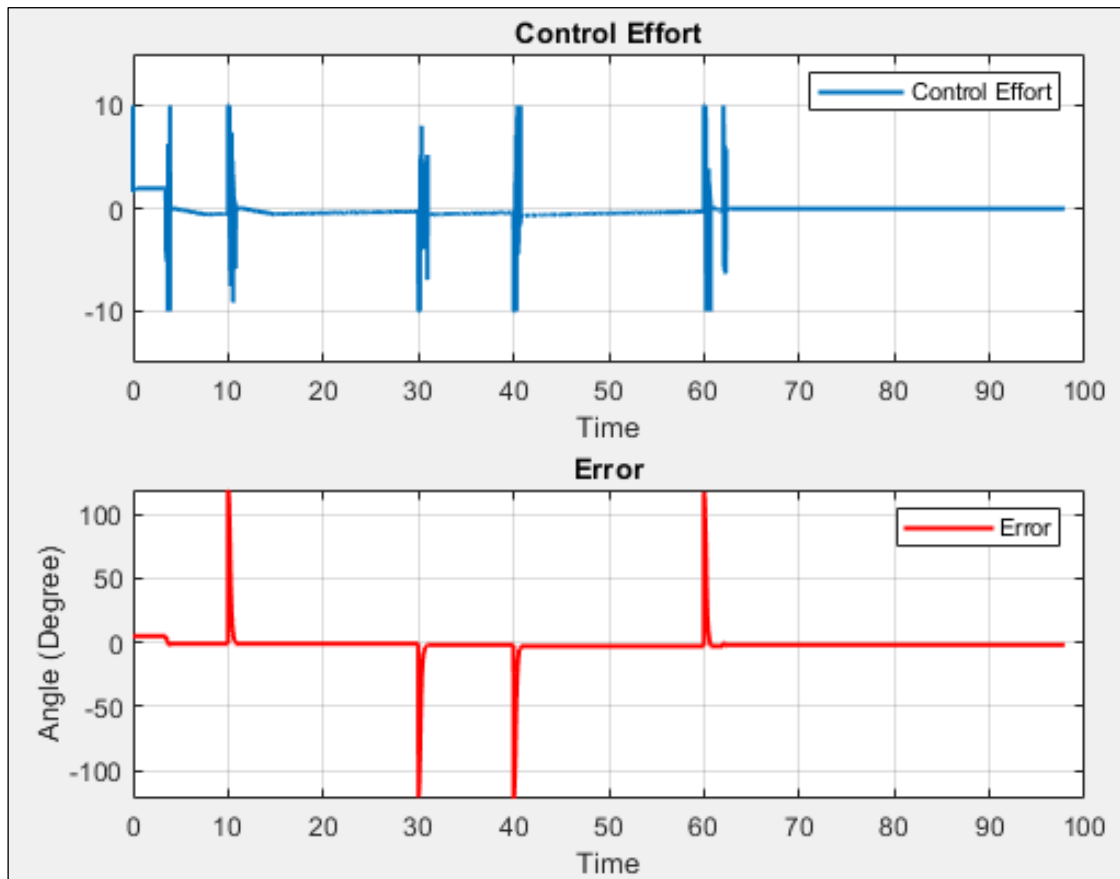
Figure 4.31 Control Effort and Error (-120º degrees, 0º degree, 120º degrees)
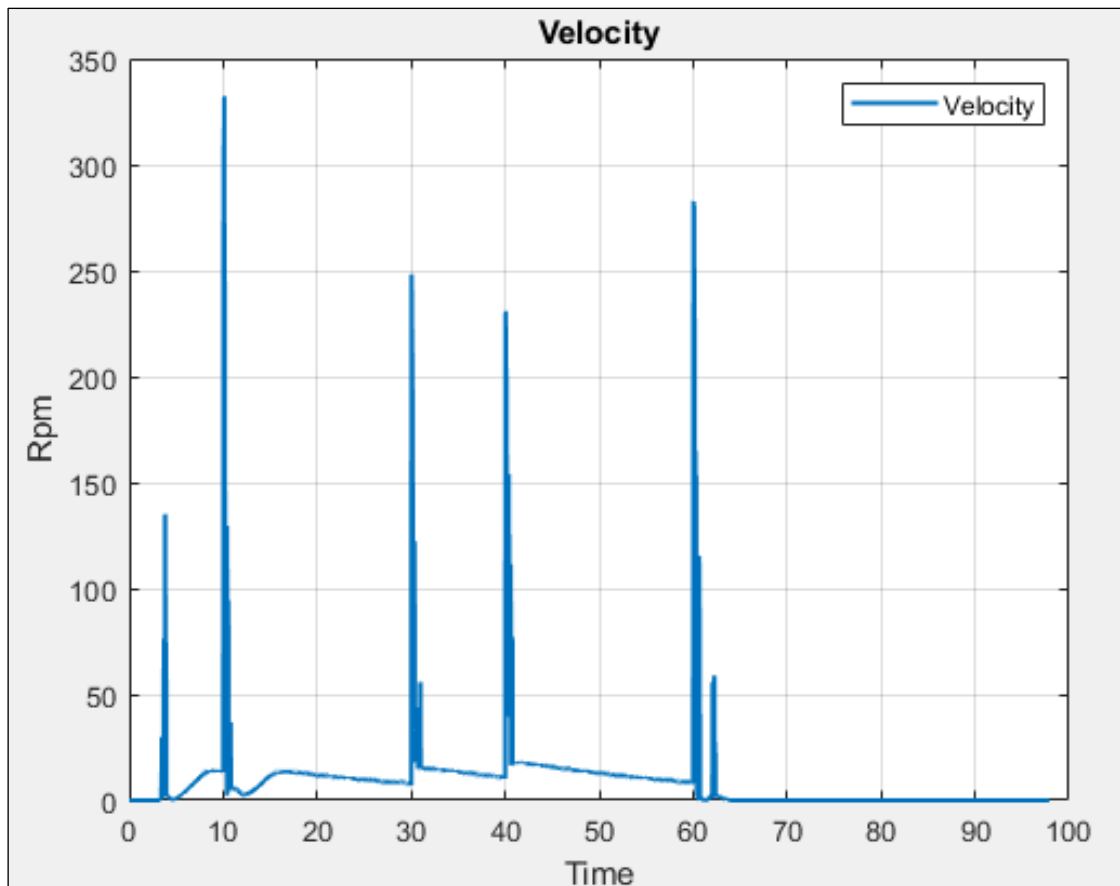
Figure 4.32 The Velocity of Motor (-120º degrees, 0º degree, 120º degrees)

4.3.4. Sine Wave Input -60º degrees and 60º degrees

The step inputs were tested successfully. the next input form is sine wave. In this section it is examined the response of system with sine reference. The reference sine wave and the response pursue each other, it can be seen in the below figure (Figure 4.33). There is no significant difference.
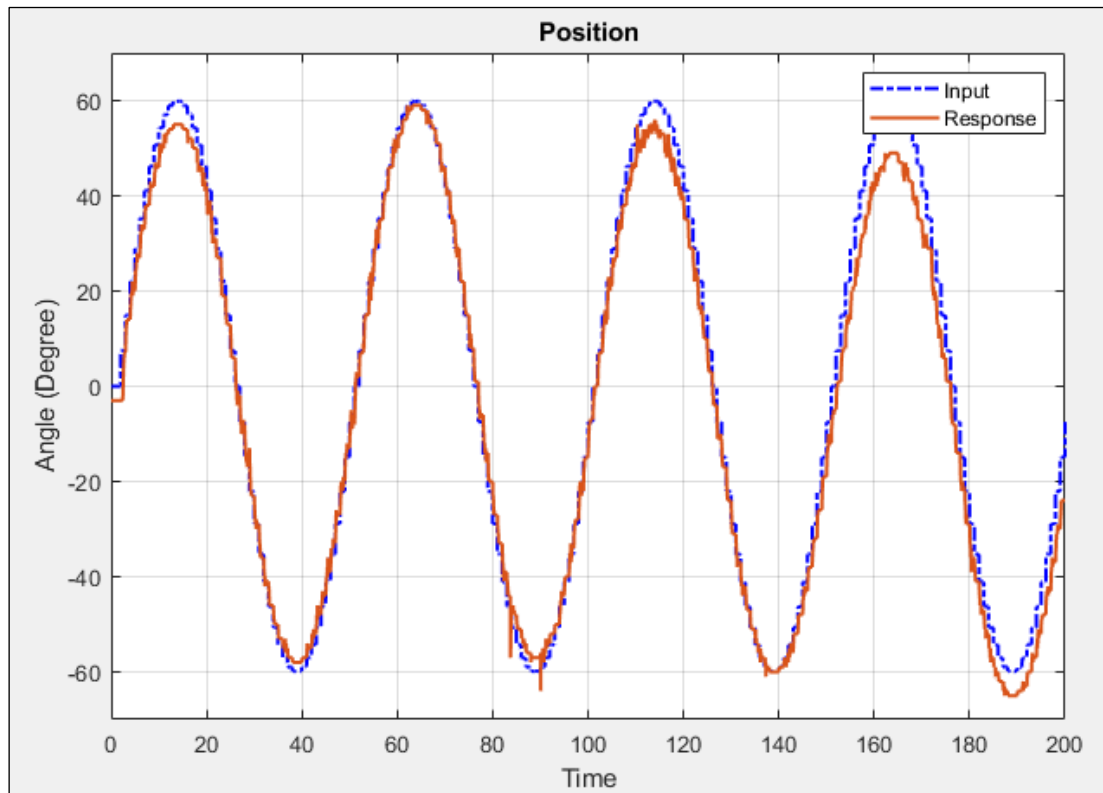
Figure 4.33 Sine Wave -60º degrees and 60º degrees

The figure (Figure 4.34) shows that the position error is between 1º degree and 10º degrees. The value of error is bigger in the final part of the graph. It is almost 10º degrees. Even so the response of the system follows the reference sine wave. This error can be caused by phase shift. The reason of this, it can be the error of measurement.

As it is known, the sine wave continues by increasing or decreasing itself during the simulation time so that the velocity of the motor is increased and decreased over time. The figure (Figure 4.36) shows the velocity of the motor. This reason affects the control effort as well. The figure (Figure 4.35) of control effort shows that the controller works intensively in every second of experiment. Finally, all results of sine wave input are acceptable.
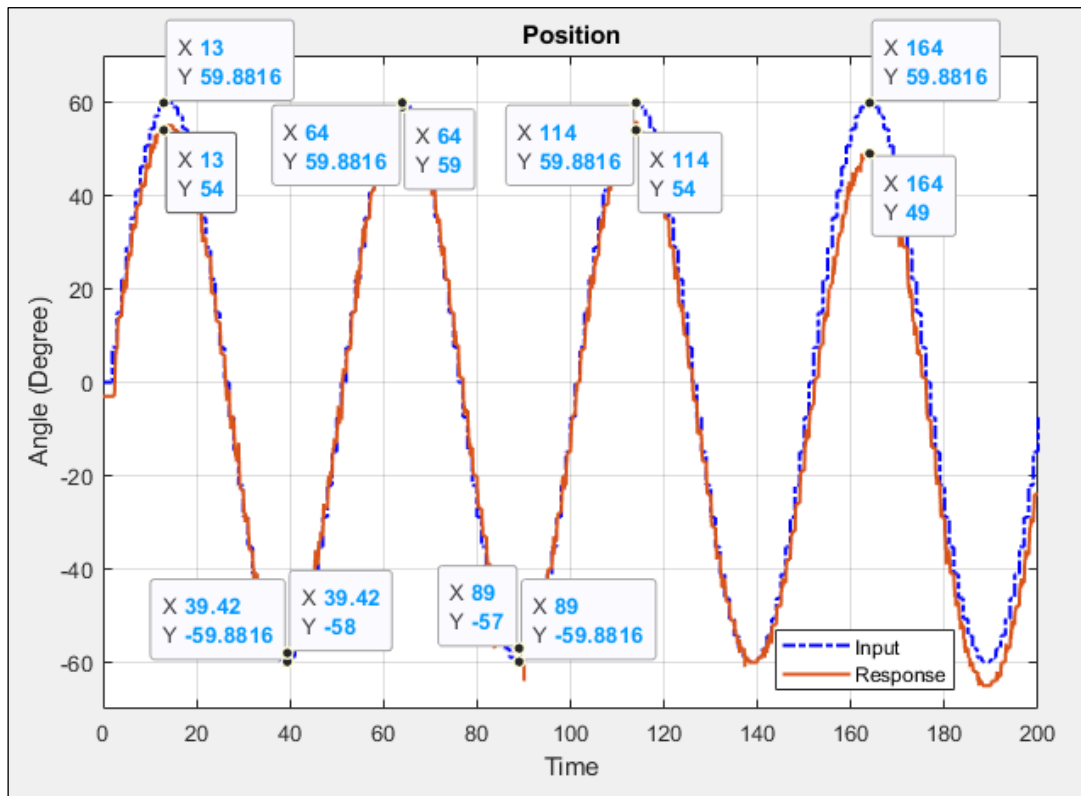
Figure 4.34 Sine Wave -60º degrees and 60º degrees with labels
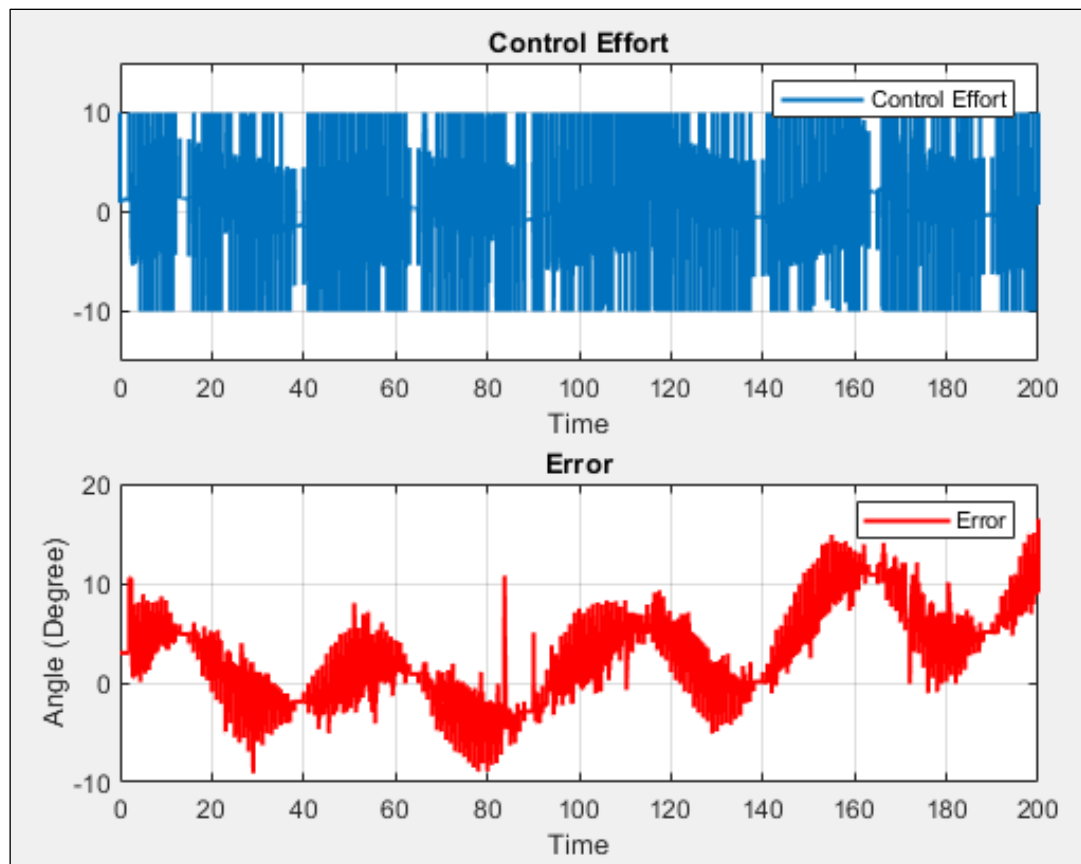
Figure 4.35 Control Effort and Error (Sine Wave -60º degrees and 60º degrees)
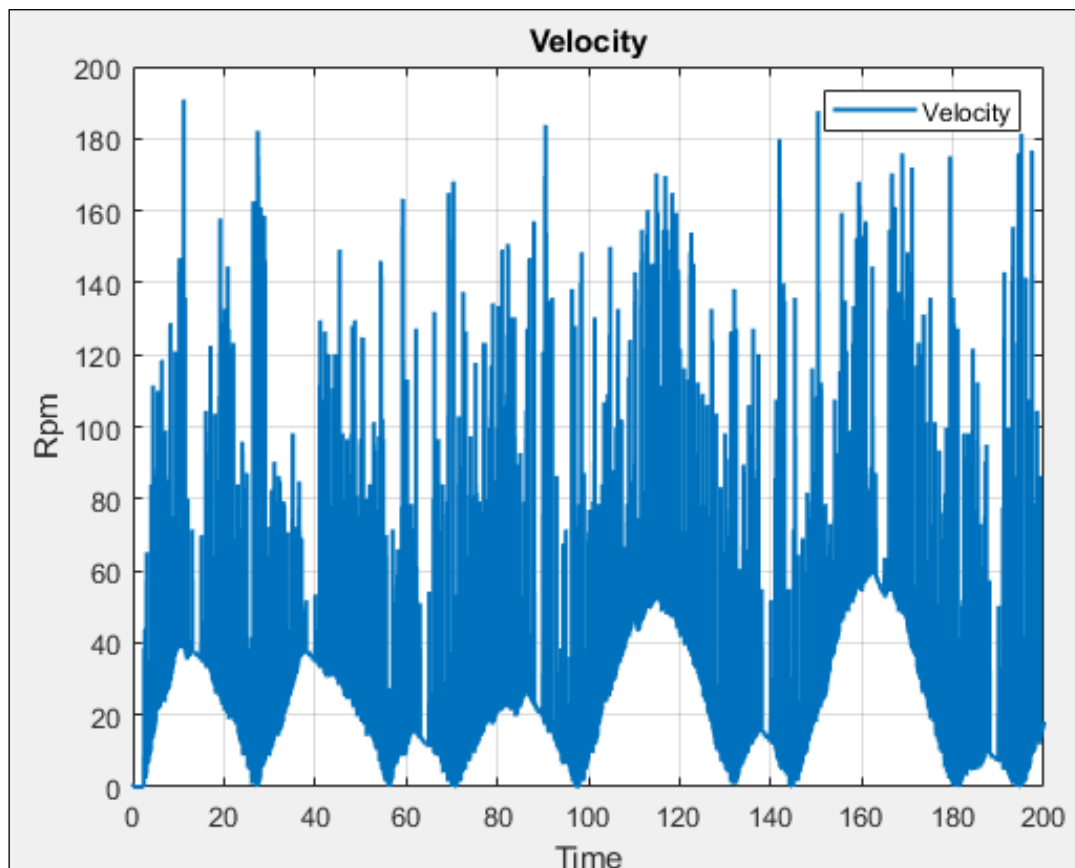
Figure 4.36 The Velocity of Motor (Sine Wave -60º degrees and 60º degrees)

4.3.5. Triangle Wave Input 0º degree, -60º and 60º degrees, -45º and 45º degrees, -30 and 30 degrees

The form of a triangle wave has a peak point, there is no smooth point or straight line. So, the reaction of the system can be different. When the response reaches the reference angle, it should be reacted faster in order to follow the reference input.

The figure (Figure 4.37) shows that the system of response follows the reference input clearly. The reference input is changeable during time for all that the error depends between 0º degree and 5º degrees (Figure 4.38). And the controller keeps the error between tolerable values.

There is a similarity between the control effort and the error. As in the previous experiments, the control effort is higher when the error is higher. The figure shows the control effort and the error. Clearly it is seen that the graph of control effort (Figure 4.39) has an intense form which is the same behavior of the error.

As it is seen that when the reference input is zero, the velocity of the motor is zero in the figure of the velocity (Figure 4.40). In addition to this, where the error is bigger, the velocity and the control effort is higher to correct the error. Finally, the experiments of the triangle wave of results are satisfactory as the results of previous experiments.
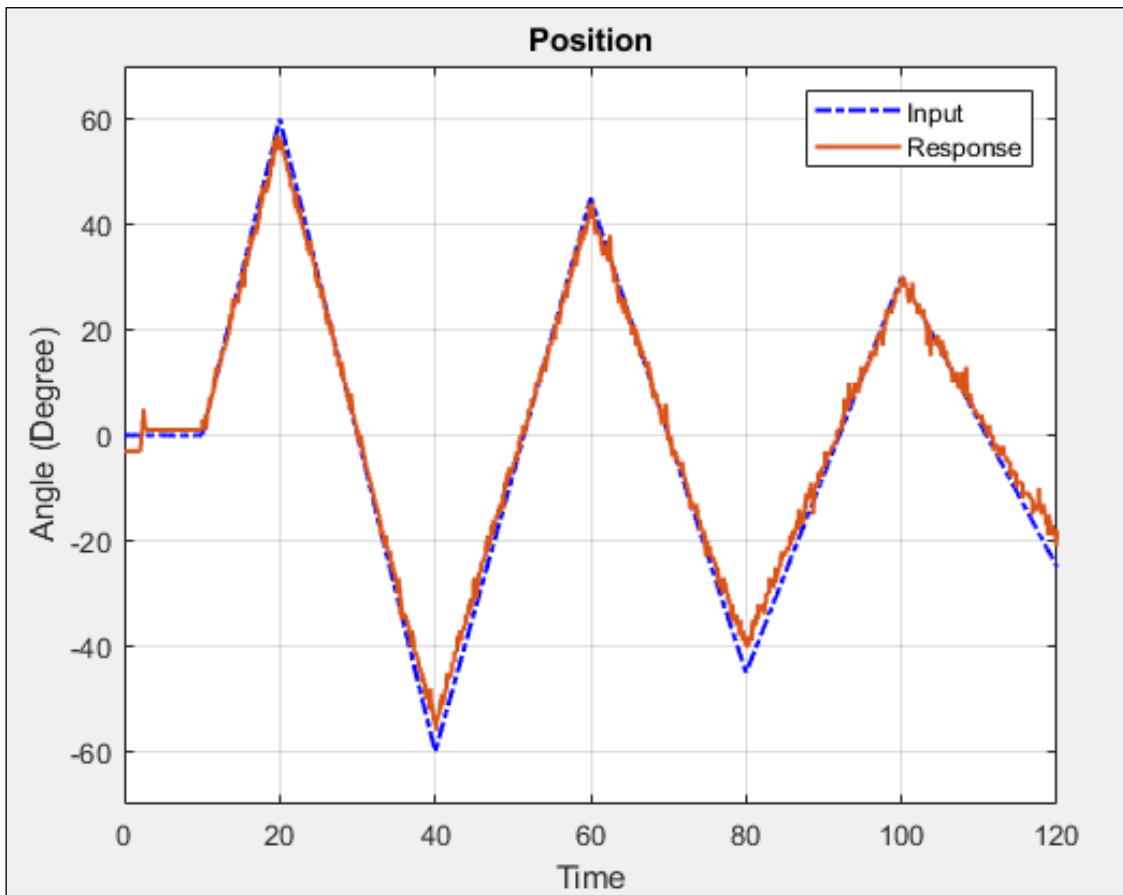
Figure 4.37 Triangle Wave 0 degree, -60 and 60 degrees, -45 and 45 degrees, -30 and 30 degrees
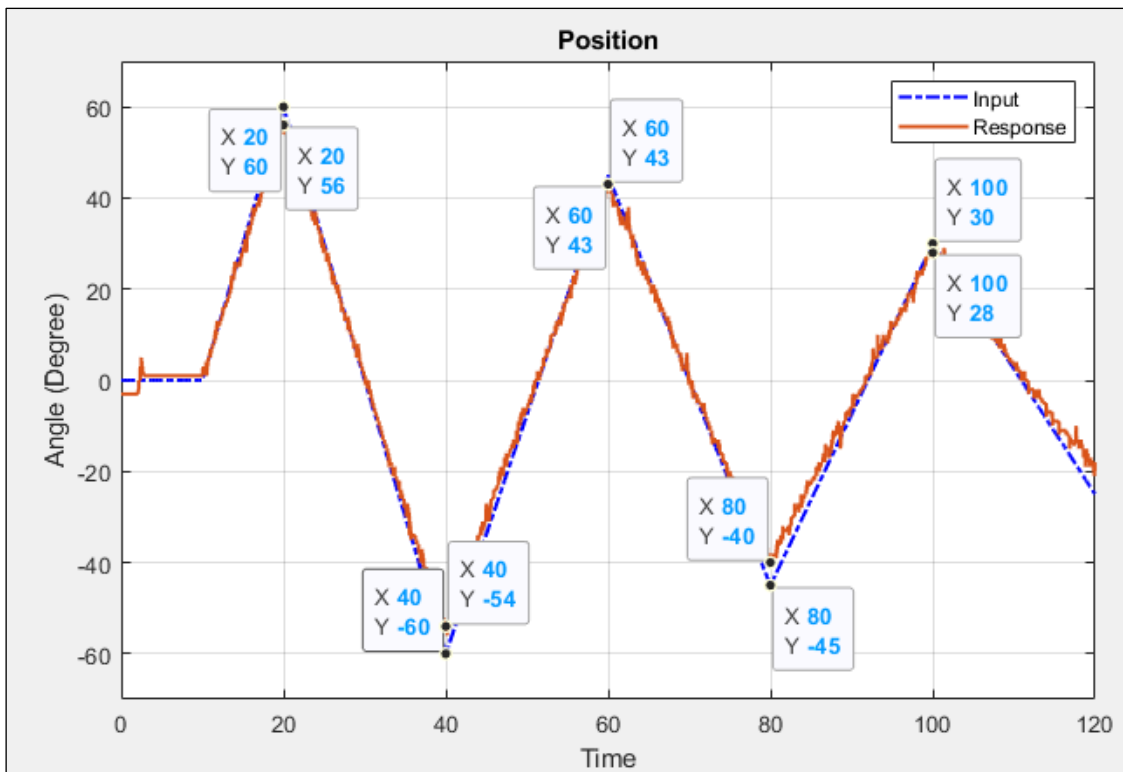
Figure 4.38 Triangle Wave 0 degree, -60 and 60 degrees, -45 and 45 degrees, -30 and 30 degrees with labels
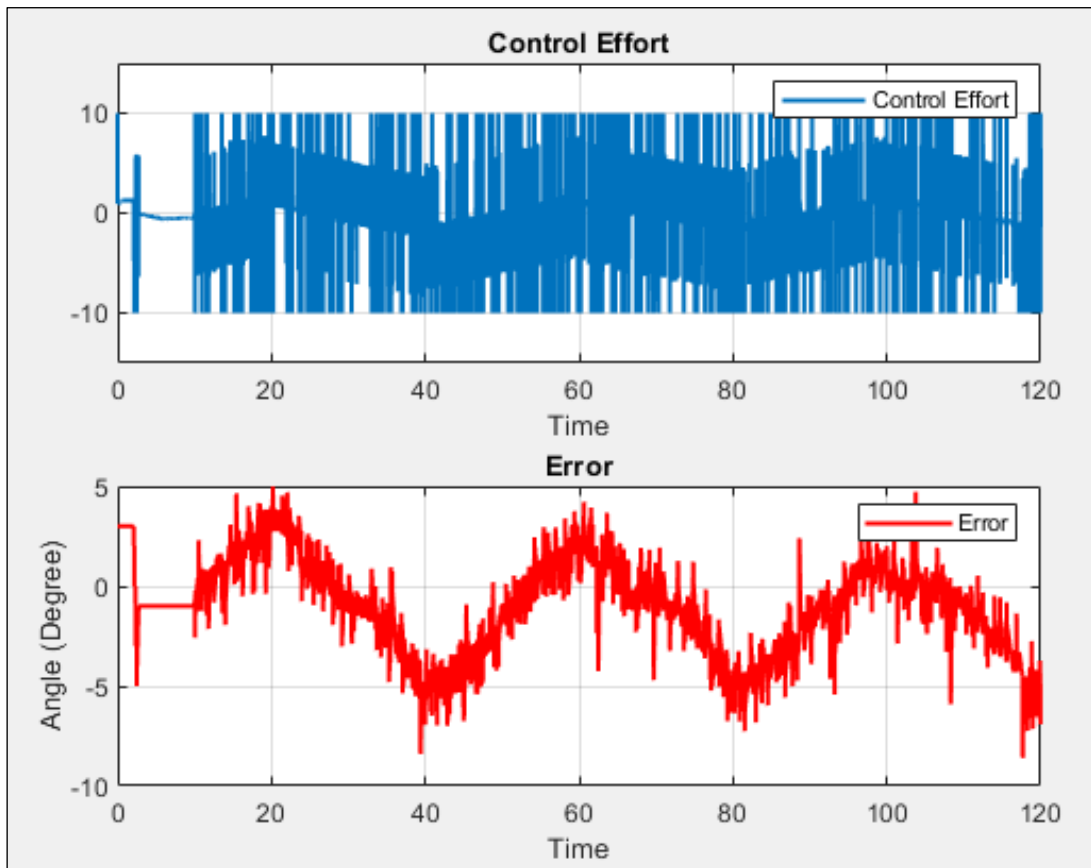
Figure 4.39 The Control Effort and Error (Triangle Wave)
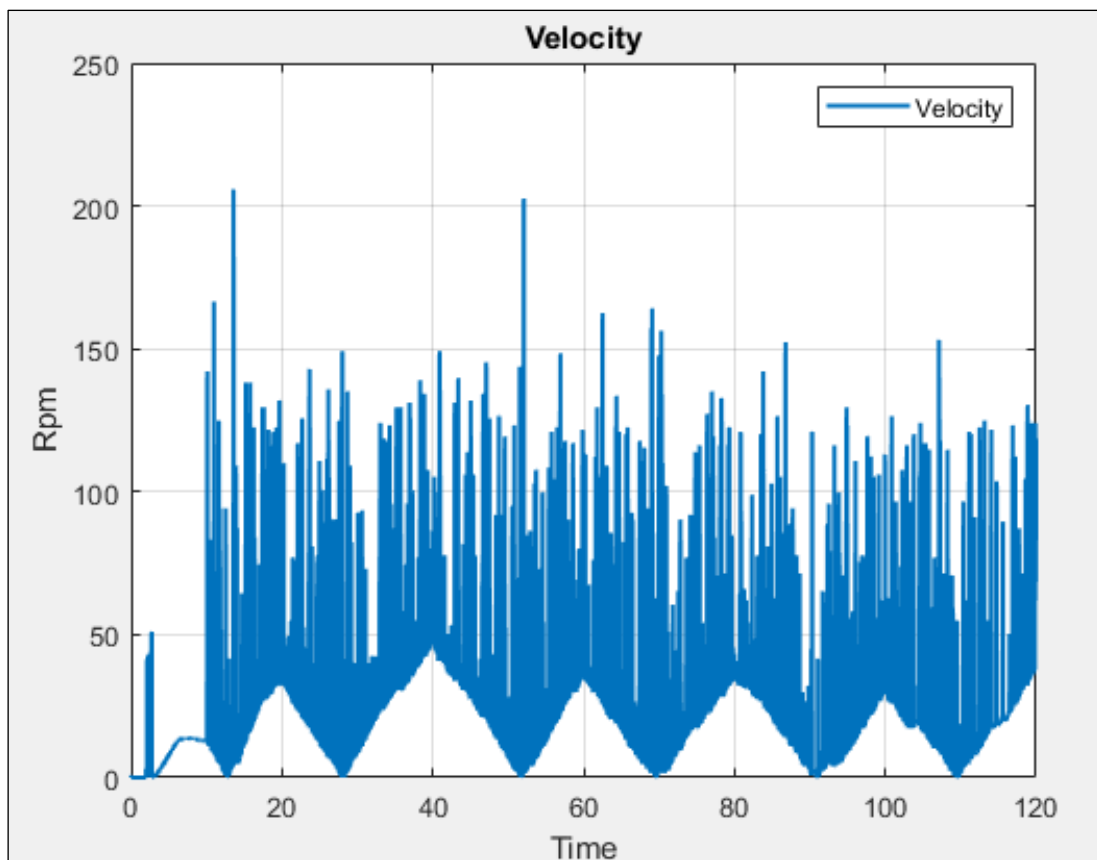
Figure 4.40 The Velocity of Motor (Triangle Wave)

5. Conclusion and Future Works

After finishing the master's thesis, most of the tasks and objectives proposed at the beginning have been completed successfully. The different inputs namely step, sine and triangle configurations are analyzed and compared in terms of the settling times, controlling in the simulation and the implementation.

The results of three-dimensional simulation within Simspace are satisfactory. All results show that the controllers and the systems work as it is expected. The joint which is used for the simulation is three degrees of freedom. The simulation part is just considered the rotation degree of freedom. The next study is to simulate with six-degrees of freedom for observing the systems behaviour in three-dimensional.

The results of the implementation are a marked achievement to control the position of the axis. The most challenging part of the implementation has been faced in terms of the connection cable. This problem is effectively dealt with using Slip Ring. The system behaviour is more stable with Slip Ring. The future suggestion of this work is to control three axes at the same time for implementation with the software (GIU)[14].

6. Budget

Three main costs are considered for the calculation of the budget. These three main costs are explained in the below.

- Material Cost
- Licensing Cost
- Work Force

Material Cost			
Material	**Unit Cost (€)**	**Unit**	**Total Cost (€)**
The base of Mechanism	€50	1	€50
The cylinder of Mechanism	€50	1	€50
Reaction Wheels	€30	2	€60
NIDEC 24H677	€9	1	€9
Arduino DUE	€30	1	€30
Sensor	€1	2	€2
Jumper Cables	€1	20	€20
Power Supply	€10	1	€10
Oscilloscope	€250	1	€250
Strong Gum	€2.5	1	€2.5
Total Cost			€465.35

Table 11 Material Cost

---

[14] CubeSat Hybrid Attitude Determination and Control Through HiL Simulation
https://www.youtube.com/watch?v=dJQngmdZaq4

The table (Table 11) shows a list with the price of the devices required for the assembly of the prototype.

The table (Table 12) shows the prices of licenses of the necessary software for the development of this project.

Licensing Cost	
Software	**Cost (€)**
SolidWorks 2020	€4000
MATLAB	€2000
Total Cost	€6000

Table 12 Licensing Cost

Assuming that the development of an application for an experienced person of per 1 hour at a cost of €20. The below table (Table 13) shows the workforce for an experienced person.

Workforce			
Activity	**Per Hour (€/h)**	**Hours (h)**	**Total Cost (€)**
Conception of the solution	€20	8	€160
Mechanical Design	€20	8	€190
Simulation	€20	100	€2000
Control Design	€20	70	€140
Assembly	€20	200	€4000
Total Cost without IVA			€6490
Total Cost with IVA			€7852.9

Table 13 Work Force

The below table (Table 14) shows the final result of the cost for developing the project.

Total Cost	
Area	**Cost (€)**
Material Cost	€465.35
Licensing Cost	€6000
Workforce Cost	€7852.9
Total Cost	€14318.25

Table 14 Total Cost

Appendices

Appendix A   Mechanical Properties
Appendix A.1   C Technical Drawing CubeSat Rail 1

Note: Master Thesis, Master's Degree in Mechatronics Engineering

	NAME	SIGNATURE	DATE
DESIGNED BY	OMAR OMEN		10.07.2021
CHECKED BY	V.CALVO		15.07.2021
APPROVED BY	V.CALVO		23.07.2021

UNIVERSITAT POLITÈCNICA DE VALÈNCIA

All dimensiones mm

TITLE

PART NUMBER: RAIL001

MATERIAL: ALUMINUM 6061

2019_001_Rail

PROJECT NAME

CONTROL OF A REACTION WHEEL BASED POSITIONING MECHANISM

A4

SCALE 1:2   SHEET 1 OF 1

Ø220

6'50

00,9

93'00

111.50

9'50

3'00

Ø220

Appendix A.2   C Technical Drawing CubeSat Rail 2

Note: Master Thesis, Master's Degree in Mechatronics Engineering

	NAME	SIGNATURE	DATE	PART NUMBER		TITLE	
DESIGNED BY	ONUR CIMEN		10.07.2021	SIDE001		2020_C3U_001_Side	
CHECKED BY	V.CALVO		15.07.2021				
APPROVED BY	V.CALVO		21.07.2021	MATERIAL		PROJECT NAME	
				ALUMINUM 6061		CONTROL OF A REACTION WHEEL BASED POSITIONING MECHANISM	A4
All dimensiones mm						SCALE 1:1 SHEET 1 OF 1	

87'00

67'00

Ø2'20

6'50

Appendix A.3   C Technical Drawing CubeSat Top and Bottom Plate

Note: Master Thesis, Master's Degree in Mechatronics Engineering

	NAME	SIGNATURE	DATE		PART NUMBER		TITLE	
DESIGNED BY	ONUR OMEN		10.07.2021		BOTTOMUP001			2019_001_Bottom
CHECKED BY	V.CALVO		15.07.2021		MATERIAL		PROJECT NAME	
APPROVED BY	V.CALVO		23.07.2021		ALUMINUM 6061		CONTROL OF A REACTION WHEEL BASED POSITIONING MECHANISM	

UNIVERSITAT POLITÈCNICA DE VALÈNCIA

All dimensiones mm

SCALE:1:1   SHEET 1 OF 1   A4

2'00

87'00

Ø 4'40

9'00

87'00

5'00

Appendix A.4   C Technical Drawing Reaction Wheel

Note: Master Thesis, Master's Degree in Mechatronics Engineering

	NAME	SIGNATURE	DATE	PART NUMBER		TITLE	
DESIGNED BY	OMAR OMEN		10.07.2021	RW001		2019_002_Reaction_Wheel	
CHECKED BY	V.CALVO		15.07.2021				
APPROVED BY	V.CALVO		23.07.2021	MATERIAL		PROJECT NAME	
				ALUMINUM 6061		CONTROL OF A REACTION WHEEL BASED POSITIONING MECHANISM	A4
						SCALE 2:1	SHEET 1 OF 1

UNIVERSITAT POLITÈCNICA DE VALÈNCIA

All dimensiones mm

Ø 34.00

Ø 4.00

1.00

10.00

Ø 40.20

Appendix A.5   C Technical Drawing CubeSat Assembly
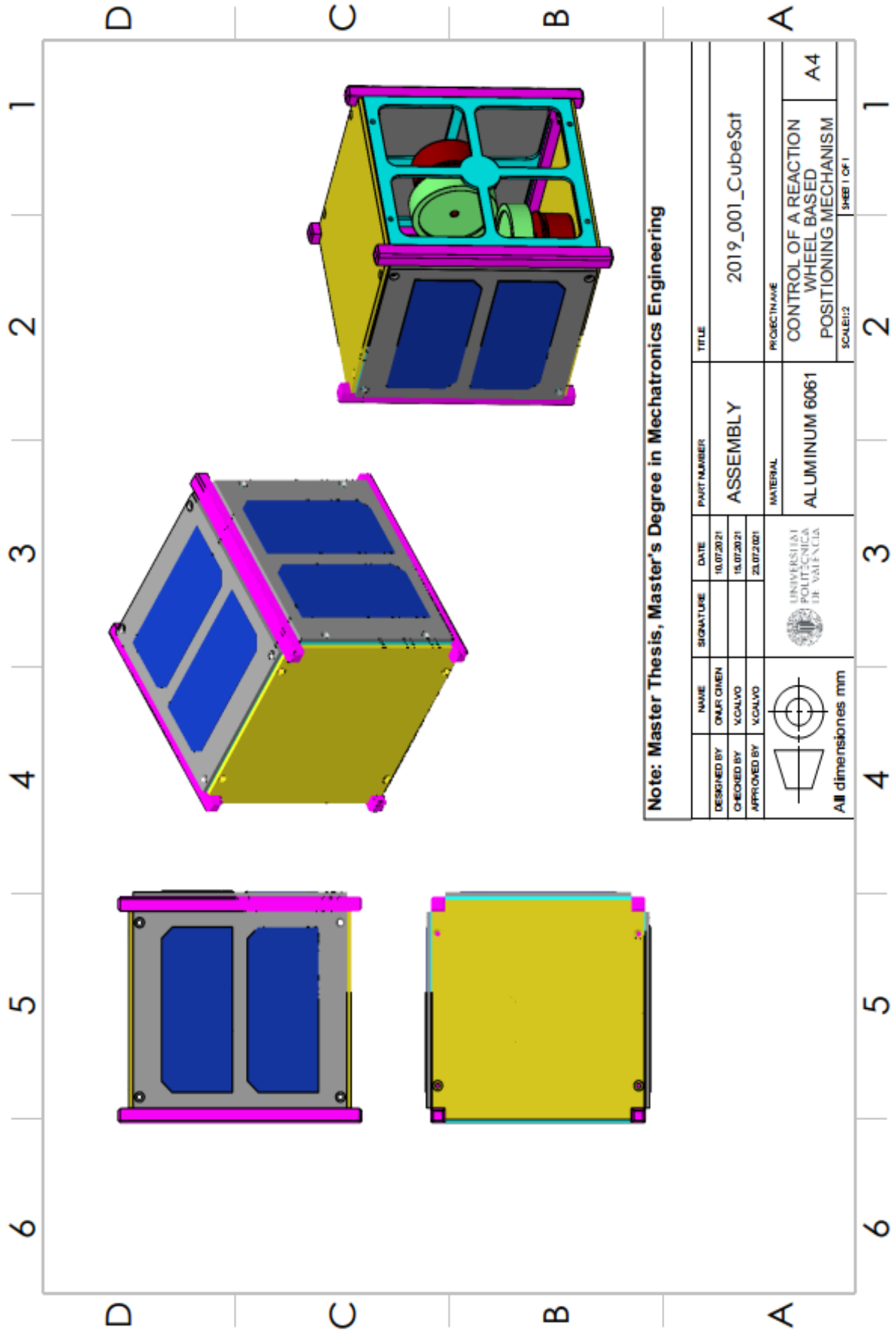
Appendix A.6   Implementation Base Technical Drawing

Note: Master Thesis, Master's Degree in Mechatronics Engineering

	NAME	SIGNATURE	DATE	PART NUMBER		TITLE	
DESIGNED BY	ONUR OMEN		10.07.2021	BASE001			2021_IMP_Base
CHECKED BY	V.CALVO		15.07.2021				
APPROVED BY	V.CALVO		23.07.2021	MATERIAL		PROJECT NAME	
				METHACRYLATE		CONTROL OF A REACTION WHEEL BASED POSITIONING MECHANISM	
						SCALE 1:5	A4

All dimensiones mm

2021_IMP_Base

BASE001

METHACRYLATE

CONTROL OF A REACTION WHEEL BASED POSITIONING MECHANISM

SCALE 1:5   SHEET 1 OF 1   A4

UNIVERSITAT POLITÈCNICA DE VALÈNCIA

295.00

320.00

$\varnothing$ 400

$\varnothing$ 42.00

$\varnothing$ 4.00

5.00

30.00

10.00

Appendix A.7   Implementation Cylinder Technical Drawing
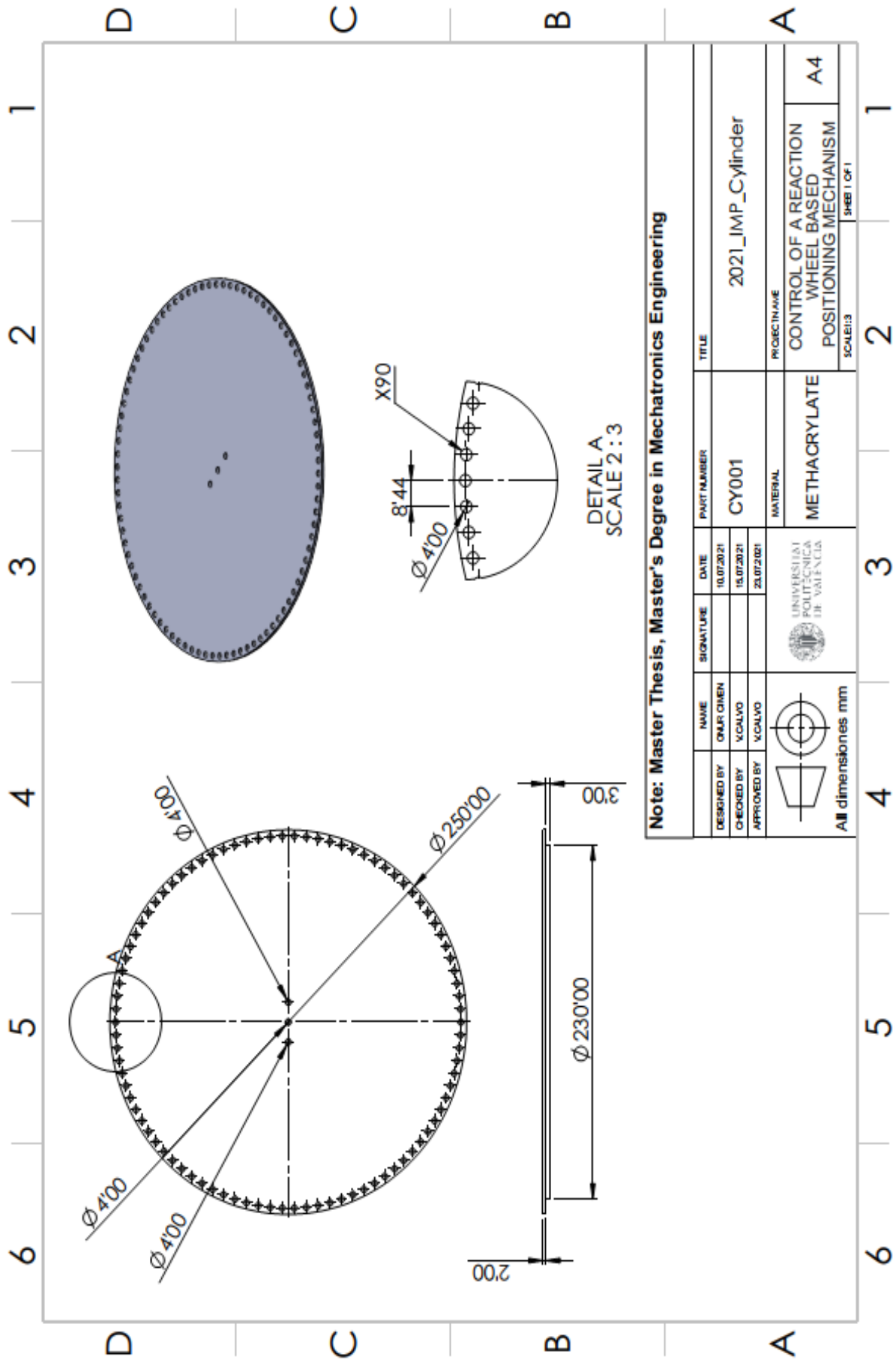
Appendix A.8   Implementation Reaction Wheel Technical Drawing

Note: Master Thesis, Master's Degree in Mechatronics Engineering

TITLE
2021_IMP_Reaction_Wheel

PART NUMBER
RW001

MATERIAL
METHACRYLATE

PROJECT NAME
CONTROL OF A REACTION
WHEEL BASED
POSITIONING MECHANISM

SCALE 1:2

A4

SHEET 1 OF 1

	NAME	SIGNATURE	DATE
DESIGNED BY	ONUR GIVEN		10.07.2021
CHECKED BY	V.CALVO		15.07.2021
APPROVED BY	V.CALVO		23.07.2021

UNIVERSITAT
POLITÈCNICA
DE VALÈNCIA

All dimensiones mm

Ø 110,00
Ø 120,00
Ø 140,00

0,80

2,00

Appendix A.9   Implementation Assembly Drawing

Note: Master Thesis, Master's Degree in Mechatronics Engineering

	NAME	SIGNATURE	DATE
DESIGNED BY	ONUR GIVEN		10.07.2021
CHECKED BY	V.CALVO		15.07.2021
APPROVED BY	V.CALVO		23.07.2021

UNIVERSITAT POLITÈCNICA DE VALÈNCIA

All dimensiones mm

PART NUMBER		TITLE	
ASSEMBLY		2021_IMP_Assembly	
MATERIAL		PROJECT NAME	
METHACRYLATE		CONTROL OF A REACTION WHEEL BASED POSITIONING MECHANISM	
SCALE 1:5			A4
			SHEET 1 OF 1

Appendix B   Mechanical and Electronic Components Properties
Appendix B.1   Maxon Flat DC Motor Datasheet

EC 32 flat ∅32 mm, brushless, 15 Watt

A mit Hallsensoren / with Hall sensors

B sensorlos / sensorless

maxon flat motor

M 1:2
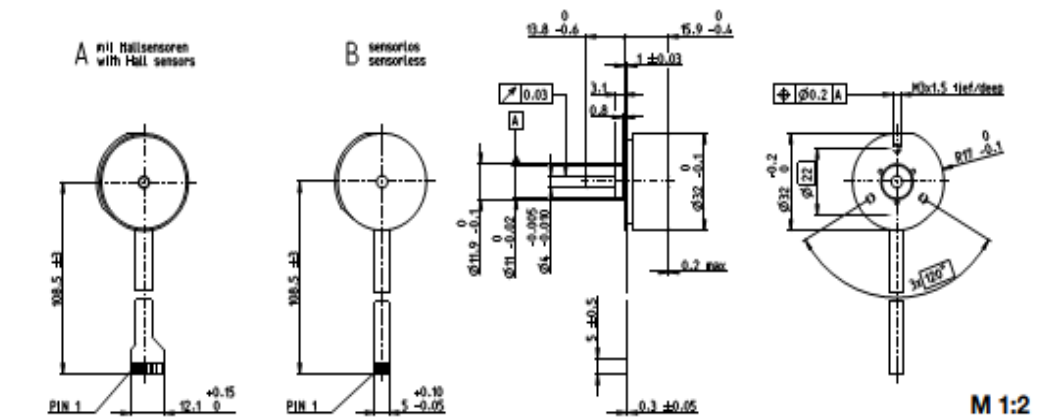
Stock program
Standard program
Special program (on request)

Part Numbers				
A with Hall sensors	339267	339268	267121	339269
B sensorless	339271	339272	226006	339273

Motor Data

	Values at nominal voltage				
1	Nominal voltage	V	9	12	24	48
2	No load speed	rpm	3720	4610	4530	4780
3	No load current	mA	74.7	75.7	36.9	19.9
4	Nominal speed	rpm	2060	2790	2760	2940
5	Nominal torque (max. continuous torque)	mNm	24.5	25	25.5	24.7
6	Nominal current (max. continuous current)	A	1.06	1	0.5	0.257
7	Stall torque¹	mNm	68.3	82.3	85.3	83.9
8	Stall current	A	3.06	3.42	1.74	0.904
9	Max. efficiency	%	71	73	73	73
	Characteristics				
10	Terminal resistance phase to phase	Ω	2.95	3.51	13.8	53.1
11	Terminal inductance phase to phase	mH	1.61	1.86	7.72	27.7
12	Torque constant	mNm/A	22.4	24.1	49	92.8
13	Speed constant	rpm/V	427	397	195	103
14	Speed/torque gradient	rpm/mNm	56.3	57.8	54.8	58.8
15	Mechanical time constant	ms	20.6	21.2	20.1	21.6
16	Rotor inertia	gcm²	35	35	35	35

Specifications

Thermal data
17 Thermal resistance housing-ambient   10.8 K/W
18 Thermal resistance winding-housing   4.99 K/W
19 Thermal time constant winding   8.78 s
20 Thermal time constant motor   120 s
21 Ambient temperature   -40...+100°C
22 Max. winding temperature   +125°C
Mechanical data (preloaded ball bearings)
23 Max. speed   10000 rpm
24 Axial play at axial load   < 5.0 N   0 mm
    > 5.0 N   typ. 0.6 mm
25 Radial play   preloaded
26 Max. axial load (dynamic)   4.8 N
27 Max. force for press fits (static)   45 N
    (static, shaft supported)   1000 N
28 Max. radial load, 5 mm from flange   14 N
Other specifications
29 Number of pole pairs   4
30 Number of phases   3
31 Weight of motor   57 g
Values listed in the table are nominal.

Connection	with Hall sensors	sensorless
Pin 1	V_cc 3.5...24 VDC	Motor winding 1
Pin 2	Hall sensor 3	Motor winding 2
Pin 3	Hall sensor 1	Motor winding 3
Pin 4	Hall sensor 2	⊥ neutral point
Pin 5	GND	
Pin 6	Motor winding 3	
Pin 7	Motor winding 2	
Pin 8	Motor winding 1	

Adapter	Part number	Part number
see p. 481	220300	220310

Connector	Part number	Part number
TE	1-84953-1	84953-4
Molex	52207-1133	52207-0433

Pin for design with Hall sensors:
FPC, 11-pol, Pitch 1.0 mm, top contact style
Wiring diagram for Hall sensors see p. 47

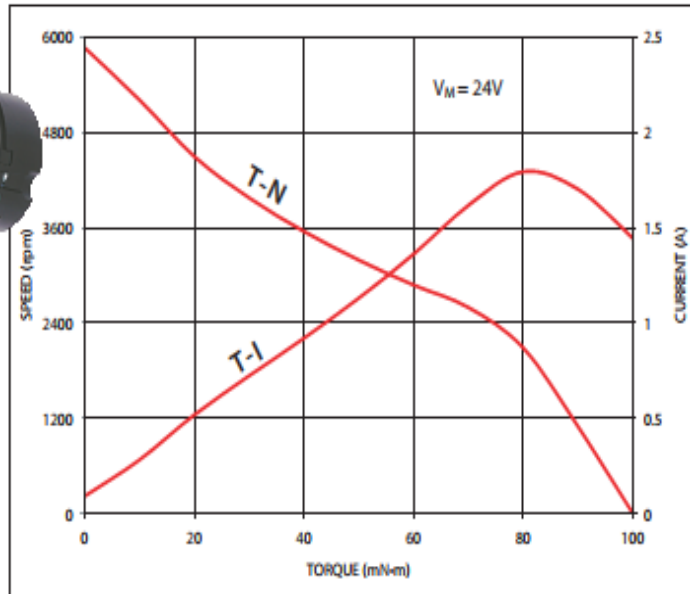¹Calculation does not include saturation effect
(p. 57/162)

April 2019 edition / subject to change

Operating Range

n [rpm]

15 W

267121

Comments

Continuous operation
In observation of above listed thermal resistance (lines 17 and 18) the maximum permissible winding temperature will be reached during continuous operation at 25°C ambient.
= Thermal limit.

Short term operation
The motor may be briefly overloaded (recurring).

Assigned power rating

maxon Modular System   Details on catalog page 36

Planetary Gearhead
∅32 mm
0.75 - 6 Nm
Page 350/353
Spur Gearhead
∅38 mm
0.1 - 0.6 Nm
Page 360

Recommended Electronics:	
Notes	Page 36
ESCON Module 24/2	454
ESCON 36/3 EC	455
ESCON Mod. 50/4 EC-S	455
ESCON Module 50/5	455
ESCON 50/5	457
DEC Module 24/2	459
DEC Module 50/5	459
EPOS4 Mod./Comp. 24/1.5	462
EPOS4 50/5	463
EPOS4 Mod./Comp. 50/5	463
MAXPOS 50/5	473

maxon EC motor 259

Appendix B.2   Nidec DC Motor Datasheet

24H Brushless DC Motors

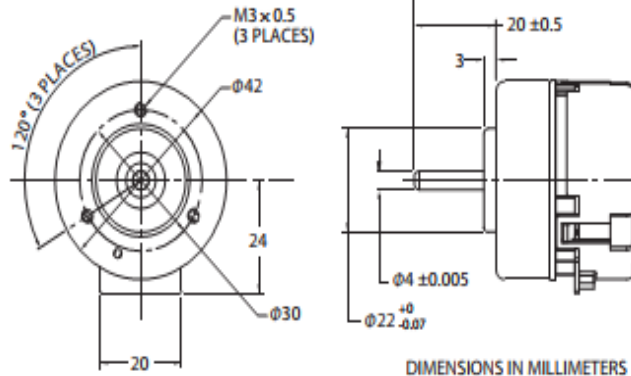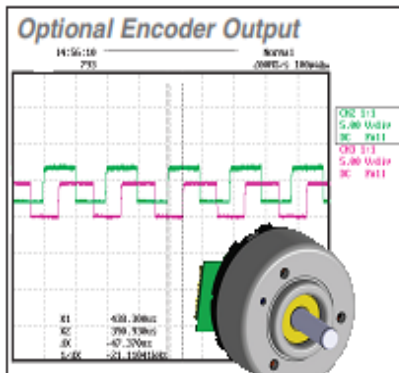## for Home Appliances and Office Equipment

- 3-Phase, 12-Pole Brushless Motors
- Logic-Controlled Clockwise or Counterclockwise Rotation
- Hall Effect Commutation
- Quiet Operation
- Low Inertia
- PWM Speed Control/Brake Function
- Open-Drain Tachometer
- Optional Dual Channel Phase-Tracking Encoder
- Locked Rotor Protection*
- Compact 42 (dia.) × 34mm Case

$V_M = 24V$

* Automatic shutdown at locked rotor condition: Restart at power OFF/ON.

Optional Encoder Output

M3 × 0.5 (3 PLACES)

Φ42

Φ30

54

20 ±0.5

3

Φ4 ±0.005

$\Phi 22 \, {}^{+0}_{-0.07}$

24

20

DIMENSIONS IN MILLIMETERS

Pinout

Pin	Function
1	Standard = No connection. Encoder option = Channel A output: 90° phase tracking, 100 pulses per revolution, HIGH = 5V, LOW = 0V.
2	Standard = Open-drain tachometer, six pulses per revolution, $I_{C(MAX)}$ = 3.0 mA. Encoder option = Channel B output: 90° phase tracking, 100 pulses per revolution, HIGH = 5V, LOW = 0V.
3	Standard = No connection. Encoder option = Logic supply, 5V ±0.5V.
4	$V_{IN(HIGH)}$ = 2.0V to 5.0V or OPEN = Clockwise, $V_{IN(LOW)}$ <= 0.6V = Counterclockwise.
5	PWM: f_{in} = 20 kHz to 30 kHz, $V_{IN(LOW)}$ <= 0.6V, $V_{IN(HIGH)}$ = 2.0V to 5.0V, duty cycle = 20% to 100%.
6	Brake: $V_{IN(HIGH)}$ = 2.0V to 5.0V = OFF, $V_{IN(LOW)}$ <= 0.6V = ON (motor stop).
7	Supply ground.
8	Motor supply voltage, 24V, nominal.

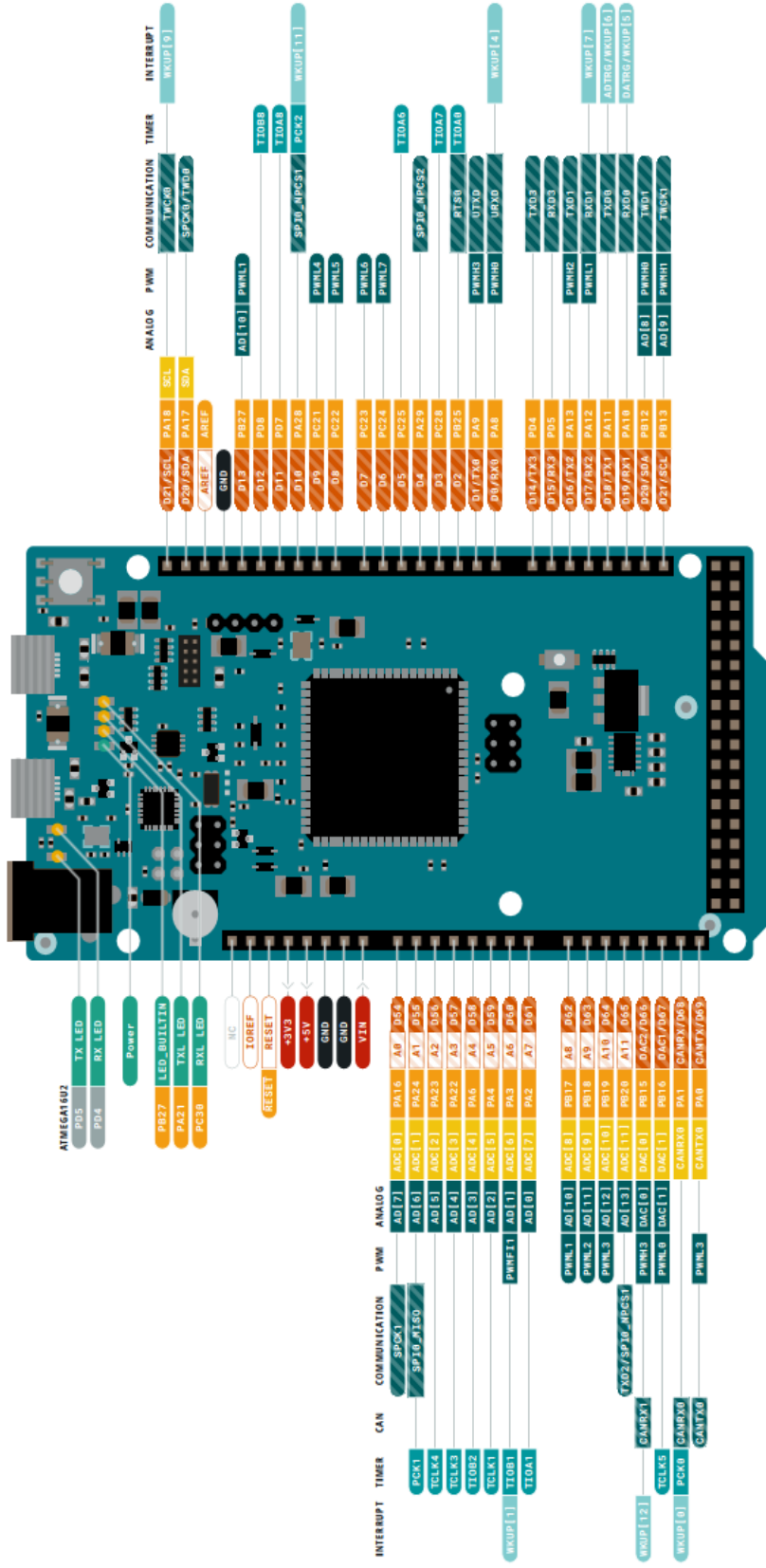**Nidec**
–All for dreams

Nidec America · phone 314-595-8186 · email motors@nidecamerica.com · www.nidecamerica.com

Appendix B.3   Arduino Due

Appendix B.4 Sensor

Lm393 Motor Speed Measuring Sensor Module For Arduino

Widely used in motor speed detection, pulse count, the position limit, etc. The DO output interface can be directly connected to a micro-controller IO port, if there is a block detection sensor, such as the speed of the motor encoder can detect.

DO modules can be connected to the relay, limit switch, and other functions, it can also with the active buzzer module, compose alarm.

Main technical characteristics:
- Dimensions: 32 x 14 x 7mm.
- The sensor reading slot has a width of 5mm.
- Two outputs, one Digital and one Analog.
- LED power indicator.
- LED indicator of the output pulses of pin D0.

Features
- Using imported trough type optical coupling sensor, groove width 5 mm.
- The output state light, lamp output level, the output low level light.
- Covered : output high level; Without sunscreen : the output low level.
- The comparator output, signal clean, good waveform, driving ability is strong, for more than 15 ma.
- The working voltage of 3.3 V to 5 V
- Output form: digital switch output (0 and 1)
- A fixed bolt hole, convenient installation
- Small board PCB size: 3.2 cm x 1.4 cm
- Use the LM393 wide voltage comparator Module

USES:
- The module without slot, the receiving tube conduction, module DO output low level, shade, the DO output high level;

Appendix B.5   SENRING H2042 Slip Ring
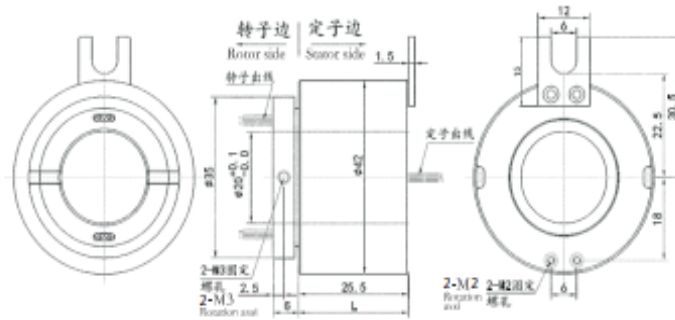
H2042 Series

H2042 series standard precise slip ring, integrated structure design, with through hole 20mm , OD42mm , suitable for rotating application which requires a through hole <=5mm (remark: if need a hole <20mm, can add a inner bushing)

Part No. Description

H2042 - Signal circuits no. - Eroduct grade

H:through hole slip ring
2042:ID 20mm, OD 42mm

Example:
06S:6circuits signal (0~5A)
12S:12circuits signal (0~5A)

Example:
C: standard level
D:Industrial level
H:High quality level

転子边 定子边
Rotor side Stator side
转子由线
定子由线

Standard Model List

H0522 series model list		
Part no.	Circuits no. (signal or 0~5A)	Length L(mm)
H2042-02S	2	25.5
H2042-03S	3	25.5
H2042-04S	4	25.5
H2042-06S	6	25.5
H2042-08S	8	37.5
H2042-10S	10	37.5
H2042-12S	12	37.5

*Remark: Circuits can be combined in parallel for bigger current,N circuits of 5A to get N*5A, such as 2 circuits of 5A in parallel for 10A use.

Technical Specification

Mechanical		Electrical		
Spec	Data	Spec	Data	
Working life	pls refer to product grade table		Power	Signal
Rotating speed	pls refer to product grade table	Rated voltage	0~240VAC/VDC	0~240VAC/VDC
Working temp.	-30°C~80°C	Insulation resistance	≥500mΩ/500VDC	≥500mΩ/500VDC
Work humidity	0~85% RH	Lead wire spec	AWG26# Silver-plated teflon	AWG26# Silver-plated teflon
Contact material	pls refer to produce grade table	Lead wire length	standard 300mm(can be customized)	
Housing material	AL alloy	Dielectric Strength	500VAC@50Hz,60s	
Torque	0.05N.m (+0.03N.m/6circuits)	Electrical noise	<0.01Ω	
IP grade	IP51			

Product Grade Table

Grade code	Max rotating speed	Working life	Contact material
C:standard	250RPM	20millisons revolutions	precious metal
D:industrical	600RPM	60millisons revolutions	precious metal
H:high quality	1000RPM	150millisons revolutions	gold alloy

H2042 Series

H Series Through Hole Slip Ring

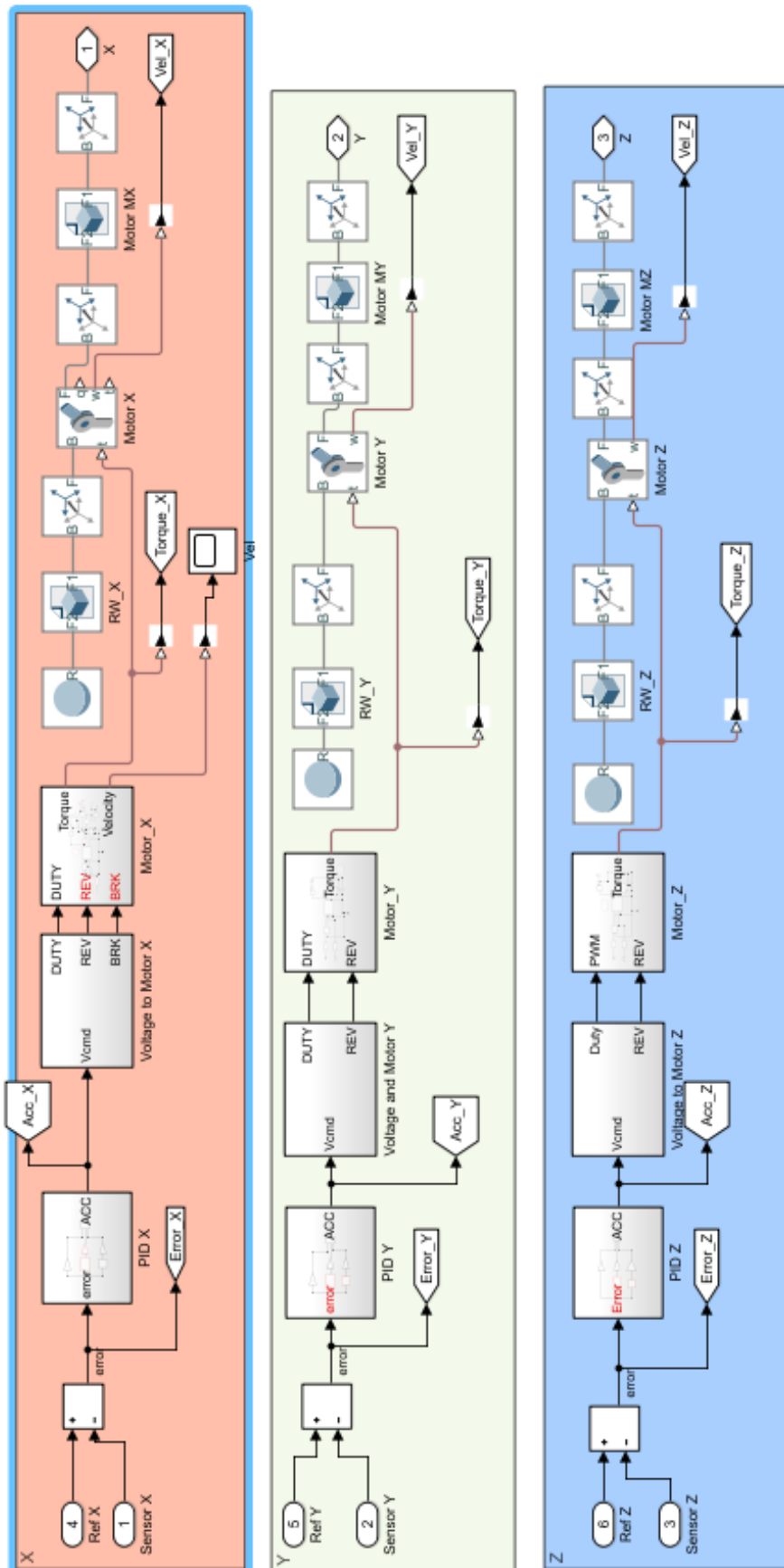## Appendix C   Simulink Simscape Model
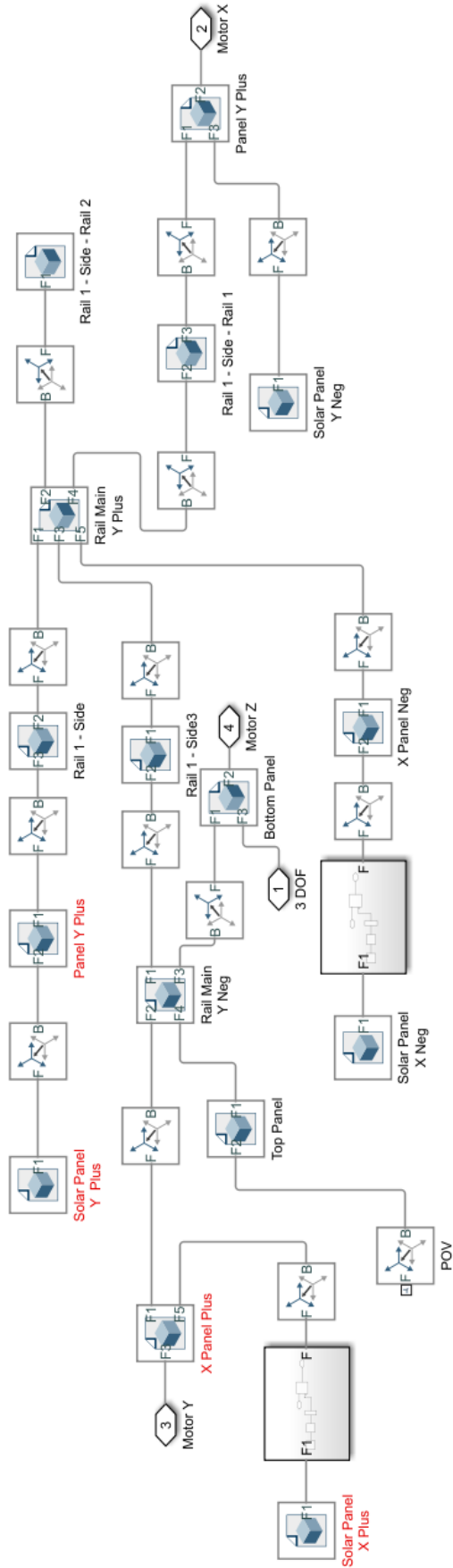### Appendix C.1   Simscape Model
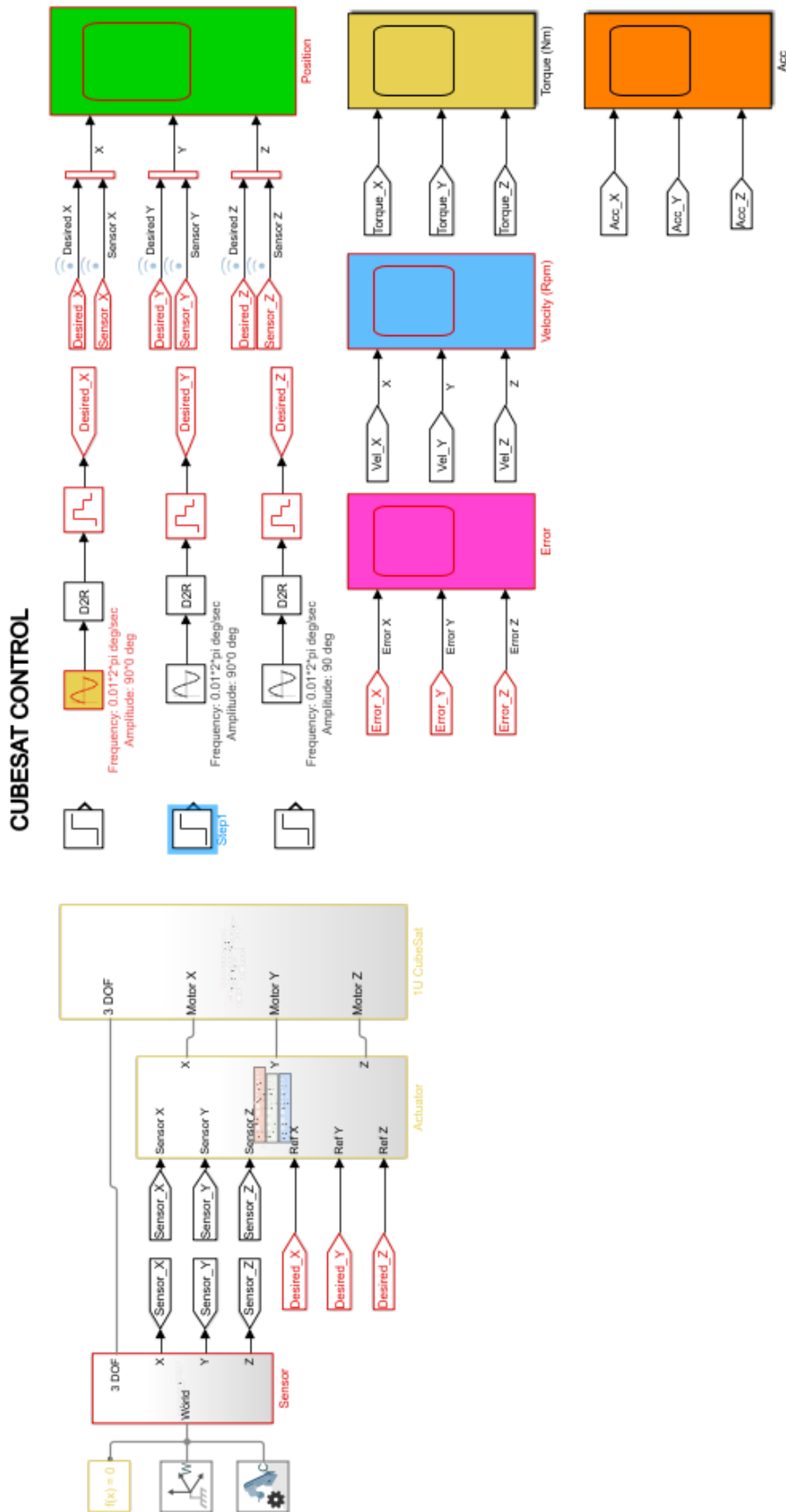
Appendix C.2   Simscape Sensor Modelling
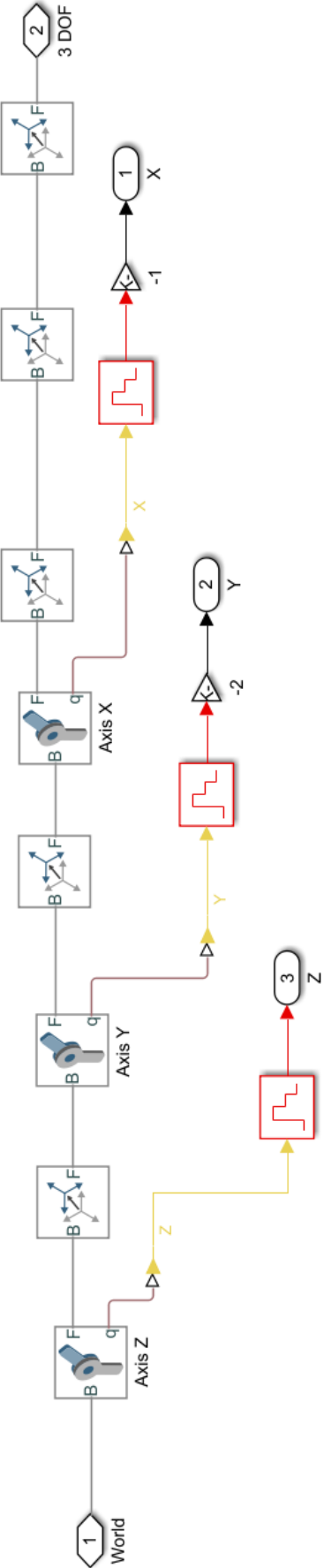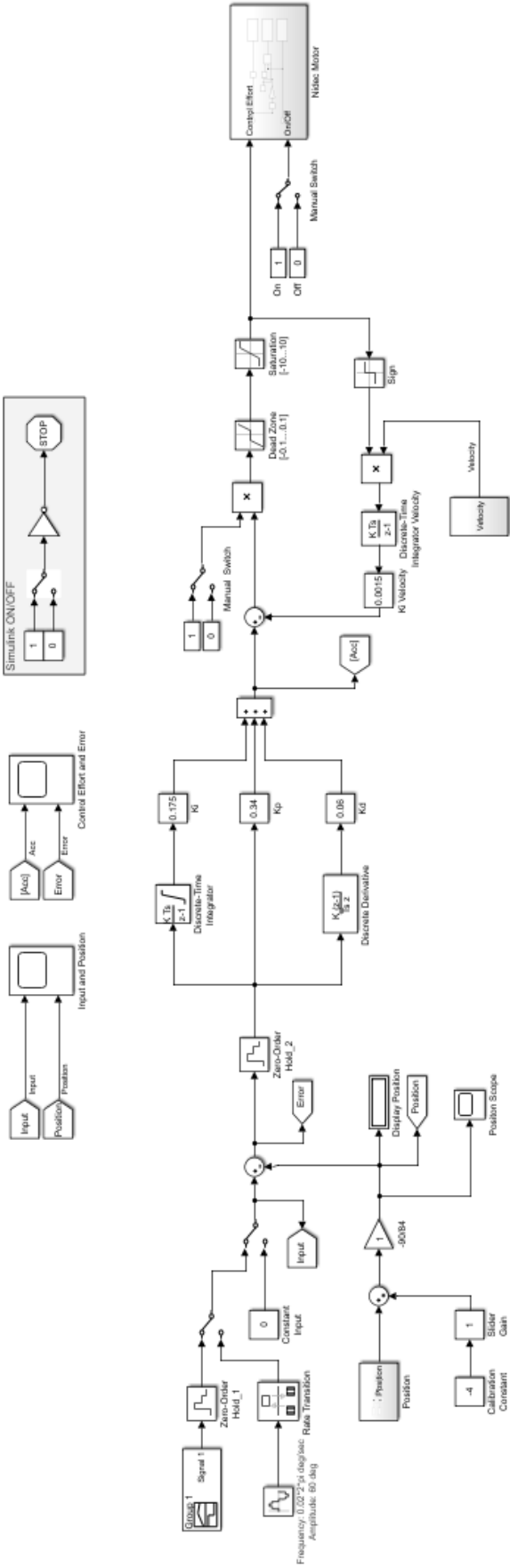
Appendix C.3   Simscape Actuators Modelling

Appendix C.4   Simscape CubeSats Model Assembly

Appendix C.5   Implementation Simulink

Bibliography

[1] A. JohnStone, "Cubesat Design Specification (1U-12U) REV14 CP-CDS-R14," California Polytechnic State University (Cal Poly), California, 2020.

[2] E. Oland and R. Schlanbusch, "Reaction Wheel Design for CubeSats," in *2009 4th International Conference on Recent Advances in Space Technologies*, Istanbul, Turkey, 11-13 June 2009.

[3] I. Zuliana and V. Renuganth, "A study of reaction wheel configurations for a 3-axis satellite," *Advances in Space Research,* vol. 15, no. 6, pp. 750-759, 15 March 2010.

[4] R. Gordon, "Quadcopter Simulation and Control Made Easy - MATLAB and Simulink Video," The MathWorks, 30 April 2017. [Online]. Available: https://www.youtube.com/watch?v=fpJZSQmqDVk, https://www.mathworks.com/campaigns/products/trials.html?s_eid=PSM_15028.

[5] M. M. I. T. a. R. D. Mohanarajah Gajamohan, "The Cubli: A Cube that can Jump Up and Balance," in *2012 IEEE/RSJ International Conference on Intelligent Robots and Systems*, Vilamoura, Algarve, Portugal, 2012.